A MULTI-SCALE ASSESSMENT OF THE COUPLING BETWEEN THE NITROGEN CYCLE AND THE TERRESTRIAL CARBON SINK UNDER GLOBAL CHANGE

by

Justin David Gay

A dissertation submitted in partial fulfillment
of the requirements for the degree

of

Doctor of Philosophy

in

Land Resources and Environmental Sciences

MONTANA STATE UNIVERSITY
Bozeman, Montana

May 2022

©COPYRIGHT

by

Justin David Gay

2022

All Rights Reserved

DEDICATION

For my parents and grandparents,

who have taught me how to work hard and to value your purpose and pursuits in life.

ACKNOWLEDGEMENTS

This body of work warrants much gratitude as it reflects the skills, dedication, and insights of the many individuals who have contributed to the process. I am grateful to my parents and brother for their endless encouragement, love, and support along my path. To my wife, Shealyn, the decision to start on this trajectory with you was the best of my life. Your unwavering love and encouragement reverberate throughout this dissertation and have kept me moving forward.

I was fortunate to be surrounded by a strong community of committee members. Drs. Paul Stoy, Ben Poulter, and Perry Miller have all been pivotal advocates for me and were sources of intellectual support, thoughtful advice, and constructive feedback. Your individual and combined efforts have made me a better scientist. A special thank you to Dr. Clain Jones, whom I had the privilege of learning from and teaching with for three semesters. Your dedication to your students and teaching craft has been an inspiration. I will be forever grateful for the opportunity to share my time at Montana State with my fellow lab mate, Bryce Currey. Much of this work is a direct reflection of your insightful collaboration. I thank you for the invaluable quantitative assistance you provided, but most importantly, for your friendship.

Lastly, none of this would have been possible without the guidance of my advisor Dr. Jack Brookshire. I am forever grateful that you took a chance on me and believed in my potential. Thank you for supporting my intellectual development, holding the bar high and demonstrating the critical skill of persistence in the pursuit of truth. This work was generously supported by Montana State Graduate School Dissertation Completion Grant.

TABLE OF CONTENTS

1. INTRODUCTION 1

Figures 7
References 8

2. THE CLIMATE MITIGATION POTENTIAL AND SOIL MICROBIAL RESPONSE OF CYANOBACTERIA-FERTILIZED BIOENERGY CROPS IN ACOOL SEMI-ARID CROPLAND 12

Contribution of Authors and Co-Authors 12
Manuscript Information 14
Abstract 16
Introduction 17
Methods 22
Site Description and Experimental Design 22
Growing Degree Days, Rain Use Efficiency, and Soil pH 23
Fertilization 24
Soil Sampling and Analysis 25
Above and Belowground Productivity and Biomass Chemistry 26
GHG Flux Collection 27
Flux Calculations 29
Statistical Analysis 30
Soil Microbial Community Analysis 32
Results 33
Soil Water, Weather Conditions, and pH 32
Above and Belowground Production 34
SOC Change 2018-2020 34
Soil Greenhouse Gas Flux 35
Above and Belowground Biomass Chemistry 36
Microbial Biodiversity Shifts 37
Discussion 38
References 49

3. THE CUMULATIVE EFFECTS OF CONIFER EXPANSION AND PRESCRIBED FIRE ON ECOSYSTEM CARBON AND NITROGEN CYCLING IN A TEMPERATE GRASSLAND 89

Contribution of Authors and Co-Authors 89
Manuscript Information 90
Abstract 91

TABLE OF CONTENTS CONTINUED

Introduction....93
Methods....97
Site Description....97
Aboveground Biomass Estimates....98
Dendrochronology....99
Prescribed Fire Management....99
Fire Severity....100
Tree Mortality Assessment....101
C and N Emission Estimates....101
Soil, Surface PyOM, and Woody Tissue Collection and Processing....102
Soil and Foliar Chemical Analysis....103
Soil Respiration Measurements....104
Statistical Analysis....104
Results....106
Tree Establishment and Growth Rates....106
Fire Severity, Tree Mortality, and C and N Biomass Loss....106
Changes in Soil Chemistry....108
PyC Production, Landscape Distribution, and Soil Respiration....109
Discussion....110
References....118

4. GLOBAL DISTRIBUTION AND CLIMATE SENSITIVITY OF THE TROPICAL MONTANE FOREST NITROGEN CYCLE....143

Contribution of Authors and Co-Authors....143
Manuscript Information....144
Abstract....145
Introduction....146
Results and Discussion....148
Elevational Patterns of Soil N and $\delta^{15}N$....148
Drivers of Tropical Soil N Content and $\delta^{15}N$....149
Global Distribution of Tropical Montane Forest Soil N pool and ^{15}N....151
Methods....154
Data Assembly....154
Quantifying Tropical Montane Forest Extent....156
Drivers of Soil N and $\delta^{15}N$....156
Mapping soil N pools and $\delta^{15}N$....158
References....160

5. SYNTHESIS....185
REFERENCES CITED....186

LIST OF TABLES

Table Page

2.1 Growing season CO_2 fluxes across fertilizer type 62

2.2 Differences in CO_2 fluxes between growing season months 63

2.3 Annual aboveground, belowground, and total annual productivity 64

2.S1 Changes in soil organic carbon 75

2.S2 Above and belowground biomass chemistry 76

2.S3 Aboveground biomass production of non-irrigated switchgrass and tall wheatgrass across the Northern Great Plains 77

2.S4 Crop rain use efficiency 78

2.S5 Soil water filled pore space by month 79

2.S6 Mean growing season fluxes of CO_2, CH_4 flux, and N_2O flux by crop type 80

2.S7 Summary of PERMANOVA for fungal and bacterial communities 81

2.S8 Relative abundances (%) of bacterial/archaeal phyla across crop types. 82

2.S9 Relative abundances (%) of major fungal classes across crop 83

2.S10 Identity & ecology of zOTUS in the fungal classes. 84

2.S11 Levene's test results for equal variance of SOC change 85

3.1 Burn severity classification and % area affected 131

3.2 Conifer biomass chemistry and total pre-fire aboveground biomass pools. 132

3.S1 KCL extractable NO_3-N, NH_4-N, and NH_4:NO_3 140

LIST OF TABLES CONTINUED

3.S2 Bray's extractable PO_4-P 141

3.S3 One-year differences in soil concentrations of %C, %N, %P, and %PyC 142

4.S1 Biophysical properties of elevational gradients 178

4.S2 Linear mixed model results (Figure 2a, 2b, 2c) 179

4.S3 Model results for drivers of tropical soil %N, N pool, and $\delta^{15}N$ 180

4.S4 Montane classification criteria and binned tropical land area estimates 181

4.S5 Global and regional extent of tropical montane forest. 182

4.S6 Previously reported tropical forest extent 183

4.S7 Total mineral soil N pool for global tropical forests 184

LIST OF FIGURES

Figure Page

1.1 Conceptual model of the coupled interactions between carbon and nitrogen in an agricultural system 7

2.1 Above and belowground biomass production 58

2.2 Three-year soil organic carbon change 59

2.3 Time series of greenhouse gas fluxes across the growing season 60

2.4 Bacterial and fungal soil community dissimilarity matrix for crop types 61

2.S1 Experimental design 65

2.S2 Switchgrass and tall wheatgrass in 2020 66

2.S3 2019 aboveground biomass across treatments 67

2.S4 2019 and 2020 growing degree days 68

2.S5 Gas flux linearity regression assessments 69

2.S6 Changes in the relative abundance of the methanogenic Euryarchaeota 70

2.S7 Dissimilarity matrix of bacterial and fungal community composition 71

2.S8 Daily precipitation during the growing season 72

2.S9 Soil organic carbon concentration shifts from 2018 to 2020 73

2.S10 Soil temperature and water filled pore space in 2020 74

LIST OF FIGURES CONTINUED

Figure Page

3.1 Woody establishment distribution and aboveground C accumulation 126

3.2 Unit D fire severity map 127

3.3 Plot level mortality and relationship with fire severity....128

3.4 Carbon and nitrogen fire fluxes and relationship with pre-fire woody cover....129

3.5 Pre and post fire differences of soil C, N, and pyrogenic carbon....130

3.S1 Aerial photograph of woody expansion in Unit D....133

3.S2 Pre and post fire photograph....134

3.S3 CO_2 fluxes from woody biochar greenhouse experiment....135

3.S4 Ordinary least square regressions pre-fire soil pyrogenic carbon and surface slope angle regression 136

3.S5 Ordinary least square regressions between the pre and post fire change in soil N concentrations and woody expansion and fire variables....137

3.S6 Ordinary least square regressions between the pre and post fire change in soil C concentrations and woody expansion and fire variables....138

3.S7 Ordinary least square regressions between the pre and post fire change in soil C concentrations and woody expansion and fire variables....139

4.1 Global distribution of tropical montane forests, soil N pools, and $\delta^{15}N$....165

4.2 Elevational distribution of soil N content, C:N ratios, and $d^{15}N$ across tropical montane forests....166

LIST OF FIGURES CONTINUED

4.3 Temperature sensitivity of tropical montane forest N 167

4.S1 Tropical forest cover extent, soil organic carbon (SOC), and MAP 168

4.S2 Georeferenced maps of sampling locations.....169

4.S3 Relationship between soil organic carbon (%)
and elevation across the transects 170

4.S4 Nonlinear relationship between bulk soil $\delta^{15}N$ and soil C:N. 171

4.S5 Elevational change in temperature across
tropical montane forests.....172

4.S6 Relationship between mean annual precipitation
(mm) and elevation. 173

4.S7 Relationships between soil $\delta^{15}N$ and N and mean annual
precipitation across the elevational transects.....174

4.S8 Changes in soil bulk density across the elevational transects.....175

4.S9 Observed vs. modeled data comparison
for $\delta^{15}N$ (‰) and N pools.. 176

4.S10 Observed versus SoilGrid 2.0 soil N.. 177

ABSTRACT

It is now unequivocal that the main driver of greenhouse gas (GHG) accumulation in Earth's atmosphere over the industrial era has been due to anthropogenic global change. Despite the recent and rapid rise in GHGs, global terrestrial ecosystems have slowed the rate of carbon dioxide accumulation in the atmosphere, and thus the rate of climate change, through the uptake and storage of carbon (C) in plant biomass and soil organic matter. However, the global cycles of C and nitrogen (N) are tightly coupled through primary production and the turnover of soil organic matter, highlighting a stoichiometric relationship that is critical to understanding the future stability and strength of the terrestrial C sink. Thus, our ability to understand the response of the terrestrial C sink to global change hinges on critical — but often overlooked — feedback with N cycling.

In this dissertation, I examine how different aspects of global change and land management practices are impacting the terrestrial C sink by evaluating interactions with the N cycle in both managed and natural ecosystems. I use observational and experimental methods to quantitatively assess C and N dynamics at plot, landscape, and global scales. I focus this work on crop- and range-lands of the Upper Missouri River Basin in the United States, and in equatorial mountain forests across the globe to address three overarching research questions:

1. What are the controls over the soil-atmosphere gas exchange of greenhouse gases, and how do they change in response to management and vegetation cover?
2. How do changes in plant community composition influence ecosystem C and N dynamics?
3. How is global change altering the stability and rate of C and N accumulation and storage?

CHAPTER ONE

INTRODUCTION

The cycling of carbon (C) and nitrogen (N) are of central importance to biosynthesis and the functioning of global ecosystems. C uptake by the terrestrial ecosystems is driven by photosynthetic primary production and is counterbalanced by ecosystem respiration, where C is released from plants, animals, and microbes as a metabolic byproduct. Together, these processes regulate atmospheric CO_2. For example, photosynthesis removes one-fifth of atmospheric C annually, which is ten times greater than anthropogenic fossil fuel emissions (T. F. Keenan & Williams, 2018; Le Quéré et al., 2018). While the processes of photosynthesis and respiration dominate the natural flow of C fluxes in and out of terrestrial ecosystems, they are fundamentally constrained by the ecosystem's nutrient status, namely the availability of N (Fay et al., 2015; Fernández-Martínez et al., 2014; Reed et al., 2011; Vicca et al., 2012). N constraint on C cycling is driven by the paradoxical fact that the largest pool of N on earth, atmospheric dinitrogen (N_2), is largely inaccessible to most organisms. Consequently, ecosystem development, organization and other functions are influenced by the limited availability of N. As such, C cycling is tightly coupled to N through biomass accumulation, decomposition, and storage (Asner et al., 1997; Vitousek & Howarth, 1991). Improving our understanding of how these dynamic processes will respond to anthropogenic global change and ongoing changes to the N cycle are paramount.

Human activity has drastically altered the C and N cycles (Vitousek et al., 1997). Through the combustion of fossil fuels and the advent of industrial fertilizer N production, the atmospheric concentration of greenhouse gases (GHG), including carbon dioxide

(CO_2), methane CH_4), and nitrous oxide (N_2O), has increased to levels unprecedented in recent evolutionary history and has led to substantial climate warming. This imbalance of terrestrial C and N has been further perturbed by large-scale human-driven land use and cover changes. For example, human appropriation of land for agriculture has led to large declines in soil C and increases in GHG emissions (Robertson & Vitousek, 2009; Sanderman et al., 2017). Moreover, human-driven changes in land cover, such as the expansion of woody plants (WPE) into grassland from fire suppression, alter the balance and location of ecosystem C and N storage. Consequently, WPE shifts the proportion of C and N from below to aboveground and causes ecosystem pools to be more vulnerable to atmospheric losses through fire. While not exhaustive, these examples highlight how human activity leads to GHG emissions and impacts the capacity of terrestrial ecosystems to absorb and store C (Friedlingstein et al., 2020; Graven et al., 2013). However, our process-based understanding of how these source-sink dynamics respond to change across temporal and spatial scales is still evolving. Furthermore, while global models capture the interannual dynamics of terrestrial C variability, their ability to predict site and ecosystem-specific terrestrial C responses to change is poor (T. F. Keenan et al., 2012; T. F. Keenan et al., 2016). Together, this suggests we need to focus research efforts on evaluating how ecosystem processes respond to change to improve our understanding of how human activity is altering source-sink C dynamics and potential feedback from N.

Despite the recent and rapid rise in anthropogenic GHG emissions, Earth's surfaces have demonstrated a large capacity to buffer current GHG emissions via uptake and storage, annually offsetting total anthropogenic emissions by ~30% (Friedlingstein et al.,

2020; Graven et al., 2013). Although the capacity of terrestrial ecosystems to store C is finite, terrestrial C storage represents a short-term but essential part of climate mitigation strategies (Matthews et al., 2022). Moreover, land management practices aimed at increasing terrestrial C have the potential to offset significant portions of anthropogenic emissions (Bossio et al., 2020; Griscom et al., 2017; Mackey et al., 2013). Despite this potential, land management practices aimed at decarbonization often fail to consider the cycling of N which can constrain C sequestration or lead to unintended consequences (Kicklighter et al., 2019; Lugato et al., 2018; van Groenigen et al., 2017). For example, climate mitigation practices that promote SOC sequestration (e.g. increasing fertilizer application) can be offset by increases in the N_2O emissions (Guenet et al., 2021 Lugato et al., 2018). Moreover, because the N cycle is highly sensitive to temperature and moisture, both of which are predicted to change under current climate models, understanding how the N cycle responds to global changes is imperative to understanding the trajectory of the terrestrial C sink due to the close coupling of both cycles (Bai et al., 2013; Firestone & Davidson, 1989; Gruber & Galloway, 2008).

This dissertation improves our understanding of how different aspects of global change alter fluxes of C and N across different ecosystems and spatial scales by addressing the following questions in the next three chapters:

1. What are the biophysical controls over the soil-atmosphere gas exchange of greenhouse gases, and how do they change in response to management and vegetation cover?

2. How do changes in plant community composition influence ecosystem C and N dynamics?
3. How will global change alter the stability and rate of C and N accumulation and storage?

To address these questions, I leverage two large geographic regions that contain ecosystems critical to global C and N cycling: 1) crop and rangelands in the Upper Missouri River Basin (UMRB) in North America's Northern Great Plains (NGP; ~800,000 km^2) and 2) high-elevation tropical montane forests across the globe (4.4 million km^2). In Chapter 1, I address the practical feasibility of a bioenergy and carbon capture and storage system (BECCS) in the semi-arid UMRB using a plot scale approach. I do this by investigating the productivity and potential biogeochemical tradeoffs of two perennial types of grass for bioenergy, switchgrass (*Panicum virgatum*; C4) and tall wheatgrass (*Thinopyrum ponticum*; C3), under dryland conditions. Specifically, I assess the biogeochemical tradeoffs by measuring soil C accumulation, GHG emissions, and above and belowground plant productivity throughout the three years during their establishment. This study also assesses the efficacy of a promising cyanobacteria biofertilizer (CBF) and its interactive effects on crop productivity. We find that the combination of a cool C3 perennial grass and CBF achieved high levels of productivity that rivaled that of synthetically fertilized bioenergy crops grown in warmer and wetter regions in the eastern UMRB, despite low soil fertility, modest N-fertilization application (50 kg N ha^{-1}), and no irrigation. Further, under C3 grasses, we document substantial gains in soil organic carbon over three years and observe consistent CH_4 uptake and low emissions of N_2O. Together, these findings

suggest that under the current climate conditions, C3 grasses offer a viable option for a BECCS climate mitigation strategy in the semi-arid regions of the UMRB.

In Chapter 2, I assess how prescribed fire influences the biogeochemistry of a temperate grassland in the NGP that is currently undergoing notable land-cover change resulting from woody plant expansion (WPE) of two conifer species (*P. ponderosa* and *J. scopulorum*). Specifically, I investigate the cumulative effects of WPE and prescribed fire, on short and long-term C and N fluxes by establishing 20 field plots across a grass-woody cover gradient and using pre/post/control experimental design. I then combine remote sensing, field measurements, and dendrochronology to estimate long-term trends in woody C accumulation, quantify fire-driven changes in soil chemistry, and estimate C and N emission loss from the consumed biomass across the woody gradient. We find that woody aboveground biomass-C has accumulated at 0.75 Mg C ha^{-1} since the 1950s. Following a low to medium severity fire prescribed by the Bureau of Land Management, we document large N emissions losses that were influenced by the combustion of the different woody species. Juniper mortality was much higher than ponderosa, and their combustion led to outsized N emission losses due to their higher foliar to woody ratio, greater %N concentration, and flammability compared to ponderosa. C losses were equal between both species, despite the greater Juniper mortality (21% vs. 90%). These findings support the notion that WPE is drastically altering grassland ecosystem structure and biogeochemical functioning and that the combustion of individual conifer species drives large N losses. However, transformations in the C and N content of soil organic matter N and C from the incomplete combustion of vegetation material offset emission losses via an increase in the

highly stable and chemically recalcitrant pyrogenic form of soil carbon (PyC). In total, the increases in soil C and N buffered emission losses by 29% and 35%, with 6% of the C offset in the form of PyC. Taken together, these findings have important implications for long-term C and N cycling in grasslands experiencing WPE. First, while WPE increases fire severity in grasslands, it also produces a small but highly stable amount of PyC that will accumulate in soil over time with each subsequent low-severity fire. Secondly, although the effects of thermally altered vegetative biomass on soil organic matter dynamics after fire are poorly understood, there is evidence that it could slow soil organic matter turnover rates based on the increased recalcitrance and inaccessibility of the PyC fraction to microbes.

In Chapter 3, I conduct a global meta-analysis of soil N measures (%N and $\delta^{15}N$) to address how climate warming might affect tropical forest N cycling and C storage by leveraging tropical mountain elevational gradients as "natural laboratories" to investigate climate-ecosystem interactions. I find a global pattern of higher N accumulation in montane compared to lowland forests and determine that this pattern is driven mainly by temperature constraints on microbially-driven N soil processes such as mineralization and denitrification. Though the tropical montane forests' tropical global footprint is small (~11% of the forested tropical area), N pools are two-fold larger than the previous estimate and account for > 16% of the tropical forest N pool. Together, these findings indicate a high temperature sensitivity of the tropical montane soil N pool and raise critical questions about the future trajectory and stability of the soil N and C pools in these rapidly warming ecosystems.

Figures

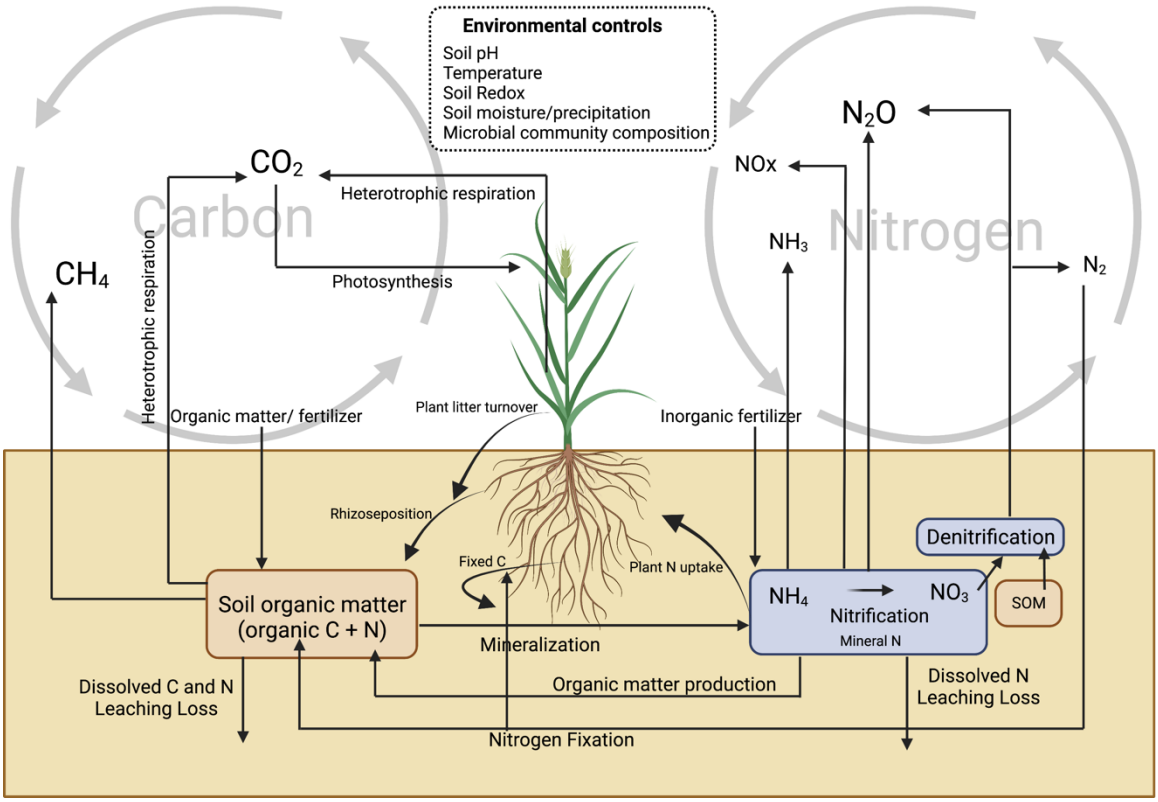


Figure 1. Conceptual model of the coupled interactions between carbon (C) and nitrogen (N) in an agricultural system. It is important to note that many of these interactions are mediated by microorganisms (mineralization, denitrification, nitrification, nitrogen fixation, decomposition of litter and rhizodeposits, methane production). Figure adapted from Guenet et al. 2020 and made in biorender.

References Cited

Asner, G. P., Seastedt, T. R., & Townsend, A. R. (1997). The Decoupling of Terrestrial Carbon and Nitrogen Cycles. *BioScience*, *47*(4), 226–234. JSTOR. https://doi.org/10.2307/1313076

Bai, E., Li, S., Xu, W., Li, W., Dai, W., & Jiang, P. (2013). A meta-analysis of experimental warming effects on terrestrial nitrogen pools and dynamics. *New Phytologist*, *199*(2), 441–451. https://doi.org/10.1111/nph.12252

Bossio, D. A., Cook-Patton, S. C., Ellis, P. W., Fargione, J., Sanderman, J., Smith, P., Wood, S., Zomer, R. J., von Unger, M., Emmer, I. M., & Griscom, B. W. (2020). The role of soil carbon in natural climate solutions. *Nature Sustainability*, 1–8. https://doi.org/10.1038/s41893-020-0491-z

Fay, P. A., Prober, S. M., Harpole, W. S., Knops, J. M. H., Bakker, J. D., Borer, E. T., Lind, E. M., MacDougall, A. S., Seabloom, E. W., Wragg, P. D., Adler, P. B., Blumenthal, D. M., Buckley, Y. M., Chu, C., Cleland, E. E., Collins, S. L., Davies, K. F., Du, G., Feng, X., … Yang, L. H. (2015). Grassland productivity limited by multiple nutrients. *Nature Plants*, *1*(7), 1–5. https://doi.org/10.1038/nplants.2015.80

Fernández-Martínez, M., Vicca, S., Janssens, I. A., Sardans, J., Luyssaert, S., Campioli, M., Chapin III, F. S., Ciais, P., Malhi, Y., Obersteiner, M., Papale, D., Piao, S. L., Reichstein, M., Rodà, F., & Peñuelas, J. (2014). Nutrient availability as the key regulator of global forest carbon balance. *Nature Climate Change*, *4*(6), 471–476. https://doi.org/10.1038/nclimate2177

Firestone, M., & Davidson, E. (1989). Microbiological Basis of NO and N2O Production and Consumption in Soil. *Exchange of Trace Gases between Terrestrial Ecosystems and the Atmosphere, 47*.

Friedlingstein, P., O'Sullivan, M., Jones, M. W., Andrew, R. M., Hauck, J., Olsen, A., Peters, G. P., Peters, W., Pongratz, J., Sitch, S., Le Quéré, C., Canadell, J. G., Ciais, P., Jackson, R. B., Alin, S., Aragão, L. E. O. C., Arneth, A., Arora, V., Bates, N. R., … Zaehle, S. (2020). *Global Carbon Budget 2020* [Preprint]. Data, Algorithms, and Models. https://doi.org/10.5194/essd-2020-286

Graven, H. D., Keeling, R. F., Piper, S. C., Patra, P. K., Stephens, B. B., Wofsy, S. C., Welp, L. R., Sweeney, C., Tans, P. P., Kelley, J. J., Daube, B. C., Kort, E. A., Santoni, G. W., & Bent, J. D. (2013). Enhanced Seasonal Exchange of CO2 by

Northern Ecosystems Since 1960. *Science*, *341*(6150), 1085–1089. https://doi.org/10.1126/science.1239207

Griscom, B. W., Adams, J., Ellis, P. W., Houghton, R. A., Lomax, G., Miteva, D. A., Schlesinger, W. H., Shoch, D., Siikamäki, J. V., Smith, P., Woodbury, P., Zganjar, C., Blackman, A., Campari, J., Conant, R. T., Delgado, C., Elias, P., Gopalakrishna, T., Hamsik, M. R., … Fargione, J. (2017). Natural climate solutions. *Proceedings of the National Academy of Sciences*, *114*(44), 11645–11650. https://doi.org/10.1073/pnas.1710465114

Gruber, N., & Galloway, J. N. (2008). An Earth-system perspective of the global nitrogen cycle. *Nature*, *451*(7176), 293–296. https://doi.org/10.1038/nature06592

Guenet, B., Gabrielle, B., Chenu, C., Arrouays, D., Balesdent, J., Bernoux, M., Bruni, E., Caliman, J.-P., Cardinael, R., Chen, S., Ciais, P., Desbois, D., Fouche, J., Frank, S., Henault, C., Lugato, E., Naipal, V., Nesme, T., Obersteiner, M., … Zhou, F. (2021). Can N2O emissions offset the benefits from soil organic carbon storage? *Global Change Biology*, *27*(2), 237–256. https://doi.org/10.1111/gcb.15342

Keenan, T. f., Baker, I., Barr, A., Ciais, P., Davis, K., Dietze, M., Dragoni, D., Gough, C. M., Grant, R., Hollinger, D., Hufkens, K., Poulter, B., McCaughey, H., Raczka, B., Ryu, Y., Schaefer, K., Tian, H., Verbeeck, H., Zhao, M., & Richardson, A. D. (2012). Terrestrial biosphere model performance for inter-annual variability of land-atmosphere CO2 exchange. *Global Change Biology*, *18*(6), 1971–1987. https://doi.org/10.1111/j.1365-2486.2012.02678.x

Keenan, T. F., Prentice, I. C., Canadell, J. G., Williams, C. A., Wang, H., Raupach, M., & Collatz, G. J. (2016). Recent pause in the growth rate of atmospheric CO 2 due to enhanced terrestrial carbon uptake. *Nature Communications*, *7*(1), 1–10. https://doi.org/10.1038/ncomms13428

Keenan, T. F., & Williams, C. A. (2018). The Terrestrial Carbon Sink. *Annual Review of Environment and Resources*, *43*(1), 219–243. https://doi.org/10.1146/annurev-environ-102017-030204

Kicklighter, D. W., Melillo, J. M., Monier, E., Sokolov, A. P., & Zhuang, Q. (2019). Future nitrogen availability and its effect on carbon sequestration in Northern Eurasia. *Nature Communications*, *10*(1), 3024. https://doi.org/10.1038/s41467-019-10944-0

Le Quéré, C., Andrew, R. M., Friedlingstein, P., Sitch, S., Pongratz, J., Manning, A. C., Korsbakken, J. I., Peters, G. P., Canadell, J. G., Jackson, R. B., Boden, T. A., Tans,

P. P., Andrews, O. D., Arora, V. K., Bakker, D. C. E., Barbero, L., Becker, M., Betts, R. A., Bopp, L., … Zhu, D. (2018). Global Carbon Budget 2017. *Earth System Science Data*, *10*(1), 405–448. https://doi.org/10.5194/essd-10-405-2018

Lugato, E., Leip, A., & Jones, A. (2018). Mitigation potential of soil carbon management overestimated by neglecting N 2 O emissions. *Nature Climate Change*, *8*(3), 219–223. https://doi.org/10.1038/s41558-018-0087-z

Mackey, B., Prentice, I. C., Steffen, W., House, J. I., Lindenmayer, D., Keith, H., & Berry, S. (2013). Untangling the confusion around land carbon science and climate change mitigation policy. *Nature Climate Change*, *3*(6), 552–557. https://doi.org/10.1038/nclimate1804

Matthews, H. D., Zickfeld, K., Dickau, M., MacIsaac, A. J., Mathesius, S., Nzotungicimpaye, C.-M., & Luers, A. (2022). Temporary nature-based carbon removal can lower peak warming in a well-below 2 °C scenario. *Communications Earth & Environment*, *3*(1), 1–8. https://doi.org/10.1038/s43247-022-00391-z

Odum, E. P. (1964). The New Ecology. *BioScience*, *14*(7), 14–16. https://doi.org/10.2307/1293228

Reed, S. C., Vitousek, P. M., & Cleveland, C. C. (2011). Are patterns in nutrient limitation belowground consistent with those aboveground: Results from a 4 million year chronosequence. *Biogeochemistry*, *106*(3), 323–336. https://doi.org/10.1007/s10533-010-9522-6

Robertson, G. P., & Vitousek, P. M. (2009). Nitrogen in Agriculture: Balancing the Cost of an Essential Resource. *Annual Review of Environment and Resources*, *34*(1), 97–125. https://doi.org/10.1146/annurev.environ.032108.105046

Sanderman, J., Hengl, T., & Fiske, G. J. (2017). Soil carbon debt of 12,000 years of human land use. *Proceedings of the National Academy of Sciences*, *114*(36), 9575–9580. https://doi.org/10.1073/pnas.1706103114

van Groenigen, J. W., van Kessel, C., Hungate, B. A., Oenema, O., Powlson, D. S., & van Groenigen, K. J. (2017). Sequestering Soil Organic Carbon: A Nitrogen Dilemma. *Environ. Sci. Technol.*, 2.

Vicca, S., Luyssaert, S., Peñuelas, J., Campioli, M., Chapin III, F. S., Ciais, P., Heinemeyer, A., Högberg, P., Kutsch, W. L., Law, B. E., Malhi, Y., Papale, D., Piao, S. L., Reichstein, M., Schulze, E. D., & Janssens, I. A. (2012). Fertile forests

produce biomass more efficiently. *Ecology Letters*, *15*(6), 520–526. https://doi.org/10.1111/j.1461-0248.2012.01775.x

Vitousek, P. M., & Howarth, R. W. (1991). Nitrogen limitation on land and in the sea: How can it occur? *Biogeochemistry*, *13*(2), 87–115. https://doi.org/10.1007/BF00002772

Vitousek, P. M., Mooney, H. A., Lubchenco, J., & Melillo, J. M. (1997). Human Domination of Earth's Ecosystems. *Science*, *277*(5325), 494–499. https://doi.org/10.1126/science.277.5325.494

CHAPTER TWO

THE CLIMATE MITIGATION POTENTIAL AND SOIL MICROBIAL RESPONSE OF CYANOBACTERIA-FERTILIZED BIOENERGY CROPS IN A COOL SEMI-ARID CROPLAND

Contribution of Authors and Co-Authors

Manuscript in Chapter 2

Author: Justin D. Gay
Contributions: Contributed to experimental design, conducted the field measurements, collected and processed field samples, analyzed and interpreted the data, and wrote the manuscript

Co-Author: Hannah Goemann
Contributions: Contributed to experimental design, conducted the field measurements, collected processed field samples; processed analyzed the microbial data, created microbial figures, and revised the manuscript

Co-Author: Bryce Currey
Contributions: Collected and processed field samples, assisted in analyzing the flux data, and revised the manuscript

Co-Author: Paul Stoy
Contributions: Conceived aspects of the project, obtained funding for Picarro gas analyzer, assisted in data interpretation, and revised the manuscript

Co-Author: Jesper Christiansen
Contributions: Assisted with flux data analysis and interpretation and revised the manuscript

Co-Author: Perry Miller
Contributions: Conceived agronomic aspects of the project, contributed to experimental design managed, agronomic field operations, and revised the manuscript

Co-Author: Ben Poulter
Contributions: Conceived the project, obtained funding, and revised the manuscript

Co-Author: Brent Peyton
Contributions: Conceived the biofertilizer aspect of the project, obtained funding, and revised the manuscript

Co-Author: Jack Brookshire
Contributions: Conceived biogeochemical aspects of the project, obtained funding for the Picarro gas analyzer, contributed to experimental design, assisted in data analysis and interpretation, and revised the manuscript

Manuscript Information

Justin D. Gay[1], HM Goemann[2,3], B Currey[1], PC Stoy[4], JR Christiansen[5], P Miller[1], B Poulter[6], BM Peyton[2,3], ENJ Brookshire[1]

Submitted to Global Change Biology: Bioenergy
April, 27th 2022

Status of Manuscript:
___ Prepared for submission to a peer-reviewed journal
__X_ Officially submitted to a peer-reviewed journal
____ Accepted by a peer-reviewed journal
____ Published in a peer-reviewed journal

Wiley

15

THE CLIMATE MITIGATION POTENTIAL AND SOIL MICROBIAL RESPONSE OF CYANOBACTERIA FERTILIZED BIOENERGY CROPS IN SEMI-ARID CROPLAND

Justin D. Gay[1], HM Goemann[2,3], B Currey[1], PC Stoy[4], JR Christiansen[5], P Miller[1], B Poulter[6], BM Peyton[2,3], ENJ Brookshire[1]

[1]Department of Land Resources and Environmental Science, Montana State University, Bozeman, MT 59715.

[2]Department of Microbiology and Cell Biology, Montana State University, Bozeman, MT 59715

[3]Center for Biofilm and Engineering, Bozeman, MT 59715

[4]Department of Biological Systems Engineering, University of Wisconsin – Madison, Madison, WI 53706

[5] Department of Geoscience and Natural Resource Management, University of Copenhagen, Copenhagen, Denmark

[6]NASA Goddard Space Flight Center, Earth Sciences Division, Biospheric Sciences Lab., Greenbelt, MD 20771

Running header: Response of GHG flux and soil microbiome to cyanobacteria-fertilized bioenergy crops

Keywords: Soil Carbon, Second Generation BECCS, Greenhouse Gas Flux, Perennial Grasses, Cyanobacteria, Microbiome

Abstract

Bioenergy carbon capture and storage (BECCS) systems can serve as decarbonization pathways for climate mitigation. Perennial grasses are a promising second-generation lignocellulosic bioenergy feedstock applicable to BECCS, but optimizing their sustainability, productivity, and climate mitigation potential requires an evaluation of their greenhouse gas (GHG) dynamics and nitrogen (N) fertilizer strategies. Land-use transitions to bioenergy cropping systems and crop-soil feedbacks from N-fertilization can lead to negative consequences including increased emissions of GHGs and loss of soil organic carbon (SOC). Soil microbiome dynamics play a role in possible environmental tradeoffs with productivity, but these are poorly understood due to the paucity of data from agroecosystems. Here, we examine the climate mitigation potential and soil microbiome response to establishing two perennial grasses, tall wheatgrass (*Thinopyrum ponticum*; C3), and switchgrass (*Panicum virgatum*; C4), in a semi-arid agroecosystem under two fertilizer applications, a novel cyanobacterial biofertilizer (CBF) and urea. Finally, we examine shifts in soil microbial composition resulting from crop establishment and fertilizer regime. In contrast to the C4 crop, the C3 crop achieved 98% greater productivity when fertilized and CBF produced the same biomass enhancement as urea. Non-CO_2 greenhouse gas fluxes across all treatments were low. We observed a three-year loss of SOC under the C4 crop and an increase under the C3 crop at a 0-30 cm soil depth. However, patterns of SOC change were partitioned by soil depth with accumulation occurring at 15-30 cm and loss at 0-15 cm. We detected crop-specific changes in the soil microbiome, including an increased relative abundance of arbuscular mycorrhizal fungi under the C3, and of pathogenic fungi

in the C4 grass. Taken together, these findings highlight the potential of CBF-fertilized C3 crops as a second-generation bioenergy feedstock in semiarid regions as a part of a climate mitigation strategy.

Introduction

Developing sustainable bioenergy and carbon capture systems (BECCS) is a critical component of global climate change mitigation (IPCC), but the environmental implications have yet to be thoroughly examined at field scales. The overarching aims of productive and sustainable second-generation bioenergy cropping systems are to 1) reduce land-use conflict with food production, 2) maximize above and belowground biomass production, 3) increase soil organic carbon (SOC) accumulation, 4) limit greenhouse gas (GHG) emissions, namely nitrous oxide (N_2O), and 5) cultivate soil health and a beneficial microbiome (Robertson et al., 2017; U.S DOE, 2014). Together, these goals support the notion that sustainable bioenergy systems – and their mitigation potential – largely hinge on understanding how these systems affect the C and N cycles of agroecosystems (Robertson et al., 2011). Given geographic variations in soil and climate, it is necessary to identify bioenergy crop species and fertilizer regimes that maximize crop yield while minimizing negative environmental impacts, including GHG emissions (ex. CH_4, CO_2, N_2O) and loss of soil organic carbon (SOC). One promising bioenergy cropping system pairs second-generation lignocellulosic perennial grass with cyanobacteria-based N-biofertilizer in semi-arid climates (Goemann et al., 2021.; Stoy et al., 2018). However, the

interactions between C and N cycling, and the potential tradeoffs between biomass production and environmental impacts have yet to be evaluated.

Semi-arid ecosystems cover 45% of the earth's land surface and are critical reservoirs for carbon sequestration (Lal, 2009; Poulter et al., 2014); however, these ecosystems often contain vast tracts of marginal land unsuitable for traditional cultivation due to environmental constraints over crop production from factors such as low precipitation and soil organic carbon content. It is unclear how BECCS expansion would influence ecosystem C, especially in response to different N fertilization regimes (Dolan et al., 2020). The Upper Missouri River Basin (UMRB) is a promising candidate region that serves as a model system for evaluating BECCS in semi-arid regions (Baik et al., 2018; Stoy et al., 2018). The UMRB spans ~800,000 km^2 across Montana, Wyoming, North and South Dakota and has over ~150,000 km^2 of land that classifies as marginal (Dolan et al., 2020). Large sections of the UMRB are connected with an existing network of infrastructure to transport feedstock and captured CO_2, and importantly, perennial grass feedstock has shown potential to be economically profitable for producers (Baik et al., 2018; Hanson et al., 2020). Furthermore, semi-arid regions can have a high capacity as a soil C sink, based on slow decomposition rates, and low SOC saturation levels (Lal, 2009; Sanderman et al., 2017). Yet, only one study in the western UMRB has reported empirical data on soil and gas C and N dynamics in a dedicated bioenergy study, and only for switchgrass (*Panicum virgatum*) (Schmer et al., 2012). Schemer et al. (2012) reported aboveground production of 6.8 Mg dry matter ha^{-1} and found that the global warming potential (GWP) was largely driven by CO_2 fluxes despite N_2O emissions with modest

fertilization rates (67 kg N ha^{-1}) and a late-season CH_4 pulse. A recent regional modeling study across the entire UMRB found that switchgrass expansion, and associated management practices, led to net losses of vegetation and soil C (Dolan et al., 2020), but was not parameterized with other potential bioenergy species that are likely to have different outcomes. These findings highlight the importance of understanding the constraints on bioenergy crop productivity in the harsher growing conditions in the western UMRB, a fundamental uncertainty in assessing regional BECCS viability (Fajardy & Dowell, 2017).

A critical aspect of developing a BECCS system is identifying crop species that are well-adapted to the regional climate and soil, achieve high levels of above- and below-ground biomass production, and have traits (e.g., biomass chemical composition) that support the efficient transfer of biomass-C to stable SOC (Carvalho et al., 2017; Córdova et al., 2018a). Perennial grasses have been widely identified as an environmentally advantageous functional plant group in bioenergy systems due to their low nutrient and irrigation requirements and ability to limit net GHG losses from soils and leaching losses of fertilizer-N (Robertson et al., 2000, Fargione et al., 2008, Abraha et al., 2019; Ledo et al., 2020). SOC accumulation in perennial grass systems depends primarily on inputs from root biomass as most of the aboveground biomass-C is annually removed. (Sainju et al., 2017). C4 perennial grasses (e.g., switchgrass (*Panicum virgatum*) and miscanthus (*Miscanthus giganteus*) are the most extensively studied based on agronomically important traits (e.g. rooting depth, yield potential, N and water use efficiency; Heaton et al., 2004). C4 grasses are generally thought to be more water-use efficient, but their productivity is

strongly limited by extended periods of cold temperatures and, therefore, may have reduced growth in cold semi-arid regions (Epstein et al., 1997; Monson et al., 1983; Paruelo & Lauenroth, 1996). Comparatively, C3 species may be better matched to the current climate of the western UMRB given they have greater cold tolerance and the ability to maximize photosynthetic capacity during the cool, moist spring growth period. There is also some evidence that C3 plants hold a competitive advantage in their ability to acquire N in semi-arid climates (Luo et al., 2018). To our knowledge, only one other study directly compared C3 versus C4 establishment and productivity in the UMRB but was conducted in central and eastern North Dakota (G.-J. Wang et al., 2014). Taken together, C3 perennial grasses may provide greater potential as bioenergy feedstocks than C4 in the semi-arid regions of the UMRB (Karp & Shield, 2008).

Fertilizer selection and management are at the core of agronomic sustainability and are critical for supporting BECCS feedstock production. Nitrogen is often the most limiting nutrient for plant productivity in agricultural systems (Burgess et al., 2012; Piringer & Steinberg, 2006)and the efficient application and retention of N fertilizer are essential for balancing crop production and minimizing N loss (Lai et al., 2018; Robertson & Vitousek, 2009). However, this balance is difficult to accomplish; fertilizer management decisions aimed at maximizing biomass production rarely account for environmental externalities such as SOC loss (Stewart et al., 2016), increased GHG emissions (Guenet et al., 2021; Lugato et al., 2018), and degradation of soil health (Robertson & Vitousek 2009). Across much of the UMRB, synthetically produced urea is the principal form in which N is applied to crops, and its mismanagement has resulted in sizeable reactive N losses (e.g., ammonia

volatilization, nitrate leaching) from the plant-soil system (R. Engel et al., 2011; John et al., 2017). Cyanobacteria-based biofertilizer (CBF) is an organic, microbial-based N-fertilizer that has the potential to replace petroleum-based fertilizer in perennial bioenergy systems (Goemann et al., 2021).5/6/22 1:48:00 PM Across field and greenhouse studies, CBF has shown the ability to promote SOC accumulation, increase nutrient availability, and increase soil N retention while maintaining crop productivity comparable to a urea fertilizer (Alvarez et al., 2021; Goemann et al., 2021). However, no study has evaluated CBF application over multiple seasons at the field scale, including its impact on soil GHG emissions and the soil microbiome (Alvarez et al., 2021; Castro et al., 2017).

The cultivation of a beneficial soil microbiome is an emerging management strategy to enhance the sustainable production of bioenergy biomass, especially in challenging environments such as marginal lands (Zhalnina et al., 2021). Feedbacks between crop species, fertilizer management, and soil type have been shown to benefit soil microbial community structure in bioenergy systems (Kasanke et al., 2021; Leichty et al., 2021; Revillini et al., 2019). Documented examples of beneficial plant-microbe interactions in agricultural settings include increases in yield via nutrient acquisition through arbuscular mycorrhizal fungi colonization (AMF; 5/6/22 1:48:00 PM , the alleviation of abiotic stresses (e.g. drought), pathogenic protection, and enhanced C sequestration (Mendes et al., 2011, Sher et al., 2020). However, mechanisms for these feedbacks remain poorly constrained, and further field-based research is needed on how soil microbial communities respond to crop and fertilizer interactions in sustainable agricultural operations (Lekberg & Helgason, 2018; Rillig et al., 2016). Plant-microbe

interactions are key for achieving climate mitigation goals as microbes perform specialist functions important in N loss pathway processes (e.g. N_2O production and nitrification) and more generalist functions such as C mineralization and the subsequent CO_2 release (heterotrophic respiration). Furthermore, microbial necromass and fungal hyphae networks are critical components in forming persistent SOM (Kallenbach et al., 2015; Six et al., 2006). To optimize these beneficial plant-microbe interactions, field-based studies are necessary to accurately quantify the magnitude and direction of microbial community shifts and examine their role in trade-offs between production-climate mitigation.

In a recent geospatial analysis, Baik et al. (2018) identified large portions of the UMRB as priority areas for deployment of BECCS in the USA. However, field-based studies assessing the potential of BECCS in the UMRB have yet to be conducted. To address this gap, we evaluate the production and environmental tradeoffs of two perennial types of grass, switchgrass (C4) and tall wheatgrass (*Thinopyrum ponticum*; C3), and compare the efficacy of a novel cyanobacteria based biofertilizer to a conventionally used urea fertilizer. Our objectives were to 1) quantify above and belowground biomass production, 2) quantify changes in SOC stocks to 30 cm, 3) assess growing season GHG flux of CO_2, CH_4, and N_2O, and 4) characterize shifts in soil microbial composition for crop and fertilizer treatments.

Methods

Site description and experimental design

The study site is located at Montana State University's (MSU) Arthur H. Post Farm in Bozeman, Montana (45.66 N, -111.15 W) at 1450 meters above sea level. Mean annual

temperature is 6.5 °C and mean annual precipitation is 408 mm yr^{-1}, most of which falls during the Spring (Miller & Holmes, 2012). Field soils at the Post Farm are classified as Amsterdam silt loam, a fine-silty, mixed, superactive, frigid Typic Haplustoll. The plot locations have low background soil fertility (SOC 1 % ± 0.03, total nitrogen (TN) 0.11% ± 0.03; Oldfield et al., 2019) and no irrigation. The study was established in a complete randomized split-plot (3.34 m^2) design with five replicates of switchgrass (Dakotah variety) and tall wheatgrass (Alkar variety). Switchgrass is a well-studied C4 species favored for second generation bioenergy production because of its chemical composition for post-processing, high ethanol yield, and significant biomass potential (Wright & Turhollow, 2010). Conversely, tall wheatgrass is a less characterized C_3 species (Martyniak et al., 2017), but has been shown to have an optimal chemical composition for efficient combustion (Xue et al., 2011), and is relatively salt-tolerant (Bleby et al., 1997). The experimental design, agronomic management, and initial soil sampling are described in detail in Goemann et al. (2021).

Growing degree days, rain use efficiency, and soil pH

Growing degree days were used to evaluate the effect of temperature on plant-specific growth rates and were calculated for each crop by subtracting the base temperature (tall wheatgrass = 0 °C, switchgrass = 10 °C; Miller et al. 2018, Clifton-Brown et al. 2011) from the daily mean temperature measured at the Post Farm in Bozeman, MT where the base temperature is defined as the lower developmental threshold of each species. Rain use efficiency (RUE) is measured as crop production per unit rainfall (kg dry matter ha^{-1} mm^{-}

^{1}) across the agricultural year (Le Houérou, 1984). Here, the agricultural year for calculating RUE was October 2019 to August 2020, as this encompasses the groundwater recharge period from the previous fall and precipitation during the primary growing season months of 2020. Soil pH was measured in the lab on air-dried soil from 0-15 cm and 15-30 cm soil depths and analyzed using a 2:1 Milli-q deionized water to soil solution and glass electrode.

Fertilization

The CBF utilized was a mixture of live *Nostoc sp.* isolated from soil directly adjacent to the field plots, and commercially available dried *Spirulina.* Due to limitations on culturing capacity, we used 20:80 Nostoc:Spirulina ratio to meet the N fertilization goal. The *Nostoc sp*. was isolated by culturing a slurry of field moist soil in BG-11_0 (nitrogen-free) media and plating the slurry on sterile petri plates of BG-11_0 agar. Repeated streaking was conducted until visual isolation of a single morphology was evident via light microscopy at which point the culture was scaled up into increasingly larger volumes of sterile liquid media. CBF cultivation was conducted as described in Goemann et al. 2021. Urea was hand-spread across the plots while the CBF was applied as a slurry from a backpack sprayer and was applied either directly before or after precipitation events to increase fertilizer-N infiltration into the soil. In 2018, 100 kg ha^{-1} of fertilizer-N was applied to maximize the harvestable yield of barley (*Hordeum vulgare*, Hayse forage variety) as an intercrop. During the subsequent two growing seasons (2019 and 2020), 50 kg N ha^{-1} of urea and CBF were applied equally across the spring months due to

production constraints of CBF. In total there were 5 replicate plots of urea, CBF, and unfertilized treatments. In 2020 plots were fertilized over three application periods May 13th, May 27th, and June 5th. After the first year, the fertilization rate was reduced from 100 kg N ha^{-1} to 50 kg N ha^{-1} to reduce potentially negative environmental effects (Lai et al., 2018).

Soil and sampling and analysis

Pre-treatment soil samples were collected before seeding in April 2018, and soils were resampled at the end of the growing season in September 2020 to assess the three-year change in SOC. In September 2020, three fixed depth soil cores (1.9 cm diameter) were taken from each plot (n = 45) and divided into 0-5 cm, 5-15 cm, and 15-30 cm depth increments, and then composited by depth for chemical and microbial analysis. In each plot, two cores were taken, one in close proximity to the base of a plant, and one was taken from an inter-row area to capture plot heterogeneity. Since baseline soil samples were only collected at 0-15 cm and 15-30 cm depths in 2018, a weighted average was calculated for the 2020 samples at the 0-15 cm depth. Before chemical analyses, soil samples were oven-dried at 40 °C for 48 hours before being sieved at 2 mm and then milled in a slow-rolling jar tumbler for 12 hr. Prior to combustion, for SOC and TN quantification, samples were acidified using 1 M and then 2 M HCl to remove the inorganic C fraction. After 48 hours, %SOC and %TN were determined via dry combustion using an ESC 4010 elemental analyzer (Costech, Valencia, CA, USA) at MSU's Environmental Analytical Laboratory. Duplicates were run for ~10% of the samples to determine analytical precision. Bulk

density was quantified using a slide hammer to reduce soil compaction by taking soil cores (5 cm diameter) at 0-15 cm and 15-30 cm adjacent to each replicate row in 2019 (n = 10; Supplemental Figure 1). Cores were then composited by depth before drying at 105 °C to a constant mass. All bulk density cores were sieved at 2 mm to be rock-free. Bulk densities of 1.28 g cm^3 at the 0-15 cm soil depth and 1.23 g cm^3 at the 15-30 cm depth were calculated and used to calculate SOC pools from 2018 and 2020.

Above and belowground productivity and biomass chemistry

Harvestable aboveground biomass (AGB) was estimated by hand-harvesting a 1 m × 1 m section 10 cm above the ground from the center of each plot on September 9th, 2020. We acknowledge that this method underestimates total annual net primary productivity because of the exclusion of the plant stubble; other estimates from tall wheatgrass plots at the Post Farm suggest this may underestimate total AGB by approximately 15% such that our measurements are a conservative estimate of AGB. AGB samples were air-dried at 40 °C until they reached a constant mass and milled to a fine powder. To assess cumulative belowground root biomass accumulation, we collected two soil cores from each plot by first clearing litter material and then using a root auger (7.5 cm diameter) to collect a 15 cm deep soil core. To calculate the mean annual production of belowground biomass, we divided the total biomass of each plot by the three years since crop establishment. Since the majority of perennial grass root biomass is usually concentrated in the surface soil layer we used 0-15 cm as a root coring depth (L. Wang et al., 2015). In total, three out of the five reps from both bioenergy crops (n = 24) were used to collect soil root cores. After

collection, root-soil cores were gently rinsed underwater in a fine-mesh sieve until all soil was removed. Retained root material was then oven-dried at 40 °C until it reached a constant dry mass before being hand-milled to a fine powder. Total C and N concentrations for all AGB and belowground biomass (BGB) samples were determined by dry combustion on a Truspec CN analyzer (LECO, St Joseph, MI, USA) at MSU. C: N ratios reported are reported by mass.

GHG flux collection

GHG fluxes (CO_2, CH_4, and N_2O) were measured over the 2020 growing season (March-October) using the closed static chamber technique. Gas measurements were taken via a portable cavity ring down spectroscopy (CRDS) gas analyzer (G2508, Picarro Inc., Santa Clara, CA, USA) that allowed for short enclosure times via its high sampling frequency and low detection limits. Dry mole fractions of CO_2, CH_4, and N_2O are reported to account for the cross-influence of H_2O during sampling. Capturing soil gas flux spatial and temporal heterogeneity are two challenging aspects of assessing ecosystem C and N dynamics. As such, sampling times and dates were scheduled to capture a range of field conditions and specific events such as fertilizer application, heavy rainfall, and freeze-thaw cycles. Measurements were made over 24 separate sampling dates from March-October 2020 for a total of 204 individual chamber measurements and were made to pair crops as closely together as possible, usually a day apart. Sampling time took approximately two hours per day and was started close to 10:00 local standard time but never exceeded 15:30 to best represent daytime flux means (Jian et al., 2018).

Collars were inserted to a 5 cm depth in early March 2020 (1 per plot) and left in place for the growing season to minimize effects of soil disturbance. Collars were installed to include a single plant from each plot, and each plant was trimmed to ensure a tight seal when the chamber was attached. Plants were trimmed for sampling throughout the growing season. During each sampling event, fluxes were measured in three out of the five replicates, and the sequence by which the plots were measured was randomized each sampling day to avoid bias. Flux measurements were made by connecting the gas analyzer via 2 m Teflon tubing to a vented and opaque polyvinyl chloride (PVC) chamber attached to a PVC collar inserted in the soil. Together the chamber and collar have a diameter of 0.032 m^2 and volume of 4.86 L. Chamber caps were left on the collar for 5 minutes and gas concentrations were measured automatically every 2 seconds, and data output was recorded in ppmv. The chamber lid was flushed via sweeping through the air three times or until a stable atmospheric baseline was met between sampling each plot. Soil temperatures were recorded with a digital thermometer for each chamber measurement and collected from a shaded location directly outside the PVC collar at a 5 cm depth. During each GHG flux measurement, small soil cores (2.5 cm diameter) to a 5 cm soil depth were collected from directly outside the collar, placed in an airtight bag, and transported back to the lab to determine water-filled pore space (WFPS). WFPS was calculated via its gravimetric soil water content after drying soil samples at 105 °C for at least 24 hours and adjusted for bulk density and soil porosity (Supplemental Methods).

Flux calculations

Fluxes were calculated from the slope of the linear increase in CO_2, N_2O, or CH_4 concentrations inside the PVC chamber over a 5-minute interval:

$$F = S\frac{V}{A \times R \times (273.15 + T)} \times 3600 \qquad (1.)$$

where S is the linear slope of the concentration versus time relationship (ppm s^{-1}), V is the volume of the chamber in liters, A is the area of the chamber in m^2, and R is the universal gas constant in L kPa K^{-1} mol^{-1} (Christiansen et al., 2015). N_2O and CH_4 fluxes are denoted as μmol m^{-2} hr^{-1} while CO_2 fluxes are μmol m^{-2} s^{-1}. Minimum detectable fluxes (MDF's) were calculated for each gas and the specific chamber dimensions by using the relationship between the analytical accuracy (Aa; ppm) of the G2508 (0.6 ppm, 0.01 ppm, 0.025 ppm for CO_2, CH_4, and N_2O, respectively), chamber volume (V; m^3), atmospheric partial pressure (P; Pa), ideal gas constant (R; m^3 Pa K^{-1} mol^{-1}), ambient soil temperature (T; K), surface area (S;m^2), total chamber enclosure time (Tc; hours), and sampling frequency of the instrument (Ps; hours) (Nickerson, 2016):

$$MDF = \frac{Aa}{Tc\sqrt{\frac{1}{Tc\ Ps}}} \cdot \left(\frac{VP}{SRT}\right) \qquad (2.)$$

which resulted in MDF_{CO2} = ±0.0003 μmol m^{-2} sec^{-1}, MDF_{CH4}= ±0.06 μmol m^{-2} hr^{-1}, MDF_{N2O}= ±0.02 μmol m^{-2} hr^{-1}. Fluxes were only used if they were above the MDF, and were otherwise excluded. Of the 202 flux measurements, only 4 of the N_2O fluxes were under the detection limit. All CO_2 and CH_4 measurements were within our analytical thresholds.

Statistical analysis

Soil organic C and N concentrations from each soil depth were converted to a mass per unit area (pools Mg ha^{-1}) by multiplying the concentrations by bulk density and the soil depth increment. Changes in SOC between sampling times were calculated by subtracting initial values from values after three years within the same plot (Liebig et al., 2008). Changes were then evaluated within plot by the fixed effects of soil depth, crop and fertilizer treatment using a linear mixed model with replicate crossed with sample day as random effects to account for unmeasured site variability and the correlation between measurements from repeated sampling using the *lmer* package (Bates et al. 2015) in R (R Core Team, 2021). Linear mixed models were also used to assess the effect of crop type and fertilizer treatments on biomass production and tissue chemistry. To evaluate if the fixed effects (and their interactions) accounted for variation in response variables, we performed type II ANOVA using the 'Anova' function in the *lmerTest* package (Kuznetsova et al. 2017). When fixed effects accounted for variation, we compared treatments using post-hoc pairwise Tukey HSD and report the model means and ± SE. We used Levene's test to evaluate the plot-level variance of SOC concentrations from 2018 to 2020 using the leveneTest in the *car* package (Fox and Weisberg 2019). The soil chemistry and biomass results are reported as model mean values (±SE). Soil pH is reported as the mean of hydrogen ion concentrations followed by a log10 back transformation with uncertainty reported as a 95% confidence interval (CI). Nitrogen use efficiency (NUE_{crop}) was calculated following represents the fraction of fertilizer N that was utilized and allocated to yield N (Congreves et al., 2021) calculated as:

$$\mathrm{NUE_{crop}} = \frac{\text{Yield } \mathrm{N_f}}{\text{Fertilizer N}} \quad (3.)$$

To calculate GHG fluxes, we quantified if each chamber gas measurement exhibited a linear increase or decrease in their concentrations over the 5-minute enclosure time (Supplemental Figure 4). We fit linear mixed models to assess the fixed effects of crop, fertilizer treatment, and time (month), soil temperature, and WFPS on daily mean GHG fluxes and included the random effects of replicate crossed with sample day. To examine the temporal differences of crop-specific fluxes, based on different plant phenology and response to environmental factors, we examined possible interactions between month and crop. WFPS and soil temperature were assessed for inclusion in all statistical flux models. To assess if the fixed effects (and their interactions) accounted for variation in daily mean and cumulative fluxes, we performed type II ANOVA using the 'Anova' function. When fixed effects accounted for variation, we compared treatments using post-hoc using pairwise Tukey HSD and report the model means and ± SE (*emmeans* package; Lenth et al. 2020). Flux uncertainty is reported as ± SE of the model means across the three replicates measured during each sampling event. All model residuals were assessed for normality, and logarithmic transformations were applied to the AGB, biomass %N (AGB and BGB), and CO_2 flux data before analysis to achieve a normal distribution. All analyses were performed in R (R Core Team 2021). Treatment significance was set *a priori* to $\alpha = 0.05$ for all analyses

Soil microbial community analysis

rRNA gene amplicon sequencing was performed to determine shifts in the composition and diversity of soil microbial communities under crop and fertilizer treatments. The soil used for sequencing was flash-frozen in an ethanol-dry ice bath in the field, and the samples were collected as subsets of the cores extracted for soil chemistry analysis to examine microbial relationships directly. Genomic DNA was extracted from 0.5 g frozen soil samples using the Fast DNA SPIN Kit for soil (MP Biomedicals, Santa Ana, CA) according to the manufacturer's instructions. We targeted the V4 region of the 16S rRNA gene using f515a and r806b (GTGYCAGCMGCCGCGGTAA and GGACTACVSGGGTATCTAAT, respectively) from the Earth Microbiome Project (Thompson et al., 2017) and the D2 hypervariable region of the fungal LSU using LR22r and LR3 (Mueller et al., 2016). Details of PCR reactions and sequencing are provided in Goemann et al. (2021). The two libraries were pooled at 4 nM and loaded onto an in-house Illumina MiSeq (Illumina, San Diego, USA). Reads were merged, trimmed, and dereplicated with USEARCH, and zero-radius operational taxonomic units (ZOTUs) were identified with UNOISE3 (v.11.0.667; Edgar, 2010). Representative 16S and LSU ZOTUs were classified against their respective databases using the online Bayesian classifier of the Ribosomal Database Project (Set 18 for bacteria, Set 11 for fungi; Wang et al., 2015). All reads classified to the chloroplast (16S), or animalia, protozoa, or viridiplantae (LSU) were removed before analysis, and datasets were randomly subsampled according to the sample with the lowest read number for statistical analysis using the R package *vegan* (Oksanen et al., 2019). The data are accessible at MG-RAST under accession numbers: mgs875156 (LSU) and mgs875153

(16S). Differences in community composition were assessed with PERMANOVA using the *vegan* package (Osanen et al., 2020) and relative abundances calculated with the *microbiome* package (Lahti and Shetty 2019). The *rstatix* package (Kassambara 2021) was used to calculate pairwise t-tests with multiple test corrections for differences in relative abundances between crops and compared to the 2018 samples.

Results

Soil WFPS, climate, and pH results

WFPS (0-5 cm) was highest in the spring and lower in the summer, with monthly means of 47% in March and 12% in August (p = 0.02; Supplemental Fig. 10). There were differences in WFPS (0-5 cm soil depth) across time (p = 0.02) with peaks in the early spring and fall (Supplemental Fig. 10). WFPS was highest under the control plots (p < 0.0001) regardless of crop or fertilizer type. Soil temperature warmed throughout the growing season from 4.9 ± 2.1 °C in March to 22.7 ± 2.1 °C in August across treatments (Supplemental Fig. 10). Weather conditions in 2020 favored tall wheatgrass (C3) growth as there were 2.8 times more growing degree days (2845 vs. 1019; Supplemental Fig. 3) and greater rain use efficiency compared to switchgrass (24.7 vs. 8.7 kg dry matter mm^{-1} rainfall; Supplemental Table 6). We report no differences in soil pH across crop type (p = 0.67) or treatment (p = 0.67) but note a higher pH at the 15-30 cm depth (8.4, CI: 7.9-8.8; p = 0.0001) compared to the 0-15 cm depth (8.0, CI: 7.5-8.4), due to the greater carbonate presence at this depth (Engel et al., 2017).

Above and belowground production

Fertilizer treatments had strong positive effects on both crops, although AGB production was much greater for tall wheatgrass ($p < 0.0001$; Fig. 2) and rivaled production output from bioenergy feedstock studies further east in warmer and wetter climates (Supplemental Table 1). AGB production in tall wheatgrass was 68% greater (6.7 ± 0.7 Mg ha^{-1}, $p = 0.0084$) and 67% greater (6.6 ± 0.7 Mg ha^{-1}, $p = 0.0016$) in the CBF and urea fertilizer treatments compared to the unfertilized control (3.3 ± 0.4 Mg ha^{-1}), respectively (Figure 1). Similarly, switchgrass AGB production was enhanced by both CBF (71%;2.3 ± 0.2 Mg ha^{-1}, $p = 0.0084$) and urea fertilization (67%;2.2 ± 0.2 Mg ha^{-1}, $p = 0.0016$) relative to the control (1.1 ± 0.1 Mg ha^{-1}). Further, we note that our estimates of switchgrass production are likely high due to the presence of weedy species not present in tall wheat grass plots. Fertilization had no measurable effect on the root biomass production in either crop ($p = 0.64$). However, mean root biomass production (0-15 cm) was 73% greater in the tall wheatgrass compared to switchgrass irrespective of fertilizer treatment (0.84 Mg ± 0.1 ha^{-1} yr^{-1} vs. 0.39 ± 0.1 Mg ha^{-1} yr^{-1}; $p < 0.0001$, Figure 1). In total, the fertilized tall wheatgrass plots were roughly three times more productive than the switchgrass plots (7.8 ± 0.8 Mg ha^{-1} vs. 2.5 ± 0.8 Mg ha^{-1}; $p < 0.0001$).

SOC change 2018-2020

The direction and magnitude of SOC change over the three-year establishment period differed across bioenergy crop type ($p = 0.009$; Figure 2) and soil depth ($p < 0.0001$), while fertilizer type did not affect SOC dynamics over the duration of this study. We observed a

net gain of 0.75 ± 0.44 Mg ha^{-1} of SOC (0.25 Mg ha^{-1} yr^{-1} accumulation rate; Supplementary Table 1) in the tall wheatgrass plots and a net loss of -0.23 ± 0.44 Mg SOC ha^{-1} (-0.08 Mg SOC ha^{-1} yr^{-1}) in the switchgrass plots across a 0-30 cm soil depth. Tall wheatgrass plots had a greater SOC increase at the 15-30 cm depth over three years (1.58 ± 0.48 Mg SOC ha^{-1} versus 0.61 ± 0.49 SOC Mg ha^{-1}). At the 0-15 cm depth, there was no change in SOC over three years in the tall wheatgrass (p = 0.32) and a three-year net loss of 1.07 ± 0.47 Mg SOC ha^{-1} in the switchgrass plots (p = < 0.0001). We find decreasing variation from 2018-2020 in SOC concentrations at the 0-15 cm soil depth, while there is increasing variation at the 15-30 cm soil depth from 2018 to 2020 across both crops (Supplemental Figure 9 and Table 11). Over the three years, no differences in bulk soil N were observed across depth, crop, or fertilizer treatments (p = 0.53, p = 0.2, p = 0.84). Thus, C:N ratios increased from a background of 7.9 ± 0.35 under tall wheatgrass by 0.51 ± 0.35 and decreased under switchgrass by 0.54 ± 0.35 across the 0-30 cm soil depth (p = 0.008).

Soil greenhouse gas flux

Soil efflux for CO_2 displayed strong seasonal variability by crop type (p < 0.0001) while CH_4 and N_2O did not (p = 0.97 and p = 0.39, respectively; Figure 3, Table). Monthly CO_2 fluxes were greater in the tall wheatgrass plots in March and April (p = 0.03 and p = 0.002) with some evidence for greater fluxes in May (p = 0.07; Table 3). This shifted in June when CO_2 fluxes converged and remained similar between crops through October. Daily CO_2 fluxes were affected by both crop type (p < 0.0001) and fertilizer treatment (p = 0.0007); Figure 3). Tall wheatgrass plots had higher mean CO_2 fluxes compared to switchgrass (1.7

± 0.19 vs. 1.2 ± 0.13 μmol CO_2 m^{-2} sec^{-1}, $p = 0.0118$) irrespective of fertilizer treatment. CO_2 fluxes were greatest under the CBF fertilization (Table 2; $p = 0.0007$). We found some evidence that CH_4 uptake was greater under tall wheatgrass (-1.00 ± 0.08 vs. - 0.81 ± 0.08 μmol CH_4 m^{-2} hr^{-1}; $p = 0.06$) but little evidence for any fertilizer effect ($p = 0.18$). All methane fluxes were negative across the sampling period. Mean N_2O emission rates were not different between fertilizer treatments or crops ($p = 0.66$, $p = 0.18$). We note that N_2O emissions were generally small. The largest N_2O flux was captured in March when WFPS was highest (2.1 μmol N_2O m^{-2} hr^{-1}; Supplemental Table 6).

CO_2 fluxes followed a general positive nonlinear relationship with soil temperature, and CO_2 fluxes under switchgrass were more sensitive to temperature than tall wheatgrass ($p = 0.05$). There was no observed effect of WFPS on CO_2 fluxes. There was some evidence for a positive relationship between CH_4 flux and WFPS under switchgrass ($p = 0.04$), but no relationship between tall wheatgrass and WFPS. There was no observed effect of temperature on CH_4 fluxes. N_2O fluxes increased linearly with WFPS ($p = 0.01$) but were not affected by soil temperature.

AGB and root biomass chemistry

The %C in switchgrass AGB and root biomass was 2.9% and 4.7% greater compared to tall wheatgrass (Supplemental Table 2; $p < 0.0001$, $p < 0.0001$) and the %N in switchgrass root biomass was 26% greater than tall wheatgrass (Supplementary Table 2; $p = 0.05$). However, we find little evidence for differences in mean root C:N ratios (53.9 versus 63.5; $p = 0.14$) or AGB C:N ratios (72.1 vs. 77.4 $p = 0.44$) between switchgrass and tall

wheatgrass. %C was greater in fertilizer treatments relative to controls irrespective of crop type ($p = 0.02$). A greater amount of biomass-N was lost from harvest (31.7 vs. 13.6 kg N ha^{-1}; $p = < 0.0001$) in the tall wheatgrass plots, suggestive of a higher nitrogen use efficiency (equation 3; NUE_{crop}). If we assume all plant N was acquired from a fertilizer source, 63% of fertilizer N was recovered in harvestable tall wheatgrass yield, while only 27% was recovered from switchgrass.

Microbial biodiversity shifts

Switchgrass and tall wheatgrass plot bacterial/archaeal and fungal community compositions significantly shifted between 2018 and 2020 (Figure. 5a, b, Supplemental Table 6). Soil depth contributed to the dissimilarity in the fungal community, with greater shifts observed in the 15-30 cm depth ($p = 0.001$, Supplemental Table 6). Fertilizer-driven treatment effects on community composition were detected in the fungi ($p = 0.01$) but not in the bacteria/archaea ($p = 0.28$). Fungal but not bacterial/archaeal alpha diversity also increased over time at the 15-30 cm soil depth, particularly in the tall wheatgrass plots (Supplemental Figure 7).

To examine the differences in community composition between crop types and their shift from the 2018 pre-establishment conditions we compared the relative abundances of major bacterial/archaeal phyla and fungal classes. In the bacterial/archaeal community, Planctomycetes relative abundance increased in both crops while Actinobacteria increased in only the tall wheatgrass and Thaumarchaeota in the switchgrass plots (Figure 4c). Gemmatimondetes and Proteobacteria decreased from 2018 to 2020 in both crops. Due to

the observed differences in CH_4 between crops, we further investigated clades of known methanogens and methanotrophs. Euryarchaeota, a clade primarily composed of methanogens, was enriched in both switchgrass and tall wheatgrass compared to the background soil and had the greatest abundance in switchgrass (Supplemental Figure 6).

In the fungal community, while Agaricomycetes increased in relative abundance in both crops, only tall wheatgrass plots exhibited significantly increased Glomeromycetes while the Sordariomycetes were enriched in the switchgrass plots (Figure 4d). A decrease in relative abundance in Tremellomycetes was observed in both crops. The fertilizer effects detected by ordination were primarily due to a higher relative abundance of Exobasidiomycetes, a class of broadly pathogenic fungi, in urea-fertilizer plots, particularly under the switchgrass. Furthermore, we detected a greater relative abundance of Ustilaginomycetes, another class of broadly pathogenic fungi, in switchgrass compared to tall wheatgrass (Supplemental Table 9), particularly under urea fertilization. BLAST analysis of the Exobasidiomycete and Ustilaginomycete zOTUs revealed that the species detected are all documented fungal pathogens of grass species (Supplemental Table 10).

Discussion

Tall wheatgrass (C3) was more productive than switchgrass (C4)

We highlight that fertilized tall wheatgrass achieved high levels of aboveground biomass production in 2020 (6.7 Mg ha^{-1}). This production rivals that of switchgrass and tall wheatgrass grown in warmer and wetter regions in the eastern UMRB (1.4 - 10.3 Mg ha^{-1} and 2.4 - 9.8, respectively: Supplemental Table 1) despite low soil fertility, modest N-

fertilization application (50 kg N ha^{-1}), and no irrigation. Switchgrass showed minimal potential as a bioenergy crop in the study area in the present, regardless of fertilization. We contend that the large differences in aboveground production between switchgrass and tall wheatgrass likely reflect an important regional climate constraint on C4 species in the cool, early-season precipitation dominated, and semi-arid climate of the western UMRB and highlight the potential of C3 species for bioenergy production despite opportunities for C4 bioenergy production in future climates (Dolan et al., 2020).

In the semi-arid western UMRB, annual productivity in dryland cropping systems is dependent on precipitation inputs and adaption to a shorter growing season. Previous studies have shown that efficient use of rainwater is critical for bioenergy crop sustainability (Hendrickson et al., 2013; Peterson et al., 1996). Our estimate of nearly three times more growing degree days and almost three times greater rain use efficiency for the C3 crop supports a hypothesis of climate limitation on the productivity and establishment of switchgrass. This finding is critical in that pairing high rain-use efficiency crops in semi-arid and non-irrigated bioenergy systems will be necessary moving forward. In addition to climate constraints, we acknowledge that other biophysical factors could have compounded the poor establishment of switchgrass. For example, we see a greater increase in the relative abundance of Ustilaginomycetes and Exobasidiomyctes, both pathogenic species, under the switchgrass plots, although disease symptoms were not assessed.

CBF matches urea crop production and did not increase non-CO_2 GHG emissions

We determined that a fertilizer regime based on CBF achieved the same biomass production in tall wheatgrass and switchgrass as traditionally used urea N-fertilizer at equivalent application rates. Furthermore, the field use of CBF did not induce any negative non-CO_2 GHG emissions tradeoffs compared to urea fertilization at a 50 kg ha^{-1} application rate. Notably, CBF's lack of effect on N_2O emissions is important as the GWP of bioenergy systems is often a function of the N_2O emissions since the 100-year GWP of N_2O (298) is much higher than CH_4 (36) and CO_2 (1) (Lawrence et al., 2021; Robertson et al., 2000). However, evaluating application rates greater than 50 kg ha^{-1} should be evaluated in the future based on the slurry in which CBF is applied as it could increase C substrate availability and WFPS, both environmentally conducive for N_2O production.

CH_4 is also a potent GHG, and quantifying how different management practices affect soil CH_4 fluxes is critical in assessing regional agricultural mitigation potential and calculating C budgets (Levine et al., 2011). In this study, CH_4 fluxes remained negative throughout the entire growing season across all crop and fertilizer treatments and were greatest under tall wheatgrass. This contrasts with Schmer et al. 2012, another bioenergy study in the UMRB, that reported positive CH_4 fluxes under switchgrass late in the growing season after harvest in September. Interestingly, we find a greater relative abundance of methanogens (CH_4 producing microbes) under switchgrass plots (Supplementary Figure 6), and this coupled with findings from Schmer et al. (2012) may warrant future exploration of upland CH_4 dynamics under switchgrass, especially for irrigated systems in the UMRB.

CO_2 fluxes drove GHG differences between crop and fertilizer treatments. The temporal trends in CO_2 flux between crops highlight plant phenology as a critical driver of C fluxes and an important consideration for evaluating seasonal GHG budgets in this system. Since the CO_2 measured in our chambers is a composite of autotrophic respiration and heterotrophic respiration, it is difficult to infer the relative contributions from each in these data. However, another study in a mixed grassland reported root respiration covarying with the season, ranging from 31%-51% of total soil respiration (Wanga et al., 2005). The greater CO_2 fluxes under tall wheatgrass across the March-May likely reflect a larger fraction of autotrophic respiration from early root growth from the cold-adapted metabolism of C3 species (Hanson et al., 2000). The similar CO_2 fluxes between crops during the June-October signal a seasonal switch to an increased ratio of heterotrophic respiration under warming temperatures for both crops. However, these similar signatures of CO_2 flux from June-October suggest a larger fraction of heterotrophic CO_2 production under switchgrass given the substantially smaller plant inputs compared to tall wheatgrass. Taken together, the divergent pattern in CO_2 flux between crops early in the season indicates a strong autotrophic C3 signature that appears to shift to a dominant imprint of heterotrophic respiration as soil temperatures rise. This pattern is important for understanding the pattern of SOC loss under switchgrass although future experimental validation would be needed to confirm this.

Despite greater CO_2 emissions under the CBF fertilizer, rates were within published values for similar agronomic systems (Oertel et al., 2016), and we identified no effect of fertilizer on SOC over the three years. Possible explanations for greater CO_2 emissions

under the CBF fertilized include: direct increases in respiration from the cyanobacterial inoculants, a decrease in microbial carbon use efficiency, or increased soil microbial respiration from the addition of a labile C substrate or a "priming effect" (Kuzyakov et al., 2000; Soong et al., 2020). Moving forward, partitioning soil respiration sources under both crop types and CBF will be critical for evaluating net ecosystem productivity and C budgets, especially heterotrophic respiration as this is a critical soil C loss vector. Furthermore, upstream production C costs are needed to develop a full carbon lifecycle assessment of CBF and assess its climate mitigation potential compared to conventional fertilizer practices.

SOC accumulation under C3 and loss under C4 crops partitioned by soil depths

We find that the establishment of tall wheatgrass led to a net gain of SOC over three years, while the establishment of switchgrass led to a net loss of SOC irrespective of fertilization. Patterns in SOC gain and loss were partitioned by different soil depths in the different crops. SOC increased under tall wheatgrass at the deeper 15-30 cm depth, while losses under switchgrass were observed at the shallower 0-15 cm depth. The strong directionality and magnitude of SOC loss under switchgrass suggest the two crops had differing effects on SOC in the topsoil. This pattern of change in SOC aligns with studies that found significant losses of SOC in topsoil, but not subsoil due to increases in labile root exudation that stimulated decomposition of older SOC through the priming effect (de Graaff et al., 2014; Salomé et al., 2010). Together, these findings align with the idea that different

regulatory mechanisms exist for SOC dynamics in the topsoil and subsoil (Fierer et al., 2003).

The rate of SOC accumulation across 0-30 cm depth under tall wheatgrass (0.25 Mg SOC ha yr^{-1}) in this study are similar to Liebig et al. at a cool site in eastern North Dakota (0.28 Mg SOC ha yr^{-1}). Furthermore, our observed SOC accumulation rate is similar to a previous study on a mix of alfalfa and three native grasses adjacent to this study (0.24 Mg SOC yr^{-1}; R. E. Engel et al., 2017). Since we focused on bulk SOC, we cannot exclude that proportional fractions of particulate or mineral associated SOC were affected by crop type or N addition, which have important implications for the long-term stability of SOC (Cotrufo et al., 2019). Despite many observations that the variability of SOC is of greater importance than bulk density for detecting changes in SOC pool changes, our SOC pool results need to be interpreted carefully as we did not measure the three-year change in bulk density (Supplementary Figure 9; Schrumpf et al., 2011). Important questions remain, including whether the SOC increases under tall wheatgrass were due to an increase in the mineral or particulate-associated carbon pools and what are the mechanisms that drive the depth partitioning of SOC. Overall, these findings are important as they point to the significant potential of SOC accumulation under C3 species on non irrigated low fertility soil in the UMRB region.

Soil microbial shifts are crop-specific and relate to plant productivity

Our results show that in both the fungal and bacterial/archaeal communities, the establishment of the two perennial crops altered the soil microbiome composition and that

crop type was a stronger driver of these shifts than the fertilization regime. In the fungal community, AMF increased in relative abundance at the 15-30 cm depth under the tall wheatgrass aligning with the observed increases of SOC at the same depth. AMF can contribute significantly to soil C stocks through the production of extraradical hyphal networks while also increasing N and phosphorus availability to roots in nutrient-limited (i.e. marginal) soils (Emery et al. 2018, Zhang 2017). Thus, our observation of increased root biomass under tall wheatgrass and greater AMF colonization could represent a positive feedback loop that led to increased accumulation of SOC possibly through mineral protection from enhanced aggregation (L. Wang et al., 2015; Wilson et al., 2009). However, this hypothesis is under the assumption that our measurements of root biomass at the 0-15 cm depth extend to the 15-30 cm and warrants future investigation and targeted experimentation to evaluate the role of AMF in tall wheatgrass productivity (Rillig et al., 2019). Switchgrass is highly dependent on mycorrhizal nutrient acquisition, so the lack of change in AMF relative abundance in the switchgrass plots further signals the imprint of low productivity or lack of their establishment (Dirks & Jackson, 2020; Hetrick et al., 2011). We also found relative increases in Agaricomycetes under the tall wheatgrass; these are a broad group of fungi that include taxa with lignin-degrading capabilities and have been found to be critical regulators of C flow into soil (Lodato et al., 2021). This increase is likely due to greater litter biomass inputs and the lower substrate quality compared to switchgrass (i.e. higher C:N ratio). Total fungal richness increased in both bioenergy crops irrespective of N fertilization type, which has previously been documented during

perennial crop establishment due to decreases in soil disturbance from tillage (Bowles et al., 2017; Helgason et al., 2010; Schmidt et al., 2019).

In contrast to the fungal community, the bacterial/archaeal community richness exhibited undetectable changes over the three years of this study. However, crop-specific changes in community composition were detected, including an increased relative abundance of Actinobacteria and Planctomycetes in the tall wheatgrass plots which play an important role in plant biomass and soil carbon turnover in low fertility soils (Bao et al., 2021; Hartman et al., 2017; Wieczorek et al., 2019). We also report an increase in the relative abundance of Thaumarchaeota in the switchgrass plots, all of which belonged to the genus *Nitrososphaera*. *Nitrososphaera* are ammonia oxidizing archaea (AOA) that perform the rate-limiting step in nitrification, a critical loss pathway since it transforms the reduced form of N (NH_4^+) to an oxidized and more mobile form (NO_3^-). The higher abundance of AOA under switchgrass may signal leaching as an important pathway for NO_3-N loss under the poorly established switchgrass crop since AOA are known to contribute to nitrate leaching in agricultural systems (Wessen et al. 2011). Interestingly, we observed the inverse response in Proteobacteria under switchgrass, which could be due to competition amongst ammonia-oxidizers as some members of the Beta- and Gammaproteobacteria are ammonia-oxidizers (AOB). Although N_2O fluxes were extremely low in this study determining the factors governing AOA vs. AOB abundance in soils will be important for future studies as AOB have been observed to produce more N_2O than AOA in some soil types (Prosser et al., 2020; Banning et al., 2015). Lastly, we observed a decrease in Gemmatimonadetes in the switchgrass and tall wheatgrass plots.

Gemmatimonadetes are overall poorly characterized in soil systems, but their mirrored decline may signal they have a negative N fertilization response as observed by Cedarland et al. (Cederlund et al., 2014)

Conclusion

Our findings provide the first multi-year evaluation of second generation BECCS perennial grass feedstock candidates in the western UMRB and establish a baseline for C3 and C4 yields for bioenergy candidate species for these cold semi-arid regions. We conclude that the combination of tall wheatgrass (a cool-season C3) and a cyanobacteria biofertilizer showed strong potential as a productive bioenergy crop-fertilizer pairing that could help meet climate mitigation goals in future bioenergy systems in semi-arid regions. Over the three-year study, we observed greater productivity in the C3 tall wheatgrass than in the C4 switchgrass crop, as well as increased SOC accumulation and fertilizer-N recovery. CBF had a strong effect on plant productivity and did not stimulate increases in non-CO_2 GHG emissions compared to urea. GHG fluxes were dominated by CO_2 across all treatments and displayed substantial seasonal variability by crop type, likely driven by phenology differences among species. The soil microbiome changed over time as we observed increases in fungal diversity and crop-specific shifts in bacterial/archaeal and fungal communities linked to the regulation of soil C turnover and nitrification. These microbial shifts may have contributed to the success of the C3 crop due to the emergence of a beneficial microbiome not observed under the C4 crop (e.g. AMF and pathogenic defense). Finally, our findings are important for both developing a microbial- and biogeochemical-

coupled model geared toward agroecosystem management (e.g. DayCent; Berardi et al., 2020; Tonitto et al., 2018).

Acknowledgments

The authors would like to thank Rosie Wallander, Adam Cook, Evan Bilbrey, Ryan Malmquist, Suzy Walsh, Sophie Grimm, Jeff Holmes, and Samuel Koeshall for field setup, sample collection, and processing. We appreciate and thank Dr. Cathy Zabinski for allowing us use of root coring equipment Additionally, we thank Shealyn Malone for providing edits on previous versions of this manuscript.

Conflict of interest

None reported

Authors contributions

JG, JB, HG, PS, BP, PM, and BMP collaborated on the study design. JG, HG, and PM were responsible for field sampling, while JG, and HG were responsible for the sample processing. JG, HG, and BC performed statistical analyses. JG, HG, BC, PS, JB, and JC contributed to data interpretation. All authors contributed to writing the manuscript.

Data availability

Sequencing data are accessible at MG-RAST under accession numbers: mgs875156 (LSU) and mgs875153 (16S). R Code for flux analysis is available at

https://github.com/jgay1459/Picarro-Analyses. Additional data are available on reasonable request.

Funding

This work was supported by the National Science Foundation under the EPSCoR Track II cooperative agreement OIA1632810

REFERENCES CITED

Alvarez, A. L., Weyers, S. L., Goemann, H. M., Peyton, B. M., & Gardner, R. D. (2021). Microalgae, soil and plants: A critical review of microalgae as renewable resources for agriculture. *Algal Research*, *54*, 102200. https://doi.org/10.1016/j.algal.2021.102200

Baik, E., Sanchez, D. L., Turner, P. A., Mach, K. J., Field, C. B., & Benson, S. M. (2018). Geospatial analysis of near-term potential for carbon-negative bioenergy in the United States. *Proceedings of the National Academy of Sciences*, *115*(13), 3290–3295. https://doi.org/10.1073/pnas.1720338115

Bao, Y., Dolfing, J., Guo, Z., Chen, R., Wu, M., Li, Z., Lin, X., & Feng, Y. (2021). Important ecophysiological roles of non-dominant Actinobacteria in plant residue decomposition, especially in less fertile soils. *Microbiome*, *9*(1), 84. https://doi.org/10.1186/s40168-021-01032-x

Berardi, D., Brzostek, E., Blanc-Betes, E., Davison, B., DeLucia, E. H., Hartman, M. D., Kent, J., Parton, W. J., Saha, D., & Hudiburg, T. W. (2020). 21st-century biogeochemical modeling: Challenges for Century-based models and where do we go from here? *GCB Bioenergy*, *12*(10), 774–788. https://doi.org/10.1111/gcbb.12730

Bleby, T. M., Aucote, M., Kennett-Smith, A. K., Walker, G. R., & Schachtman, D. P. (1997). Seasonal water use characteristics of tall wheatgrass [Agropyron elongatum (Host) Beauv.] in a saline environment. *Plant, Cell & Environment*, *20*(11), 1361–1371. https://doi.org/10.1046/j.1365-3040.1997.d01-29.x

Bowles, T. M., Jackson, L. E., Loeher, M., & Cavagnaro, T. R. (2017). Ecological intensification and arbuscular mycorrhizas: A meta-analysis of tillage and cover crop effects. *Journal of Applied Ecology*, *54*(6), 1785–1793. https://doi.org/10.1111/1365-2664.12815

Burgess, M. H., Miller, P. R., & Jones, C. A. (2012). Pulse Crops Improve Energy Intensity and Productivity of Cereal Production in Montana, USA. *Journal of Sustainable Agriculture*, *36*(6), 699–718. https://doi.org/10.1080/10440046.2012.672380

Carvalho, J. L. N., Hudiburg, T. W., Franco, H. C. J., & DeLucia, E. H. (2017). Contribution of above- and belowground bioenergy crop residues to soil carbon. *GCB Bioenergy*, *9*(8), 1333–1343. https://doi.org/10.1111/gcbb.12411

Castro, J. de S., Calijuri, M. L., Assemany, P. P., Cecon, P. R., de Assis, I. R., & Ribeiro, V. J. (2017). Microalgae biofilm in soil: Greenhouse gas emissions, ammonia volatilization and plant growth. *Science of The Total Environment*, *574*, 1640–1648. https://doi.org/10.1016/j.scitotenv.2016.08.205

Cederlund, H., Wessén, E., Enwall, K., Jones, C. M., Juhanson, J., Pell, M., Philippot, L., & Hallin, S. (2014). Soil carbon quality and nitrogen fertilization structure bacterial

communities with predictable responses of major bacterial phyla. *Applied Soil Ecology*, *84*, 62–68. https://doi.org/10.1016/j.apsoil.2014.06.003

Congreves, K. A., Otchere, O., Ferland, D., Farzadfar, S., Williams, S., & Arcand, M. M. (2021). Nitrogen Use Efficiency Definitions of Today and Tomorrow. *Frontiers in Plant Science*, *12*, 912. https://doi.org/10.3389/fpls.2021.637108

Córdova, S. C., Olk, D. C., Dietzel, R. N., Mueller, K. E., Archontouilis, S. V., & Castellano, M. J. (2018). Plant litter quality affects the accumulation rate, composition, and stability of mineral-associated soil organic matter. *Soil Biology and Biochemistry*, *125*, 115–124. https://doi.org/10.1016/j.soilbio.2018.07.010

Cotrufo, M. F., Ranalli, M. G., Haddix, M. L., Six, J., & Lugato, E. (2019). Soil carbon storage informed by particulate and mineral-associated organic matter. *Nature Geoscience*, 1–6. https://doi.org/10.1038/s41561-019-0484-6

de Graaff, M.-A., Jastrow, J. D., Gillette, S., Johns, A., & Wullschleger, S. D. (2014). Differential priming of soil carbon driven by soil depth and root impacts on carbon availability. *Soil Biology and Biochemistry*, *69*, 147–156. https://doi.org/10.1016/j.soilbio.2013.10.047

Dirks, A. C., & Jackson, R. D. (2020). Community Structure of Arbuscular Mycorrhizal Fungi in Soils of Switchgrass Harvested for Bioenergy. *Applied and Environmental Microbiology*, *86*(19). https://doi.org/10.1128/AEM.00880-20

Dolan, K. A., Stoy, P. C., & Poulter, B. (2020). Land management and climate change determine second-generation bioenergy potential of the US Northern Great Plains. *GCB Bioenergy*, *12*(7), 491–509. https://doi.org/10.1111/gcbb.12686

Edgar, R. C. (2010). Search and clustering orders of magnitude faster than BLAST. *Bioinformatics*, *26*(19), 2460–2461. https://doi.org/10.1093/bioinformatics/btq461

Engel, R. E., Miller, P. R., McConkey, B. G., & Wallander, R. (2017). Soil Organic Carbon Changes to Increasing Cropping Intensity and No-Till in a Semiarid Climate. *Soil Science Society of America Journal*, *81*(2), 404–413. https://doi.org/10.2136/sssaj2016.06.0194

Engel, R., Jones, C., & Wallander, R. (2011). Ammonia Volatilization from Urea and Mitigation by NBPT following Surface Application to Cold Soils. *Soil Science Society of America Journal*, *75*(6), 2348–2357. https://doi.org/10.2136/sssaj2011.0229

Epstein, H. E., Lauenroth, W. K., Burke, I. C., & Coffin, D. P. (1997). Productivity Patterns of C3 and C4 Functional Types in the U.s. Great Plains. *Ecology*, *78*(3), 722–731. https://doi.org/10.1890/0012-9658(1997)078[0722:PPOCAC]2.0.CO;2

Fajardy, M., & Dowell, N. M. (2017). Can BECCS deliver sustainable and resource efficient negative emissions? *Energy & Environmental Science*, *10*(6), 1389–1426. https://doi.org/10.1039/C7EE00465F

Fierer, N., Allen, A. S., Schimel, J. P., & Holden, P. A. (2003). Controls on microbial CO2 production: A comparison of surface and subsurface soil horizons. *Global Change Biology*, *9*(9), 1322–1332. https://doi.org/10.1046/j.1365-2486.2003.00663.x

Goemann, H. M., Gay, J. D., Mueller, R. C., Brookshire, E. N. J., Miller, P., Poulter, B., & Peyton, B. M. (2021). Aboveground and belowground responses to cyanobacterial biofertilizer supplement in a semi-arid, perennial bioenergy cropping system. *GCB Bioenergy*. https://doi.org/10.1111/gcbb.12892

Halvorson, A. D., Wienhold, B. J., & Black, A. L. (2002). Tillage, Nitrogen, and Cropping System Effects on Soil Carbon Sequestration. *Soil Science Society of America Journal*, *66*(3), 906–912. https://doi.org/10.2136/sssaj2002.9060

Hanson, E., Ritten, J., Miller, P., Nagler A., Gerace, S. et al. (2020). Is growing switchgrass economically feasible? *University of Wyoming Extension*. https://www.wyoextension.org/agpubs/pubs/B-1360-1-switchgrass-web.pdf

Hanson, P. J., Edwards, N. T., Garten, C. T., & Andrews, J. A. (2000). Separating root and soil microbial contributions to soil respiration: A review of methods and observations. *Biogeochemistry*, *48*(1), 115–146. https://doi.org/10.1023/A:1006244819642

Harmoney, K. R. (2015). Cool-Season Grass Biomass in the Southern Mixed-Grass Prairie Region of the USA. *BioEnergy Research*, *8*(1), 203–210. https://doi.org/10.1007/s12155-014-9514-9

Hartman, W. H., Ye, R., Horwath, W. R., & Tringe, S. G. (2017). A genomic perspective on stoichiometric regulation of soil carbon cycling. *The ISME Journal*, *11*(12), 2652–2665. https://doi.org/10.1038/ismej.2017.115

Heaton, E., Voigt, T., & Long, S. P. (2004). A quantitative review comparing the yields of two candidate C4 perennial biomass crops in relation to nitrogen, temperature and water. *Biomass and Bioenergy*, *27*(1), 21–30. https://doi.org/10.1016/j.biombioe.2003.10.005

Helgason, B. L., Walley, F. L., & Germida, J. J. (2010). No-till soil management increases microbial biomass and alters community profiles in soil aggregates. *Applied Soil Ecology*, *46*(3), 390–397. https://doi.org/10.1016/j.apsoil.2010.10.002

Hendrickson, J. R., Schmer, M. R., & Sanderson, M. A. (2013). Water Use Efficiency by Switchgrass Compared to a Native Grass or a Native Grass Alfalfa Mixture. *BioEnergy Research*, *6*(2), 746–754. https://doi.org/10.1007/s12155-012-9290-3

Hetrick, B. A. D., Kitt, D. G., & Wilson, G. T. (2011). Mycorrhizal dependence and growth habit of warm-season and cool-season tallgrass prairie plants. *Canadian Journal of Botany*. https://doi.org/10.1139/b88-193

Jackson, R. B., Canadell, J., Ehleringer, J. R., Mooney, H. A., Sala, O. E., & Schulze, E. D. (1996). A global analysis of root distributions for terrestrial biomes. *Oecologia*, *108*(3), 389–411. https://doi.org/10.1007/BF00333714

Jian, J., Steele, M. K., Day, S. D., Quinn Thomas, R., & Hodges, S. C. (2018). Measurement strategies to account for soil respiration temporal heterogeneity across diverse regions. *Soil Biology and Biochemistry*, *125*, 167–177. https://doi.org/10.1016/j.soilbio.2018.07.003

John, A. A., Jones, C. A., Ewing, S. A., Sigler, W. A., Bekkerman, A., & Miller, P. R. (2017). Fallow replacement and alternative nitrogen management for reducing nitrate leaching in a semiarid region. *Nutrient Cycling in Agroecosystems*, *108*(3), 279–296. https://doi.org/10.1007/s10705-017-9855-9

Kallenbach, C. M., Grandy, A. S., Frey, S. D., & Diefendorf, A. F. (2015). Microbial physiology and necromass regulate agricultural soil carbon accumulation. *Soil Biology and Biochemistry*, *91*, 279–290. https://doi.org/10.1016/j.soilbio.2015.09.005

Karp, A., & Shield, I. (2008). Bioenergy from plants and the sustainable yield challenge. *New Phytologist*, *179*(1), 15–32. https://doi.org/10.1111/j.1469-8137.2008.02432.x

Kasanke, C. P., Zhao, Q., Bell, S., Thompson, A. M., & Hofmockel, K. S. (2021). Can switchgrass increase carbon accrual in marginal soils? The importance of site selection. *GCB Bioenergy*, *13*(2), 320–335. https://doi.org/10.1111/gcbb.12777

Kuzyakov, Y., Friedel, J. K., & Stahr, K. (2000). Review of mechanisms and quantification of priming effects. *Soil Biology and Biochemistry*, *32*(11), 1485–1498. https://doi.org/10.1016/S0038-0717(00)00084-5

Lai, L., Hong, C. O., Kumar, S., Osborne, S. L., Lehman, R. M., & Owens, V. N. (2018). Soil nitrogen dynamics in switchgrass seeded to a marginal cropland in South Dakota. *GCB Bioenergy*, *10*(1), 28–38. https://doi.org/10.1111/gcbb.12475

Lal, R. (2009). Sequestering carbon in soils of arid ecosystems. *Land Degradation & Development*, *20*(4), 441–454. https://doi.org/10.1002/ldr.934

Lawrence, N. C., Tenesaca, C. G., VanLoocke, A., & Hall, S. J. (2021). Nitrous oxide emissions from agricultural soils challenge climate sustainability in the US Corn Belt. *Proceedings of the National Academy of Sciences*, *118*(46). https://doi.org/10.1073/pnas.2112108118

Le Houérou, H. N. (1984). Rain use efficiency: A unifying concept in arid-land ecology. *Journal of Arid Environments*, *7*(3), 213–247. https://doi.org/10.1016/S0140-1963(18)31362-4

Leichty, S. I., Kasanke, C. P., Bell, S. L., & Hofmockel, K. S. (2021). Site and Bioenergy Cropping System Similarly Affect Distinct Live and Total Soil Microbial Communities. *Frontiers in Microbiology*, *12*, 3086. https://doi.org/10.3389/fmicb.2021.725756

Lekberg, Y., & Helgason, T. (2018). In situ mycorrhizal function – knowledge gaps and future directions. *New Phytologist*, *220*(4), 957–962. https://doi.org/10.1111/nph.15064

Levine, U. Y., Teal, T. K., Robertson, G. P., & Schmidt, T. M. (2011). Agriculture's impact on microbial diversity and associated fluxes of carbon dioxide and methane. *The ISME Journal*, *5*(10), 1683–1691. https://doi.org/10.1038/ismej.2011.40

Liebig, M. A., Schmer, M. R., Vogel, K. P., & Mitchell, R. B. (2008). Soil Carbon Storage by Switchgrass Grown for Bioenergy. *BioEnergy Research*, *1*(3), 215–222. https://doi.org/10.1007/s12155-008-9019-5

Lodato, M. B., Boyette, J. S., Smilo, R. A., Jackson, C. R., Halvorson, H. M., & Kuehn, K. A. (2021). Functional importance and diversity of fungi during standing grass litter decomposition. *Oecologia*, *195*(2), 499–512. https://doi.org/10.1007/s00442-020-04838-y

Luo, W., Wang, X., Sardans, J., Wang, Z., Dijkstra, F. A., Lü, X.-T., Peñuelas, J., & Han, X. (2018). Higher capability of C3 than C4 plants to use nitrogen inferred from nitrogen stable isotopes along an aridity gradient. *Plant and Soil*, *428*(1), 93–103. https://doi.org/10.1007/s11104-018-3661-2

Martyniak, D., Żurek, G., & Prokopiuk, K. (2017). Biomass yield and quality of wild populations of tall wheatgrass [Elymus elongatus (Host.) Runemark]. *Biomass and Bioenergy*, *101*, 21–29. https://doi.org/10.1016/j.biombioe.2017.03.025

Mendes, R., Kruijt, M., Bruijn, I. de, Dekkers, E., Voort, M. van der, Schneider, J. H. M., Piceno, Y. M., DeSantis, T. Z., Andersen, G. L., Bakker, P. A. H. M., & Raaijmakers, J. M. (2011). Deciphering the Rhizosphere Microbiome for Disease-Suppressive Bacteria. *Science*. https://doi.org/10.1126/science.1203980

Miller, P. R., & Holmes, J. A. (2012). Short Communication: Comparative soil water use by annual crops at a semiarid site in Montana. *Canadian Journal of Plant Science*, *92*(4), 803–807. https://doi.org/10.4141/cjps2011-191

Monson, R. K., Littlejohn, R. O., & Williams, G. J. (1983). Photosynthetic adaptation to temperature in four species from the Colorado shortgrass steppe: A physiological model for coexistence. *Oecologia*, *58*(1), 43–51. https://doi.org/10.1007/BF00384540

Mueller, R. C., Gallegos-Graves, L. V., & Kuske, C. R. (2016). A new fungal large subunit ribosomal RNA primer for high-throughput sequencing surveys. *FEMS Microbiology Ecology*, *92*(fiv153). https://doi.org/10.1093/femsec/fiv153

Neff, J. C., Townsend, A. R., Gleixner, G., Lehman, S. J., Turnbull, J., & Bowman, W. D. (2002). Variable effects of nitrogen additions on the stability and turnover of soil carbon. *Nature*, *419*(6910), 915–917. https://doi.org/10.1038/nature01136

Oertel, C., Matschullat, J., Zurba, K., Zimmermann, F., & Erasmi, S. (2016). Greenhouse gas emissions from soils—A review. *Geochemistry*, *76*(3), 327–352. https://doi.org/10.1016/j.chemer.2016.04.002

Oldfield, E. E., Bradford, M. A., & Wood, S. A. (2019). Global meta-analysis of the relationship between soil organic matter and crop yields. *SOIL*, *5*(1), 15–32. https://doi.org/10.5194/soil-5-15-2019

Paruelo, J. M., & Lauenroth, W. K. (1996). Relative Abundance of Plant Functional Types in Grasslands and Shrublands of North America. *Ecological Applications*, *6*(4), 1212–1224. https://doi.org/10.2307/2269602

Peterson, G. A., Schlegel, A. J., Tanaka, D. L., & Jones, O. R. (1996). Precipitation Use Efficiency as Affected by Cropping and Tillage Systems. *Journal of Production Agriculture*, *9*(2), 180–186. https://doi.org/10.2134/jpa1996.0180

Piringer, G., & Steinberg, L. J. (2006). Reevaluation of Energy Use in Wheat Production in the United States. *Journal of Industrial Ecology*, *10*(1–2), 149–167. https://doi.org/10.1162/108819806775545420

Poulter, B., Frank, D., Ciais, P., Myneni, R. B., Andela, N., Bi, J., Broquet, G., Canadell, J. G., Chevallier, F., Liu, Y. Y., Running, S. W., Sitch, S., & van der Werf, G. R. (2014). Contribution of semi-arid ecosystems to interannual variability of the global carbon cycle. *Nature*, *509*(7502), 600–603. https://doi.org/10.1038/nature13376

Prosser, J. I., Hink, L., Gubry-Rangin, C., & Nicol, G. W. (2020). Nitrous oxide production by ammonia oxidizers: Physiological diversity, niche differentiation and potential mitigation strategies. *Global Change Biology*, *26*(1), 103–118. https://doi.org/10.1111/gcb.14877

Revillini, D., Wilson, G. W. T., Miller, R. M., Lancione, R., & Johnson, N. C. (2019). Plant Diversity and Fertilizer Management Shape the Belowground Microbiome of Native Grass Bioenergy Feedstocks. *Frontiers in Plant Science*, *10*, 1018. https://doi.org/10.3389/fpls.2019.01018

Rillig, M. C., Aguilar-Trigueros, C. A., Camenzind, T., Cavagnaro, T. R., Degrune, F., Hohmann, P., Lammel, D. R., Mansour, I., Roy, J., Heijden, M. G. A. van der, & Yang, G. (2019). Why farmers should manage the arbuscular mycorrhizal symbiosis. *New Phytologist*, *222*(3), 1171–1175. https://doi.org/10.1111/nph.15602

Rillig, M. C., Sosa-Hernández, M. A., Roy, J., Aguilar-Trigueros, C. A., Vályi, K., & Lehmann, A. (2016). Towards an Integrated Mycorrhizal Technology: Harnessing Mycorrhiza for

Sustainable Intensification in Agriculture. *Frontiers in Plant Science*, *7*. https://doi.org/10.3389/fpls.2016.01625

Robertson, G. P., Hamilton, S. K., Barham, B. L., Dale, B. E., Izaurralde, R. C., Jackson, R. D., Landis, D. A., Swinton, S. M., Thelen, K. D., & Tiedje, J. M. (2017). Cellulosic biofuel contributions to a sustainable energy future: Choices and outcomes. *Science*, *356*(6345). https://doi.org/10.1126/science.aal2324

Robertson, G. P., Hamilton, S. K., Grosso, S. J. D., & Parton, W. J. (2011). The biogeochemistry of bioenergy landscapes: Carbon, nitrogen, and water considerations. *Ecological Applications*, *21*(4), 1055–1067. https://doi.org/10.1890/09-0456.1

Robertson, G. P., Paul, E. A., & Harwood, R. R. (2000). Greenhouse Gases in Intensive Agriculture: Contributions of Individual Gases to the Radiative Forcing of the Atmosphere. *Science*, *289*(5486), 1922–1925. https://doi.org/10.1126/science.289.5486.1922

Robertson, G. P., & Vitousek, P. M. (2009). Nitrogen in Agriculture: Balancing the Cost of an Essential Resource. *Annual Review of Environment and Resources*, *34*(1), 97–125. https://doi.org/10.1146/annurev.environ.032108.105046

Sainju, U. M., Allen, B. L., Lenssen, A. W., & Mikha, M. (2017). Root and soil total carbon and nitrogen under bioenergy perennial grasses with various nitrogen rates. *Biomass and Bioenergy*, *107*, 326–334. https://doi.org/10.1016/j.biombioe.2017.10.021

Salomé, C., Nunan, N., Pouteau, V., Lerch, T. Z., & Chenu, C. (2010). Carbon dynamics in topsoil and in subsoil may be controlled by different regulatory mechanisms. *Global Change Biology*, *16*(1), 416–426. https://doi.org/10.1111/j.1365-2486.2009.01884.x

Sanderman, J., Hengl, T., & Fiske, G. J. (2017). Soil carbon debt of 12,000 years of human land use. *Proceedings of the National Academy of Sciences*, *114*(36), 9575–9580. https://doi.org/10.1073/pnas.1706103114

Schmer, M. R., Liebig, M. A., Hendrickson, J. R., Tanaka, D. L., & Phillips, R. L. (2012). Growing season greenhouse gas flux from switchgrass in the northern great plains. *Biomass and Bioenergy*, *45*, 315–319. https://doi.org/10.1016/j.biombioe.2012.05.026

Schmer, M. R., Vogel, K. P., Varvel, G. E., Follett, R. F., Mitchell, R. B., & Jin, V. L. (2014). Energy Potential and Greenhouse Gas Emissions from Bioenergy Cropping Systems on Marginally Productive Cropland. *PLOS ONE*, *9*(3), e89501. https://doi.org/10.1371/journal.pone.0089501

Schmidt, R., Mitchell, J., & Scow, K. (2019). Cover cropping and no-till increase diversity and symbiotroph:saprotroph ratios of soil fungal communities. *Soil Biology and Biochemistry*, *129*, 99–109. https://doi.org/10.1016/j.soilbio.2018.11.010

Schrumpf, M., Schulze, E. D., Kaiser, K., & Schumacher, J. (2011). How accurately can soil organic carbon stocks and stock changes be quantified by soil inventories? *Biogeosciences*, *8*(5), 1193–1212. https://doi.org/10.5194/bg-8-1193-2011

Six, J., Frey, S. D., Thiet, R. K., & Batten, K. M. (2006). Bacterial and Fungal Contributions to Carbon Sequestration in Agroecosystems. *Soil Science Society of America Journal*, *70*(2), 555–569. https://doi.org/10.2136/sssaj2004.0347

Skinner, R. H., & Comas, L. H. (2010). Root Distribution of Temperate Forage Species Subjected to Water and Nitrogen Stress. *Crop Science*, *50*(5), 2178–2185. https://doi.org/10.2135/cropsci2009.08.0461

Smith and Read. (2008). *Mycorrhizal Symbiosis*. Elsevier.

Soong, J. L., Fuchslueger, L., Marañon-Jimenez, S., Torn, M. S., Janssens, I. A., Penuelas, J., & Richter, A. (2020). Microbial carbon limitation: The need for integrating microorganisms into our understanding of ecosystem carbon cycling. *Global Change Biology*, *26*(4), 1953–1961. https://doi.org/10.1111/gcb.14962

Stewart, C. E., Follett, R. F., Pruessner, E. G., Varvel, G. E., Vogel, K. P., & Mitchell, R. B. (2016). N fertilizer and harvest impacts on bioenergy crop contributions to SOC. *GCB Bioenergy*, *8*(6), 1201–1211. https://doi.org/10.1111/gcbb.12326

Stoy, P. C., Ahmed, S., Jarchow, M., Rashford, B., Swanson, D., Albeke, S., Bromley, G., Brookshire, E. N. J., Dixon, M. D., Haggerty, J., Miller, P., Peyton, B., Royem, A., Spangler, L., Straub, C., & Poulter, B. (2018). Opportunities and Trade-offs among BECCS and the Food, Water, Energy, Biodiversity, and Social Systems Nexus at Regional Scales. *BioScience*, *68*(2), 100–111. https://doi.org/10.1093/biosci/bix145

Thompson, L. R., Sanders, J. G., McDonald, D., Amir, A., Ladau, J., Locey, K. J., Prill, R. J., Tripathi, A., Gibbons, S. M., Ackermann, G., Navas-Molina, J. A., Janssen, S., Kopylova, E., Vázquez-Baeza, Y., González, A., Morton, J. T., Mirarab, S., Zech Xu, Z., Jiang, L., … Knight, R. (2017). A communal catalogue reveals Earth's multiscale microbial diversity. *Nature*, *551*(7681), 457–463. https://doi.org/10.1038/nature24621

Tonitto, C., Woodbury, P. B., & McLellan, E. L. (2018). Defining a best practice methodology for modeling the environmental performance of agriculture. *Environmental Science & Policy*, *87*, 64–73. https://doi.org/10.1016/j.envsci.2018.04.009

U.S DOE. (2014). *Research for sustainable bioenergy: Linking genomic and ecosystem sciences*. U.S. Department of Energy Office of Science. https://genomicscience.energy.gov/sustainability/SustainableBiofuels-HR.pdf

Wang, G.-J., Nyren, P., Xue, Q.-W., Aberle, E., Eriksmoen, E., Tjelde, T., Liebig, M., Nichols, K., & Nyren, A. (2014). Establishment and Yield of Perennial Grass Monocultures and Binary Mixtures for Bioenergy in North Dakota. *Agronomy Journal*, *106*(5), 1605–1613.

Wang, L., Qian, Y., Brummer, J. E., Zheng, J., Wilhelm, S., & Parton, W. J. (2015). Simulated biomass, environmental impacts and best management practices for long-term switchgrass systems in a semi-arid region. *Biomass and Bioenergy*, *75*, 254–266. https://doi.org/10.1016/j.biombioe.2015.02.029

Wang, L., Qian, Y. L., Brummer, J., Wilhelm, S. J., & Leach, J. E. (2019). Biomass Production and Soil Carbon Analysis of Switchgrass under Rainfed or Minimal Irrigation in a Semiarid Environment. *Agronomy Journal*, *111*(4), 1704–1711. https://doi.org/10.2134/agronj2018.09.0568

Wanga, W., Ohse, K., Liu, J., Mo, W., & Oikawab, T. (2005). Contribution of root respiration to soil respiration in a C3/C4 mixed grassland. *Journal of Biosciences*, *30*(4), 507–514. https://doi.org/10.1007/BF02703725

Wieczorek, A. S., Schmidt, O., Chatzinotas, A., von Bergen, M., Gorissen, A., & Kolb, S. (2019). Ecological Functions of Agricultural Soil Bacteria and Microeukaryotes in Chitin Degradation: A Case Study. *Frontiers in Microbiology*, *10*. https://www.frontiersin.org/article/10.3389/fmicb.2019.01293

Wilson, G. W. T., Rice, C. W., Rillig, M. C., Springer, A., & Hartnett, D. C. (2009). Soil aggregation and carbon sequestration are tightly correlated with the abundance of arbuscular mycorrhizal fungi: Results from long-term field experiments. *Ecology Letters*, *12*(5), 452–461. https://doi.org/10.1111/j.1461-0248.2009.01303.x

Wright, L., & Turhollow, A. (2010). Switchgrass selection as a “model” bioenergy crop: A history of the process. *Biomass and Bioenergy*, *34*(6), 851–868. https://doi.org/10.1016/j.biombioe.2010.01.030

Xue, Q., Nyren, P. E., Wang, G., Eriksmoen, E., Bradbury, G., Halverson, M., Aberle, E., Nichols, K., & Liebig, M. (2011). Biomass composition of perennial grasses for biofuel production in North Dakota, USA. *Biofuels*, *2*(5), 515–528. https://doi.org/10.4155/bfs.11.123

Zhalnina, K., Hawkes, C., Shade, A., Firestone, M. K., & Pett-Ridge, J. (2021). Managing Plant Microbiomes for Sustainable Biofuel Production. *Phytobiomes Journal*, *5*(1), 3–13. https://doi.org/10.1094/PBIOMES-12-20-0090-E

Figures

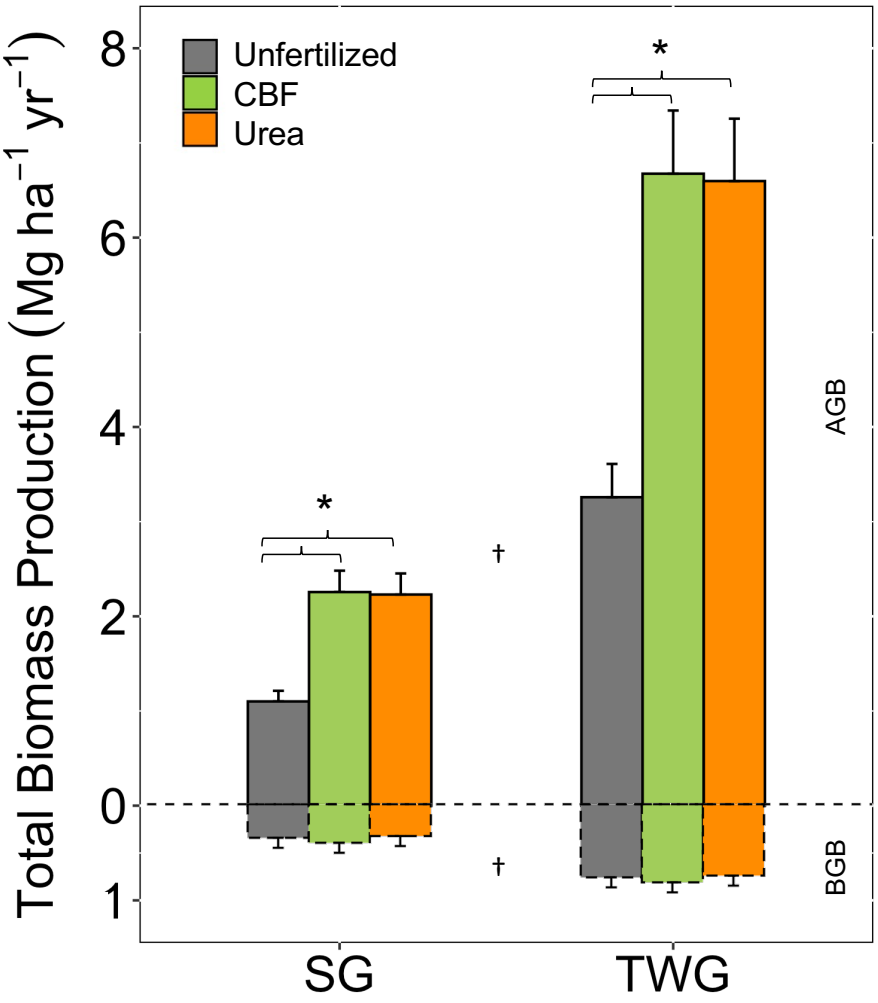


Figure 1. Above and belowground (0-15 cm) biomass production in 2020 for switchgrass (SG) and tall wheatgrass (TWG). * Denotes significance from Tukey's HSD post-hoc ($\alpha = 0.05$) between N fertilizer treatments and the unfertilized control while † denotes differences between crop type biomass pools, irrespective of fertilizer treatment. AGB = aboveground biomass and BGB = belowground biomass.

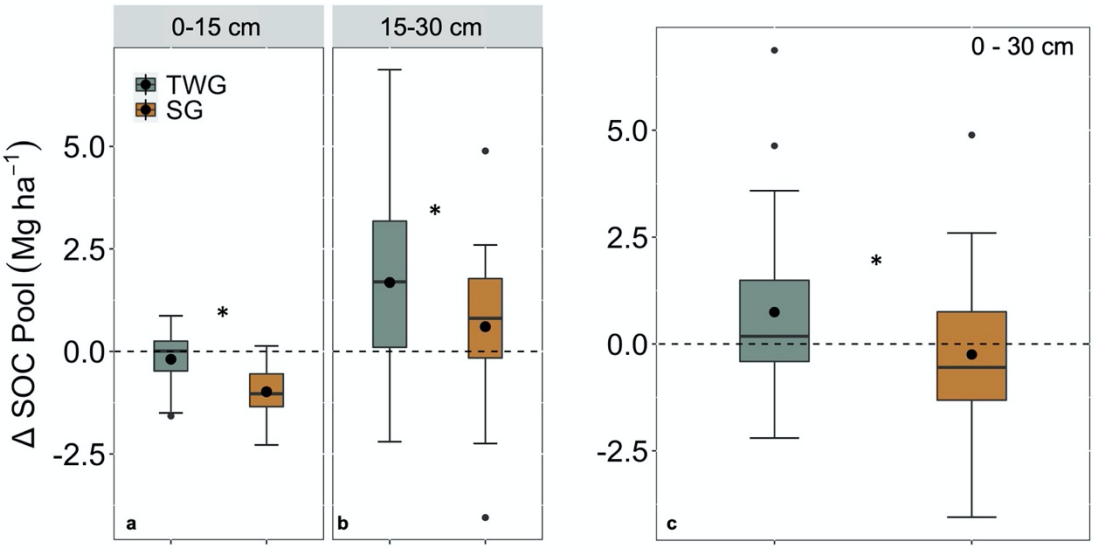


Figure 2. Box plots (median, 5th and 95th percentiles) of the three-year SOC change, with fertilizer treatment controlled for, at soil depth increments of 0-15 (a) and 15-30 (b) and 0-30 cm (c) across tall wheatgrass (TWG) and switchgrass (SG) plots. Black dots are least squared means and * denotes significance from Tukey's HSD post-hoc test (α = 0.05). Large black circles depict mean values.

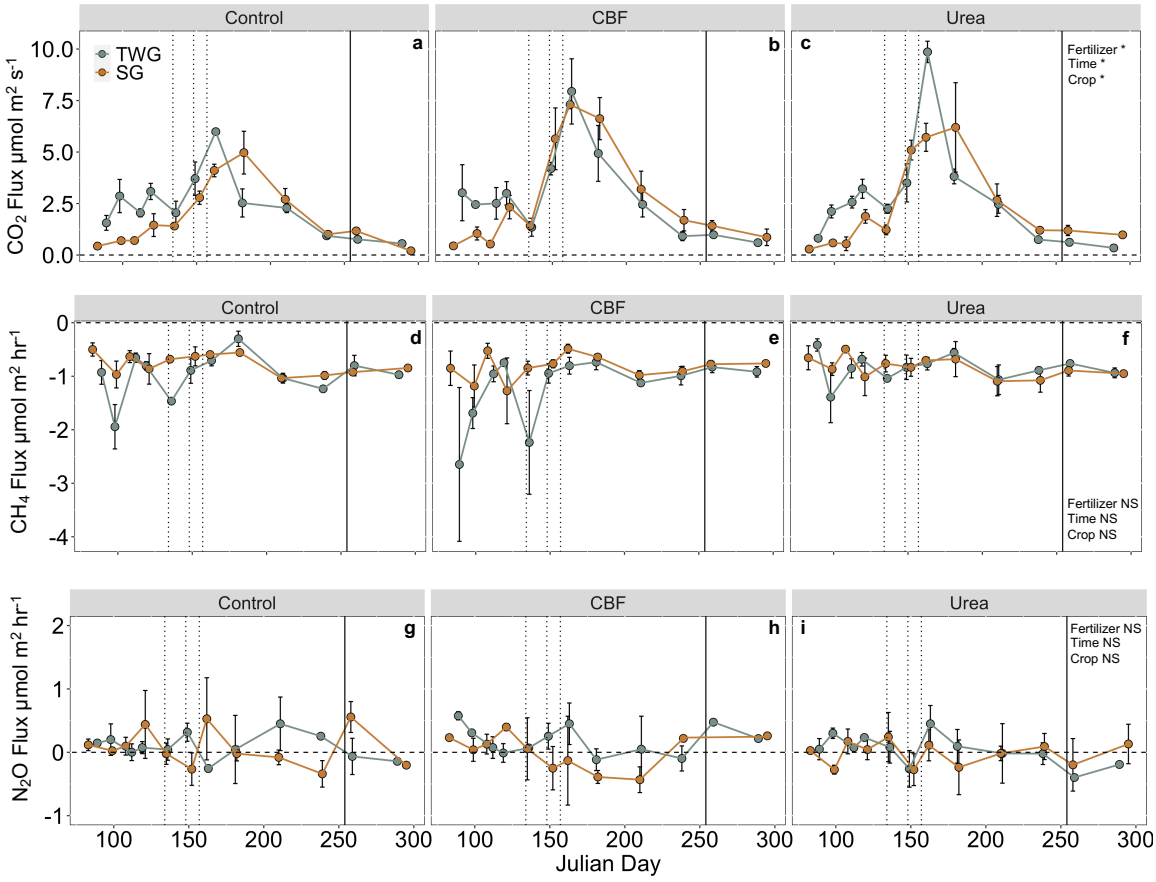


Figure 3. Time series of greenhouse gas fluxes of CO_2, CH_4, and N_2O across tall wheatgrass and switchgrass fertilizer treatments. Dotted black lines identify fertilizer application dates, and the solid black line represents the September harvest of aboveground biomass. Data points represent the mean (±SE) of the three reps measured during each sampling date. * Denotes significance from Tukey's HSD post-hoc (α = 0.05) of the fixed effects.

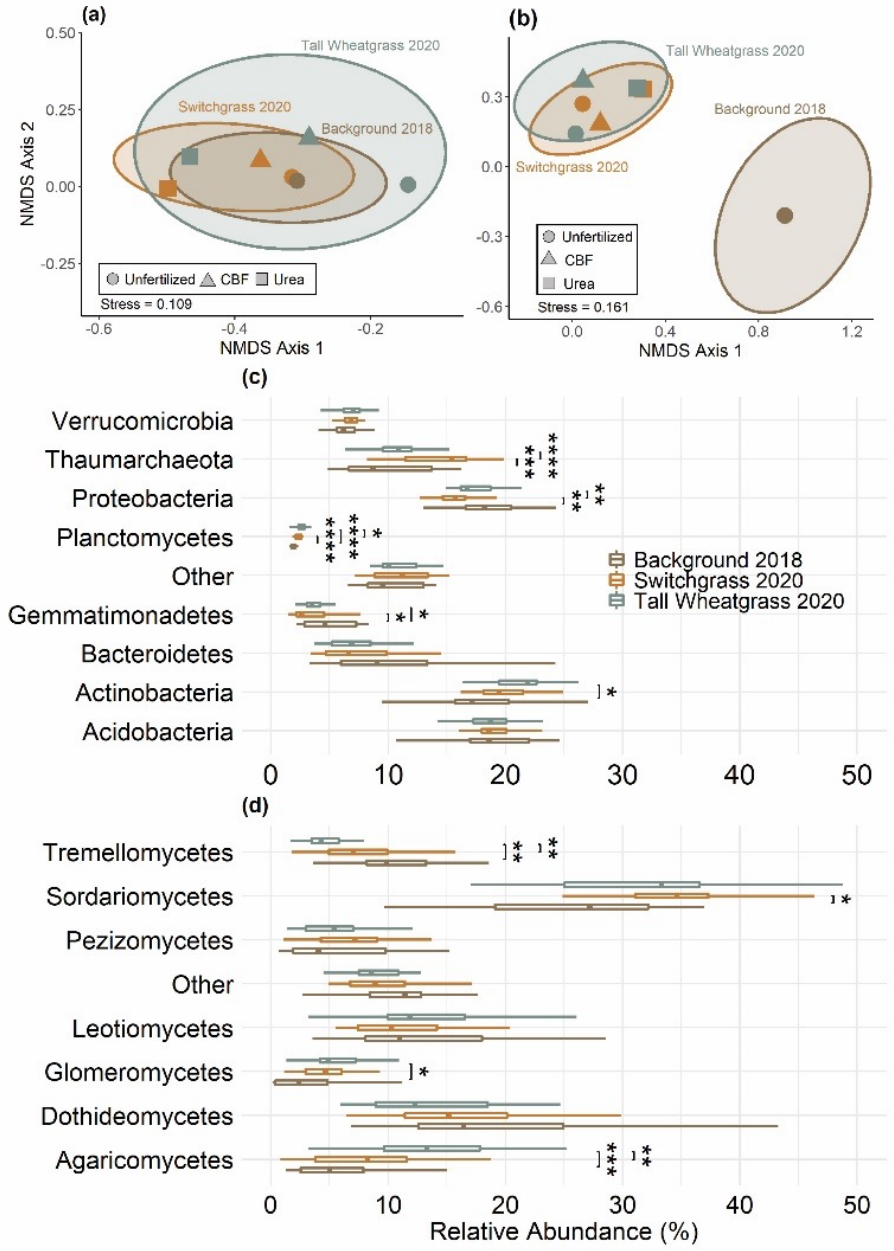


Figure 4. Bacterial (a) and fungal (b) soil community dissimilarity matrix for switchgrass and tall wheatgrass in 2020 and 2018 background soil conditions at 15-30 cm soil depth. Shapes represent centroids of n=3 samples for each fertilizer treatment (Unfertilized, CBF, or Urea). Comparisons of the relative abundance for bacterial (c; phylum level) and fungal (d; class level) communities between crop types in 2020 and background soil in 2018. * denote significance criteria * $p < 0.05$, ** $p < 0.01$, *** $p < 0.001$.

Tables

Table 1. Growing season CO_2 fluxes (least squared mean ± SE) by crop type and fertilizer treatment ($p = 0.002$). For each flux value temperature, moisture, and the other treatment variable (e.g., crop type or fertilizer) were controlled for as fixed effects in the model. Tall wheatgrass = (TWG), switchgrass = (SG), and cyanobacteria biofertilizer = (CBF).

Crop	Fertilizer Treatment	CO_2 (µmol m^{-2} s^{-1})
TWG	Control	1.86 (± 0.42)
SG	Control	1.33 (± 0.30)
TWG	CBF	2.29 (± 0.52)
SG	CBF	1.63 (± 0.37)
TWG	Urea	1.85 (± 0.41)
SG	Urea	1.32 (± 0.30)

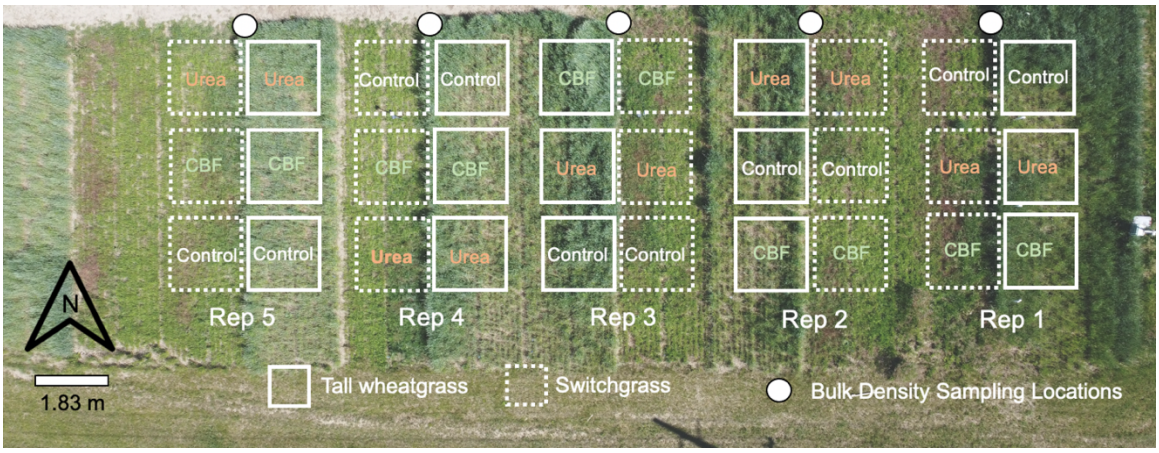
Table 2 Differences in CO_2 fluxes (μmol m^{-2} s^{-1}) between growing season months. Values are least squared means (± SE) with fertilizer type and soil temperature controlled for as a fixed effect.

Crop Type	Mar	Apr	May	Jun	July	Aug	Sept	Oct
Switchgrass	0.43(± 0.20)	0.65(± 0.16)	1.54(± 0.36)	4.38(± 1.11)	3.49(± 0.86)	1.06(± 0.38)	1.14(± 0.37)	0.42(± 0.16)
Tall Wheatgrass	1.54(± 0.54)	2.61(± 0.51)	2.98(± 0.70)	7.02(± 2.42)	2.91(± 0.70)	0.76(± 0.27)	0.72(± 0.24)	0.56(± 0.12)
p -value	0.026	0.0016	0.0746	0.2711	0.5860	0.4778	0.3366	0.5183

Table 3. Annual aboveground, belowground, and total annual productivity (to 15 cm soil depth). Values are reported as least square means with (±SE). Total biomass is calculated off the subset of plot replicates (n=9) that have paired aboveground biomass (AGB) and belowground biomass (BGB) measurements for each crop type.

	Tall wheatgrass		
Fertilizer	**AGB (n = 15)**	**BGB (n= 9)**	**Total Biomass (n = 9)**
Control	3.3 (±0.4)	0.82 (±0.1)	3.8 (±0.4)
Urea	6.6 (±0.7)	0.81 (±0.1)	7.5 (±0.9)
CBF	6.7 (±0.7)	0.88 (±0.1)	7.3 (±0.9)
p-value	< 0.0001	0.63	< 0.0001
	Switchgrass		
Control	1.1 (±0.1)	0.38 (±0.1)	1.3 (±0.2)
Urea	2.3 (±0.2)	0.43 (±0.1)	2.6 (±0.3)
CBF	2.2 (±0.2)	0.36 (±0.1)	2.5 (±0.3)
p-value	< 0.0001	0.63	0.0003

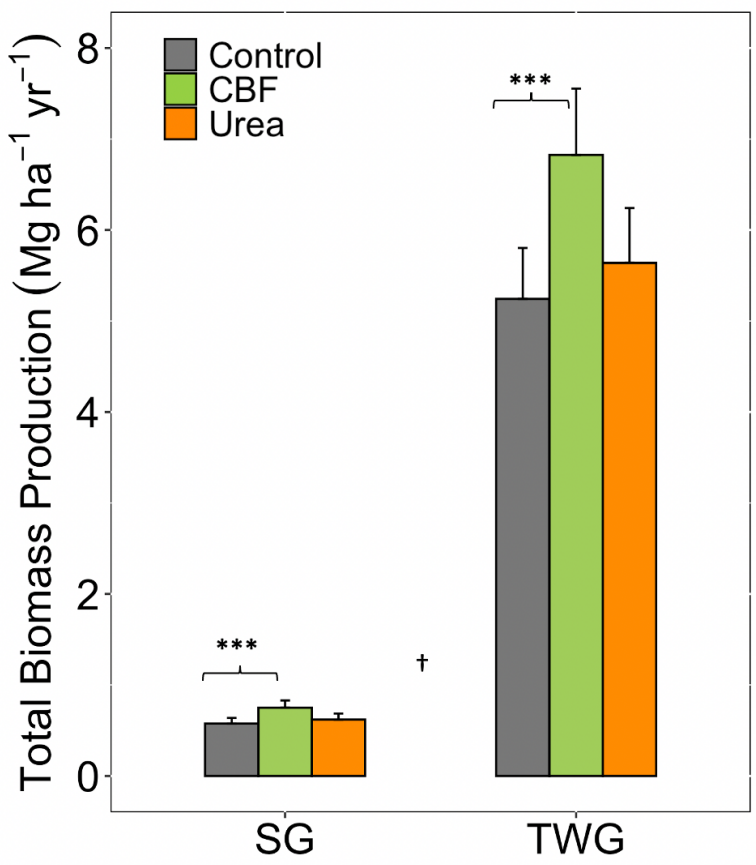
Supplemental Figures



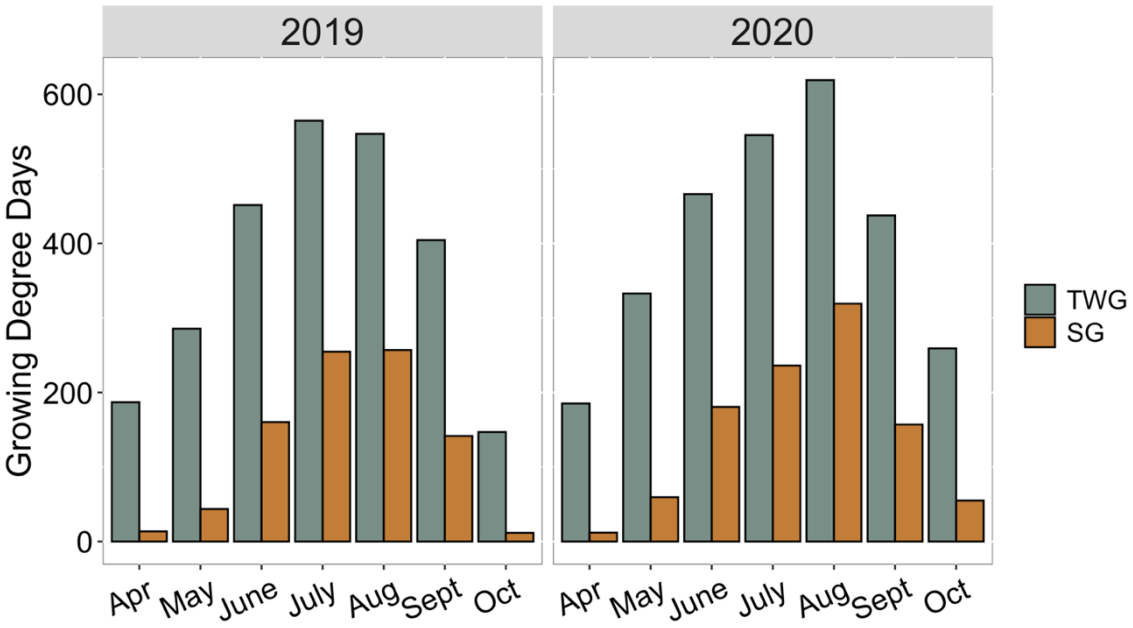
Supplemental Figure 1**.** The split-plot and randomized experimental design for this study on the Post Farm in Bozeman, MT, USA. Bulk density locations shown were used for the area scale measurements of soil organic carbon (SOC).



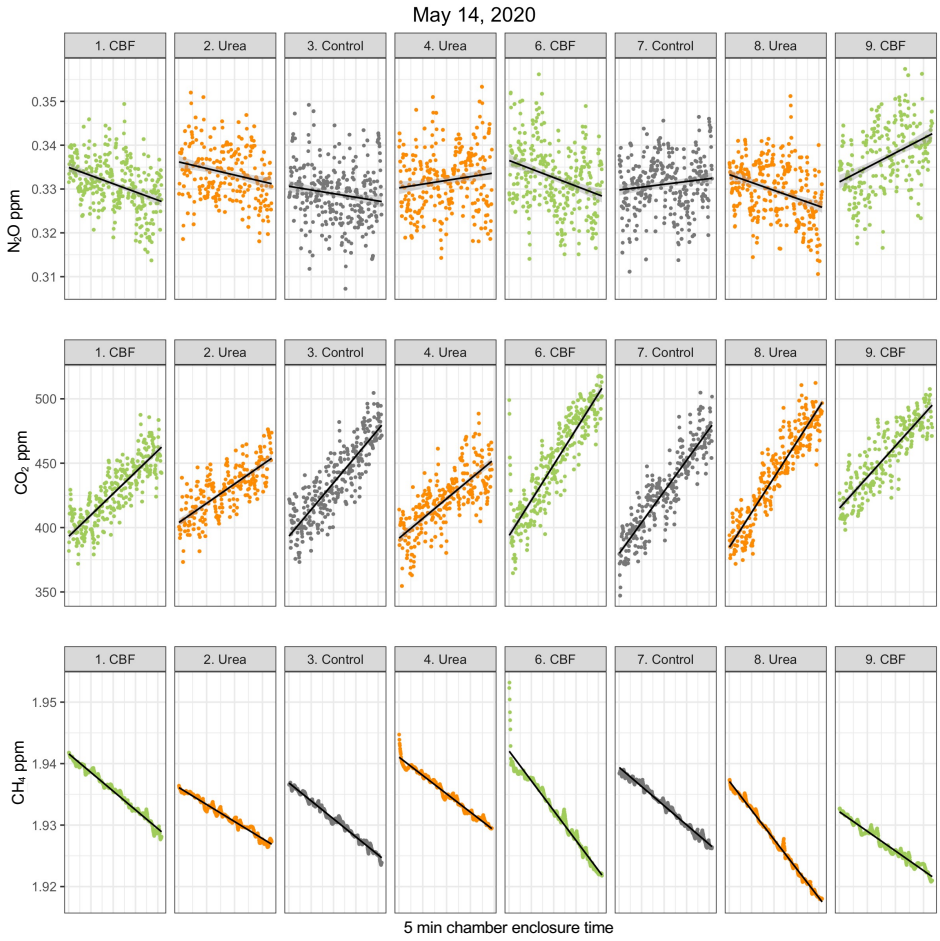
Supplemental Figure 2. Switchgrass and tall wheatgrass at the Post Farm, July 2020.



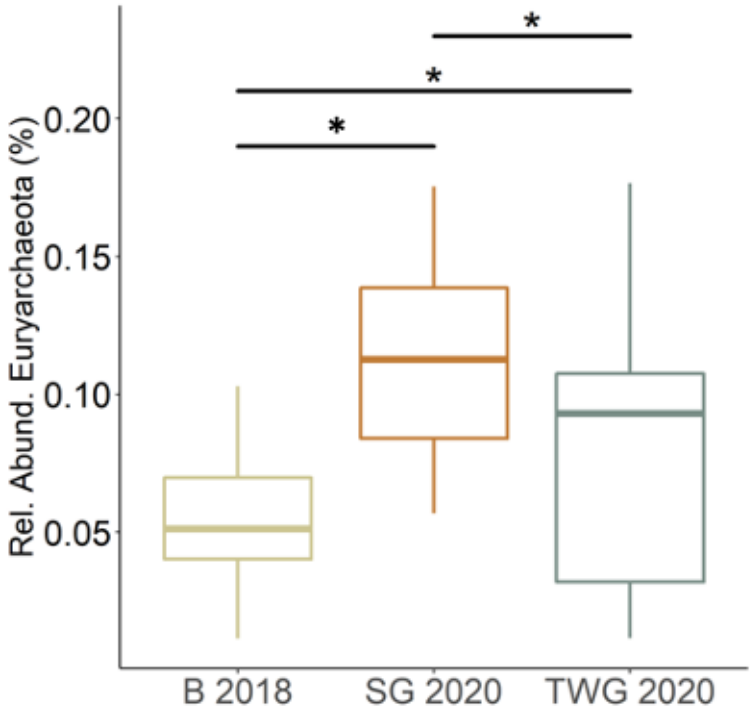
Supplemental Figure 3. Above ground biomass in 2019 for switchgrass (SG) and tall wheatgrass (TWG). *** Denotes significance from Tukey's HSD post-hoc ($\alpha = 0.05$) between N fertilizer treatments and the unfertilized control while † denotes differences between crop type biomass pools, irrespective of fertilizer treatment. Values are least square means ±SE



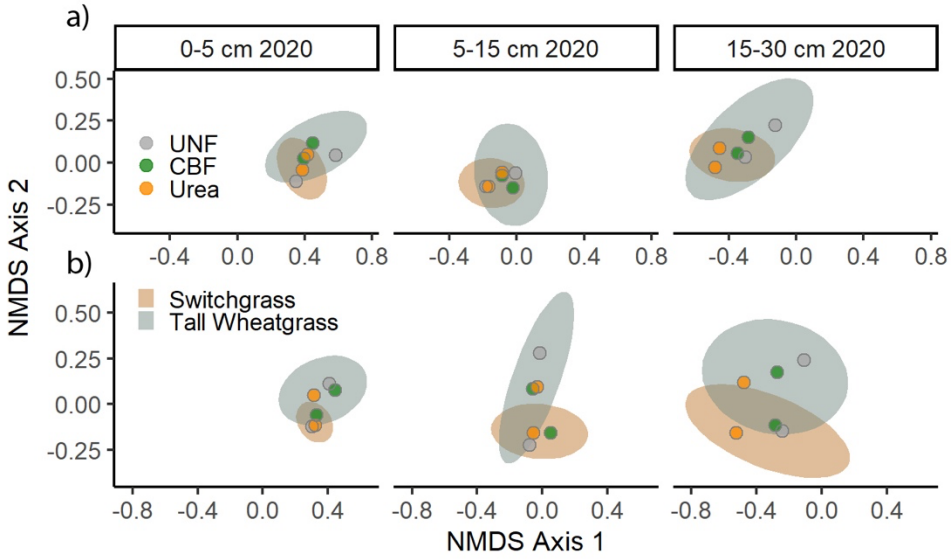
Supplemental Figure 4. Growing degree days for each bioenergy crop species in 2019 and 2020. Across both growing seasons tall wheatgrass (TWG) had 3 times more total growing degree days compared to switchgrass (SG, 5432 vs. 1902).



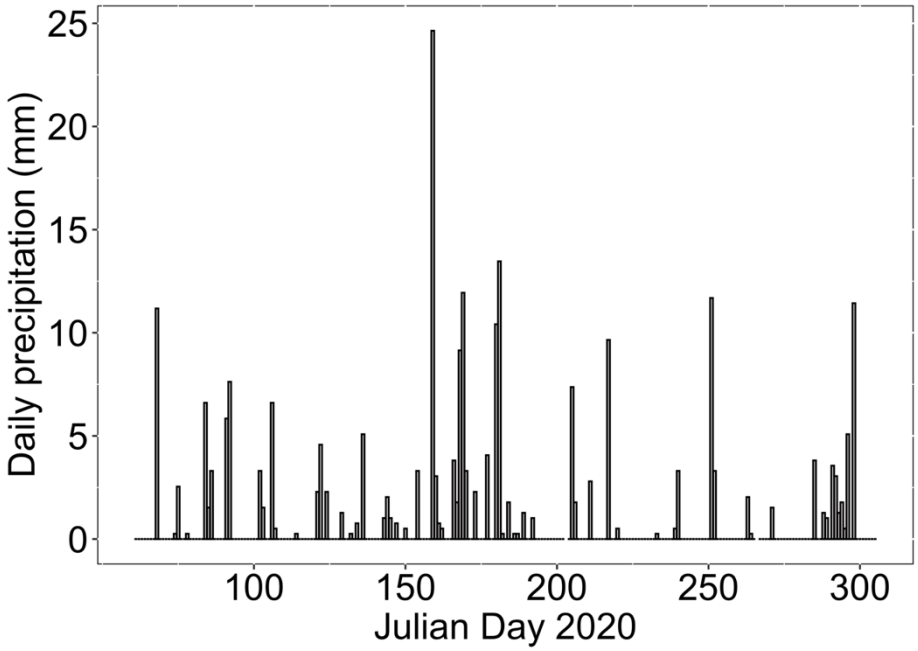
Supplemental Figure 5. An example of the regressions that were plotted after soil gas flux sampling to assess the linearity of flux development over the chamber deployment time. The ordinate indicates the GHG concentration and the abscissa for all graphs is the 5-minute deployment time.



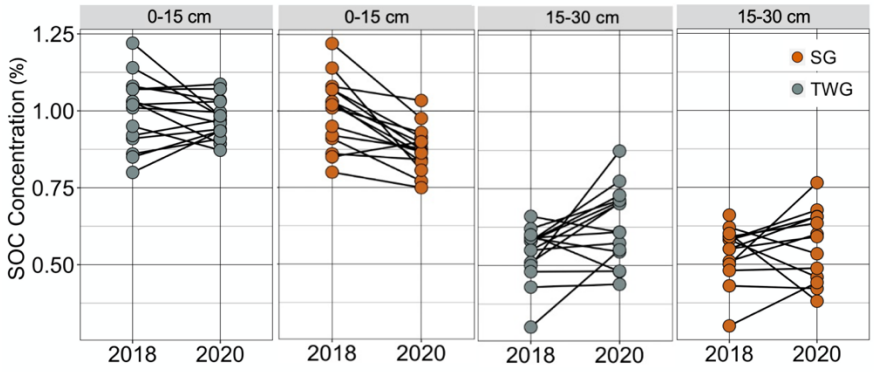
Supplemental Figure 6. Changes in the relative abundance of the methanogenic Euryarchaeota in soil from 2018 to 2020. B = Background, SG = Switchgrass, TWG = Tall wheatgrass. * Denotes significance from Tukey's HSD post-hoc ($\alpha = 0.05$).



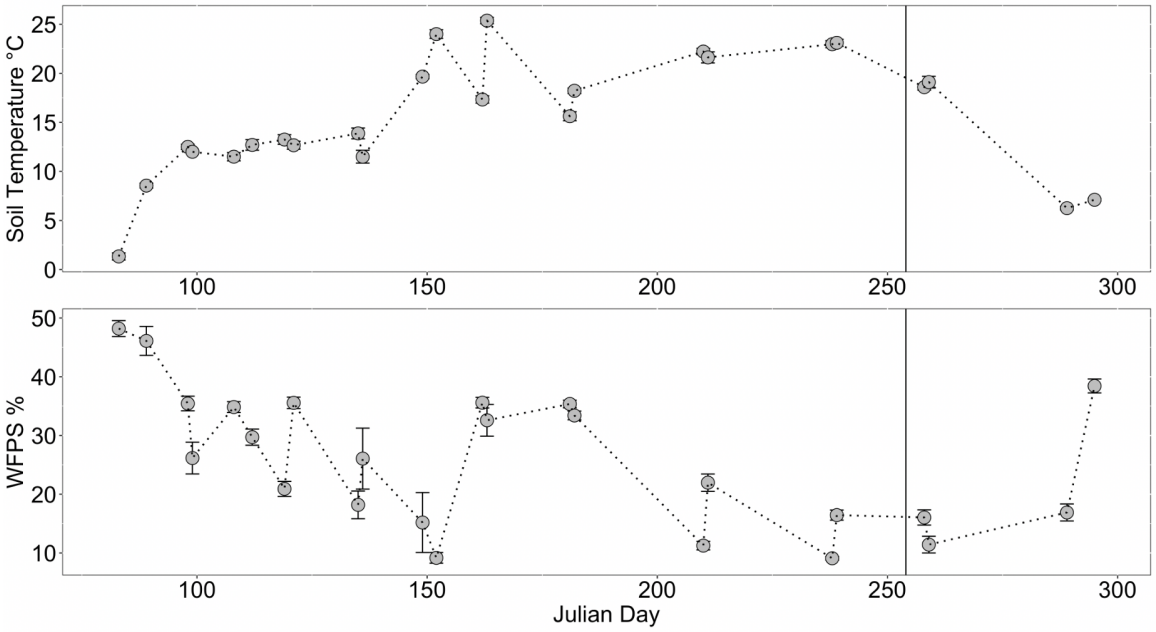
Supplemental Figure 7. Dissimilarity matrix of Bacterial/archaeal (a) and fungal (b) community composition across fertilizer and crop treatments at different soil depths in 2020. UNF = unfertilized control and CBF = cyanobacteria fertilizer.



Supplemental Figure 8. Daily precipitation (mm) during the 2020 growing season (March-October).



Supplemental Figure 9. Soil organic carbon (SOC) shifts from 2018 (pre-treatments) to 2020 at soil depths of 0-15 cm and 15-30 cm. Lines connect paired plot measurements and slope direction depicts an increase or decrease in SOC between the two-time points.



Supplemental Figure 10. Soil temperature and water-filled pore space across the sampling period in 2020. Collections aligned with GHG flux measurements, and the solid line depicts when crops were harvested. Values are modeled means with ±SE.

Supplemental Tables

Supplemental Table 1. Changes in soil organic carbon (SOC; Mg ha^{-1}) at binned soil depths, crop type, and SOC fluxes (Mg SOC ha^{-1} yr^{-1}). Values are Least squared mean ±SE

Tall Wheatgrass		
Soil depth cm	Δ SOC 2018-2020	SOC flux
0-15	-0.08 (±0.5)	-0.02 (±0.2)
15-30	1.57 (±0.5)	0.52 (±0.2)
0-30	0.75 (±0.4)	0.25 (±0.2)
Switchgrass		
0-15	-1.09 (±0.5)	-0.36 (±0.2)
15-30	0.56 (±0.5)	0.18 (±0.2)
0-30	-0.23 (±0.5)	-0.08 (±0.2)

Supplemental Table 2**.** Above and belowground biomass chemistry of each crop species. Values are reported as least squared means ±SE and have the other variable controlled (e.g. crop or fertilizer treatment) for in model outputs. TWG = tall wheatgrass, SG = switchgrass, CBF = cyanobacteria biofertilizer.

Crop	**AGB %C**	**BGB %C**	**AGB %N**	**BGB %N**	**AGB C:N**	**BGB C:N**
TWG	44.1(±0.22)	43.6(±0.35)	0.59(±0.05)	0.81(±0.11)	77.4(±5.1)	63.5(±4.6)
SG	45.4(±0.23)	45.7(±0.35)	0.67(±0.05)	1.05(±0.08)	72.1(±4.9)	53.9(±4.6)
p-value	< 0.0001	< 0.0001	0.24	0.05	0.44	0.14
Fertilizer						
Control	44.1(±0.28)	44.5(±0.4)	0.55(±0.05)	0.80(±0.10)	83.5(±6.2)	65.5(±5.6)
Urea	45.1(±0.27)	44.6(±0.4)	0.68(±0.06)	1.0(±0.12)	71.4(±6)	56.0(±5.6)
CBF	45.0(±0.27)	45.0(±0.4)	0.67(±0.06)	0.97(±0.12)	69.5(±6)	54.6(±5.6)
p-value	0.02	0.64	0.21	0.32	0.20	0.34

Supplemental Table 3. Aboveground biomass production of non-irrigated switchgrass and tall wheatgrass across the Northern Great Plains region in the U.S. Mean growing season precipitation (MGSP) and mean growing season temperature (MGST). [1](Wang et al., 2019),[2](Schmer et al., 2012), [3](Liebig et al., 2008), [4](Harmoney, 2015), [5](Wang et al., 2015)

Location	**Range in yield (Mg ha^{-1} yr^{-1})**	**Mean yield (Mg ha^{-1} yr^{-1})**	**Fertilization**	**MGSP (mm)**	**MGST(°C)**	**Length (yrs.)**	**Crop**
Fort Collins, Co[1]	4.1-7.1	5.6	50N & 45P kg ha^{-1}	420*	NA	4	Switchgrass
Mandan, ND[2]	5.2-11.1	8.1	N 67 kg ha^{-1}	315	19.1	1	Switchgrass
Ethan, SD[3]	0.6-4.9	2.8	N, 67-112 kg ha^{-1}	453	16.8	2	Switchgrass
Huron, SD[3]	3.1-7.4	5.3	N, 67-112 kg ha^{-1}	404	16.5	2	Switchgrass
Highmore, SD[3]	0.1-2.7	1.4	N, 67-112 kg ha^{-1}	316	16.5	2	Switchgrass
Bristol, SD[3]	5.5-10.1	7.8	N, 67-112 kg ha^{-1}	398	15.7	2	Switchgrass
Streeter, ND[3]	3.1-7.4	5.3	N, 67-112 kg ha^{-1}	372	13.3	2	Switchgrass
Munich, ND[3]	1.5-7.9	4.7	N, 67-112 kg ha^{-1}	454	12	2	Switchgrass
Carrington, ND[5]	7.5-13.9	10.3	Not reported	385	15.4	5	Switchgrass
Streeter, ND[5]	3.1-9.8	5.1	Not reported	348	14.3	5	Switchgrass
Minot, ND[5]	3.0-9.0	5.9	Not reported	334	14.7	5	Switchgrass
Williston, ND[5]	1.1-4.4	2.4	Not reported	294	15.7	5	Switchgrass
Hays, KS[4]	2.6-9.7	4.6	N, 56 kg ha^{-1} yr^{-1}, 112 kg ha P_2O_5	576 (annual)	NA	4	Tall wheatgrass
Carrington, ND[5]	8.9-10.5	9.8	Not reported	385	15.4	5	Tall wheatgrass
Streeter, ND[5]	5.2-7.7	6.1	Not reported	348	14.3	5	Tall wheatgrass
Minot, ND[5]	5.7-8.8	7.7	Not reported	334	14.7	5	Tall wheatgrass
Williston, ND[5]	1.6-3.6	2.4	Not reported	294	15.7	5	Tall wheatgrass
Mean range		1.4-10.3					Switchgrass
Mean range		2.4-9.8					Tall wheatgrass
This study	0.4-2.9	2.2	N, 56 kg ha^{-1} yr^{-1},	342	11.4	3	Switchgrass
This study	2.5- 11.1	6.8	N, 56 kg ha^{-1} yr^{-1},	342	11.4	3	Tall wheatgrass

Supplemental Table 4. Crop rain use efficiency (RUE; kg dry matter mm precipitation^{-1}) of each crop and fertilizer treatment in 2020.

Switchgrass	**RUE**
Control	4.1
Urea	8.6
CBF	8.2
Tall wheatgrass	
Control	12.3
Urea	24.9
CBF	24.5

Supplemental Table 5. Soil waterfilled pore space (WFPS; %) by month during the growing season. Least square means are reported (± SE).

	Mar	Apr	May	Jun	July	Aug	Sept	Oct
Control	0.49(± 0.07)	0.32 (± 0.04)	0.25 (± 0.05)	0.28(± 0.06)	0.28(± 0.05)	0.15(± 0.07)	0.16(± 0.07)	0.30(± 0.07)
CBF	0.46(± 0.07)	0.28 (± 0.04)	0.22 (± 0.05)	0.24 (± 0.06)	0.24 (± 0.05)	0.11 (± 0.07)	0.12 (± 0.07)	0.26 (± 0.07)
Urea	0.47(± 0.07)	0.29 (± 0.04)	0.23 (± 0.05)	0.26 (± 0.06)	0.25 (± 0.05)	0.12 (± 0.07)	0.13 (± 0.07)	0.28 (± 0.07)

Supplemental Table 6. Mean growing season fluxes of CO_2, CH_4 flux, and N_2O flux by crop type with fertilizer treatment temperature and moisture controlled for as fixed effects. Values are reported as least squared means (± SE).

	***p* value**	**Mean**	**Min**	**Max**	**n**
N_2O ($\mu mol\ m^{-2}\ hr^{-1}$)	0.11				
Switchgrass		0.05 (±0.08)	-0.84	1.8	92
Tall wheatgrass		0.15 (±0.08)	-0.62	2.1	88
CH_4 ($\mu mol\ m^{-2}\ hr^{-1}$)	0.06				
Switchgrass		-0.80 (± 0.08)	-2.5	-0.1	106
Tall wheatgrass		-1.00 (± 0.08)	-5.5	-0.2	99
CO_2 ($\mu mol\ m^{-2}\ s^{-1}$)	0.27				
Switchgrass		1.4 (± 0.1)	0.14	10.4	106
Tall Wheatgrass		2.0 (± 0.2)	0.22	10.8	99

Supplemental Table 7**.** Summary of PERMANOVA statistics and p-values for fungal and bacterial/archaeal communities. Significant p-values (Bonferroni-corrected) are bolded at ($\alpha = 0.05$).

Fungal Community	**Pseudo F-statistic**	**P-value**
Crop	7.89	**0.001**
Treatment	1.54	**0.011**
Depth	4.41	**0.001**
Betadisper$Crop	5.66	**0.001**
Betadisper$Treatment	.062	0.948
Betadisper$Depth	1.50	0.217
Bacterial/Archaeal Community		
Crop	4.61	**0.001**
Treatment	1.17	0.276
Depth	1.54	0.064
Betadisper$Crop	10.5	**0.001**
Betadisper$Treatment	1.58	0.226
Betadisper$Depth	1.44	0.231

Supplemental Table 8. Relative abundances (%) of major bacterial/archaeal phyla across crop types (SG 2020 = Switchgrass in 2020, TWG 2020 = Tall Wheatgrass in 2020) and compared to the 2018 background soil (B 2018). Letters indicate Bonferroni-corrected differences at ($\alpha = 0.05$).

Bacterial/Archaeal Phyla	**B 2018**	**SG 2020**	**TWG 2020**
Acidobacteria	18.9±1.94	18.9±0.666	18.6±1.04
Actinobacteria	16.3±1.97^{b}	18.05±0.666^{b}	19.7±1.14^{a}
Bacteroidetes	11.1±3.82	7.42±1.22	7.48±1.41
Chloroflexi	1.49±0.167^{b}	1.56±0.0826^{b}	2.11±0.316^{a}
Gemmatimonadetes	5.03±1.10^{a}	3.36±0.637^{b}	3.58±0.411^{b}
Other (< 1%)	10.2±1.54	11.3±1.09	10.4±0.953
Planctomycetes	1.87±0.129^{c}	2.36±0.124^{b}	2.67±0.172^{a}
Proteobacteria	18.6±1.46^{a}	15.9±0.596^{b}	17.8±0.857^{a}
Thaumarchaeota	10.1±1.93^{b}	14.4±1.24^{a}	10.7±1.10^{b}
Verrucomicrobia	6.32±0.618	6.68±0.389	6.99±0.445

Supplemental Table 9. Relative abundances (%) of major fungal classes across crop types (SG 2020 = Switchgrass in 2020, TWG 2020 = Tall Wheatgrass in 2020) and compared to the 2018 background soil (B 2018). Letters indicate Bonferroni-corrected differences at differences at ($\alpha = 0.05$).

Fungal Class	**B 2018**	**SG 2020**	**TWG 2020**
Agaricomycetes	6.41±2.83[b]	8.56±2.39[b]	15.0±3.49[a]
Blastocladiomycetes	1.31±0.957	0.224±0.198	0.238±0.107
Chytridiomycetes	2.17±1.14	1.74±0.925	1.76±0.679
Dothideomycetes	20.3±5.72	15.6±2.29	14.2±2.99
Eurotiomycetes	2.12±0.497	3.02±0.729	2.74±0.625
Glomeromycetes	3.04±1.55[b]	4.79±0.907[ab]	5.92±1.34[a]
Leotiomycetes	12.3±4.76	11.5±1.90	13.3±2.33
Other (< 1%)	1.40±0.568	1.83±0.570	1.05±0.399
Pezizomycetes	6.02±2.55	7.63±2.02	5.71±1.39
Sordariomycetes	27.2±5.25[b]	34.8±2.64[a]	32.0±3.29[ab]
Tremellomycetes	11.7±4.05	7.71±1.61	4.91±0.970
Ustilaginomycetes	0.187±0.0754[ab]	0.267±0.0567[a]	0.118±0.0392[b]
Zygomycota_incertae_sedis	4.02±1.16	2.57±0.636	3.13±0.606

Supplemental Table 10. Identity & ecology of zOTUS in the fungal classes Exobasidiomycetes and Ustilaginomycetes. See supplemental citations section.

ID	Species	Ecology
Zotu175	*Tranzscheliella yupeitaniae*	Grass pathogen (Harmoney, 2015)
Zotu557	*Ustilago avenae*	Loose smut of barley (Hu et al., 2018)
Zotu750	*Tilletia puccinelliae*	Grass smut (Bao et al., 2010)
Zotu836	*Malassezia restricta*	Endoparasitic nematode-associated soil fungi(Elhady et al., 2017) Mammalian yeast pathogen(Prohic et al., 2016)
Zotu1477	*Ustilago calamagrostidis*	Leaf smut(Kruse et al., 2018)
Zotu1907	*Urocystis alopecuri*	Foxtail smut(Bauer et al., 2008; McKenzie & Vánky, 2001)

Supplemental Table 11. Levene's test results for equal variance of SOC change from 2018-2020 for both crops at 0-15 cm and 15-30 cm.

SG	F-value	p - value
0-15 cm	2.6018	0.12
15-30 cm	1.8968	0.18
TWG		
0-15 cm	3.6286	0.07
15-30 cm	2.5014	0.13

Supplemental Methods

Water filled pore space

WFPS (0- 5 cm soil depth) was by calculated via the equation 1a. Mean bulk density for 0 - 5cm (1.12 g/cm^2) was calculated from samples taken in each plot across 3 reps of both crops (n =18) and a standard soil particle density of 2.66 g/cm^3 was used.

$$\frac{100 * \text{(gravimetric soil moisture content * bulk density)}}{(1 - \text{particle density})}$$

References

Bao, X., Carris, L. M., Huang, G., Luo, J., Liu, Y., & Castlebury, L. A. (2010). Tilletia puccinelliae, a new species of reticulate-spored bunt fungus infecting Puccinellia distans. *Mycologia*, *102*(3), 613–623. https://doi.org/10.3852/09-135

Bauer, R., Lutz, M., Begerow, D., Piątek, M., Vánky, K., Bacigálová, K., & Oberwinkler, F. (2008). Anther smut fungi on monocots. *Mycological Research*, *112*(11), 1297–1306. https://doi.org/10.1016/j.mycres.2008.06.002

Elhady, A., Giné, A., Topalovic, O., Jacquiod, S., Sørensen, S. J., Sorribas, F. J., & Heuer, H. (2017). Microbiomes associated with infective stages of root-knot and lesion nematodes in soil. *PLOS ONE*, *12*(5), e0177145. https://doi.org/10.1371/journal.pone.0177145

Harmoney, K. R. (2015). Cool-Season Grass Biomass in the Southern Mixed-Grass Prairie Region of the USA. *BioEnergy Research*, *8*(1), 203–210. https://doi.org/10.1007/s12155-014-9514-9

Hu, J., Yang, J. Y., Li, J., Gao, T., Yang, G. W., & Ren, H. Y. (2018). First report of Ustilago avenae causing loose smut of oat (Avena sativa) in Shandong China. *Journal of Plant Pathology*, *100*(1), 123–123. https://doi.org/10.1007/s42161-018-0016-z

Kassambara (2021). rstatix: Pipe-Friendly Framework for Basic Statistical Tests. R package version 0.7.0. https://CRAN.R-project.org/package=rstatix

Kruse, J., Dietrich, W., Zimmermann, H., Klenke, F., Richter, U., Richter, H., & Thines, M. (2018). Ustilago species causing leaf-stripe smut revisited. *IMA Fungus*, *9*(1), 49–73. https://doi.org/10.5598/imafungus.2018.09.01.05

Lahti L, Shetty S (2012-2019). "microbiome R package."

Li, Y.-M., Shivas, R. G., & Cai, L. (2017). Cryptic diversity in Tranzscheliella spp. (Ustilaginales) is driven by host switches. *Scientific Reports*, *7*(1), 43549. https://doi.org/10.1038/srep43549

Liebig, M. A., Schmer, M. R., Vogel, K. P., & Mitchell, R. B. (2008). Soil Carbon Storage by Switchgrass Grown for Bioenergy. *BioEnergy Research*, *1*(3), 215–222. https://doi.org/10.1007/s12155-008-9019-5

McKenzie, E. H. C., & Vánky, K. (2001). Smut fungi of New Zealand: An introduction, and list of recorded species. *New Zealand Journal of Botany*, *39*(3), 501–515. https://doi.org/10.1080/0028825X.2001.9512753

Oksanen, J., Blanchet, F. G., Friendly, M., Kindt, R., Legendre, P., McGlinn, D., . . . Wagner, H. (2019). Community Ecology Package (Version 2.5-6). CRAN. Retrieved from (Prohic et al., 2016), https://github.com/vegandevs/vegan

Prohic, A., Jovovic Sadikovic, T., Krupalija-Fazlic, M., & Kuskunovic-Vlahovljak, S. (2016). Malassezia species in healthy skin and in dermatological conditions. *International Journal of Dermatology*, *55*(5), 494–504. https://doi.org/10.1111/ijd.13116

Schmer, M. R., Liebig, M. A., Hendrickson, J. R., Tanaka, D. L., & Phillips, R. L. (2012). Growing season greenhouse gas flux from switchgrass in the northern great plains. *Biomass and Bioenergy*, *45*, 315–319. https://doi.org/10.1016/j.biombioe.2012.05.026

Wang, L., Qian, Y., Brummer, J. E., Zheng, J., Wilhelm, S., & Parton, W. J. (2015). Simulated biomass, environmental impacts and best management practices for long-term switchgrass systems in a semi-arid region. *Biomass and Bioenergy*, *75*, 254–266. https://doi.org/10.1016/j.biombioe.2015.02.029

Wang, L., Qian, Y. L., Brummer, J., Wilhelm, S. J., & Leach, J. E. (2019). Biomass Production and Soil Carbon Analysis of Switchgrass under Rainfed or Minimal Irrigation in a Semiarid Environment. *Agronomy Journal*, *111*(4), 1704–1711. https://doi.org/10.2134/agronj2018.09.0568

CHAPTER THREE

THE CUMULATIVE EFFECTS OF CONIFER EXPANSION AND PRESCRIBED FIRE ON ECOSYSTEM CARBON AND NITROGEN CYCLING IN A TEMPERATE GRASSLAND

Contribution of Authors and Co-Authors

Manuscript in Chapter 3

Author: Justin D. Gay
Contributions: Helped conceive the project and sampling design, established field plots, collected and processed field samples, analyzed the data and created figures; drafted the initial manuscript

Co-Author: Bryce Currey
Contributions: Helped conceive the project and sampling design; established field plots, collected and processed field samples, analyzed data, and revised the manuscript

Co-Author: ENJ Brookshire
Contributions: Conceived the project; established field plots, assisted with data interpretation, revised and read the manuscript.

Manuscript Information

Justin D. Gay, Bryce Currey, ENJ Brookshire
Ecosystems

Status of Manuscript:
__x__ Prepared for submission to a peer-reviewed journal
____ Officially submitted to a peer-reviewed journal
____ Accepted by a peer-reviewed journal
____ Published in a peer-reviewed journal

THE CUMULATIVE EFFECTS OF CONIFER EXPANSION AND PRESCRIBED FIRE ON ECOSYSTEM CARBON AND NITROGEN CYCLING IN A TEMPERATE GRASSLAND

J.D. Gay[1], B. Currey[1], E.N.J. Brookshire[1]

[1]Land Resources and Environmental Science. Montana State University. 334 Leon Johnson Hall. P.O. Box 173120. Bozeman, MT 59717-3120, USA

Keywords

Grassland, Prescribed fire, Pyrogenic organic matter, Woody plant expansion, Nitrogen, Carbon, Conifer

Abstract

Woody plant expansion (WPE) into grasslands is a well-documented phenomenon, but its effect on biogeochemical processes remain poorly understood, particularly in response to fire. Fire is essential for maintaining grassland ecosystem structure and biogeochemical function; however, it is unclear how recent WPE might influence the cycling of carbon (C) and nitrogen (N). For example, WPE leads to a redistribution of biomass C and N aboveground, increasing the risk of volatilization loss during fire. However, the incomplete combustion of woody vegetation produces pyrogenic organic matter (PyOM), which can buffer overall emission loss and influences post-fire soil organic matter processes but is rarely quantified in fire C and N budgets. To investigate the effects of WPE and fire on

grassland ecosystem C and N cycling, we used long-term monitoring plots in a region of the northern Great Plains that has experienced dramatic conifer expansion (*Pinus ponderosa and Juniperus spp.)* and associated biomass-C accumulation since 1950. We assess soil C and N in response to a single, low-severity prescribed fire, and employ a space-for-time experimental design to determine the effects of fire across a grassland-savanna gradient. The 2018 fire led to significant losses of C and N via emissions. Juniper mortality drove N loss while each species equally contributed to C losses, despite less ponderosa mortality. However, one-year post-fire we observed transformations in the mineral organic matter, with soil C and N concentrations increasing due to the incorporation of PyOM. Together these results show that the interactions of WPE and fire have significant impacts on the biogeochemistry of transitional grassland-savannas and are critical for understanding future nitrogen limitation, evaluating regional C sequestration potential, and informing management.

Highlights

- Pre-fire woody biomass C accumulated at 0.75 ± 0.23 Mg C ha^{-1} since 1950.
- The combustion of *Juniperus* biomass led to outsized emission losses of N compared to *P. Ponderosa.*
- A low-severity prescribed fire led to one-year increases in mineral soil C and N

Introduction

The expansion of woody plants (WPE) into grasslands is a global phenomenon that can drastically alter ecosystem processes, including the cycling of carbon (C) and nutrients critical to primary production and soil organic matter turnover, including nitrogen (N; Barger et al., 2011; Liao et al., 2008; Reich et al., 2001). Fire exclusion is a key factor responsible for conifer WPE in many temperate grasslands and has been shown to accelerate WPE, increase stand density, and replace grassy understory with bare ground and needle litter (Currey et al. in preparation, Covington and Sackett 1992). Over a period of decades, the cumulative effects of WPE and fire exclusion have caused many grassland ecosystems to shift towards savanna-grassland mosaics, leading to large accumulations in woody biomass and litter C and N that, compared to grasses, are differentially susceptible to volatile loss upon the return of fire (MacKenzie et al., 2004; Tilman et al., 2000). However, the magnitude and trajectory of C and N loss or gain in response to fire in areas of recent WPE remain unclear but likely depend on three critical factors: 1) fire severity and frequency, 2) the quantity and quality of vegetation fuel, and 3) the amount of incompletely combusted biomass, or pyrogenic organic matter (PyOM), that returns to the soil and offsets emission losses.

Vegetation fire exerts substantial impacts on the biogeochemistry of ecosystems across a range of temporal scales and is influenced by fire characteristics (i.e., severity and frequency) and vegetation fuel (McLauchlan et al., 2020; Pellegrini et al., 2020). From an immediate perspective, vegetation fires cause significant net losses of C and N through their emissions to the atmosphere (van der Werf et al., 2017), but over decades, these

ecosystems can shift back to C sinks, depending on the rate of vegetation regrowth (Dore et al., 2008). Conversely, N pools may take centuries to recover after fire in some ecosystems due to the slow rate of atmospheric deposition and biological fixation (Johnson et al., 1998). Thus, woody vegetation biomass may be a large and important vector for C and N loss in grasslands experiencing WPE since C and N storage is shifted from below- to above-ground biomass pools, increasing vulnerability to fire. While estimates of C loss from vegetation are common, they are rarely reported for N. The few studies that have reported N emissions in response to fire document large and ecologically significant losses (Boby et al., 2010; Harden et al., 2002; Johnson et al., 1998), emphasizing the need to better understand fire-driven N-cycling dynamics in grasslands affected by WPE. In contrast to the large and immediate atmospheric losses of biomass C and N from vegetation fire, soils act as C and N sources or sinks depending on the severity or frequency of fire (Pellegrini et al., 2018). For example, during low to moderate severity fires, the soil profile does not reach sufficiently high temperatures for C and N volatilization. Further, while areas subjected to repeated and higher intensity burns display substantial loss of mineral soil C and N, responses from single fires are more equivocal (Pellegrini et al. 2020). The mechanisms for C and N increases from single fires are unclear but likely depend on an interaction between plant community composition traits and fire severity and highlight the uncertainty of how C and N cycling in an area experiencing WPE will respond to fire.

Fire alters the structure of ecosystems directly via fire-induced mortality but can also initiate changes the functional composition of plant communities over long periods of time (Pellegrini et al. 2021). For example, because fire results in significant heat stress and

high volatile losses of N, frequent fire filters tree species that are more tolerant to fire and have conservative nutrient strategies. Species with low tissue nutrient concentrations can better tolerate low nutrient environments characteristic of frequent fire (Hobbie 2015) and is an important example of how fire regimes can influence ecosystem cycling of C and N through plant community dynamics. However, a field-based evaluation aimed at better understanding how the return of fire, after long absences, interacts with the morphology and stichometry of individual species to drive ecosystem C and N losses via vegetation combustion losses has not been previously conducted.

Prescribed burning is a common restoration treatment to counter WPE in previously fire-suppressed regions (Scholes & Archer, 2003; Ryan et al., 2013), and from an ecological perspective, represents a unique opportunity to evaluate how ecosystem processes respond to single, low-severity fires (Hiers et al., 2020). Often, prescribed fires are burned in the wet spring months and at low intensities and reduces C and N volatilization loss from the soil via the decreased burn efficiency because of the high moisture content of spring litter. Together, these factors may lead to transformations in mineral soil organic matter C and N and concentrations through the accumulation of incompletely combusted pyrogenic organic matter (PyOM; Johnson & Curtis, 200; Pellegrini et al., 2021). PyOM tends to persist in soil for millennia based on its chemical resistance to decomposition (PyC; Kuhlbusch, 1998; J. Lehmann et al., 2008; Santin et al. 2015). To date, many estimates of C loss due to fire fail to account for PyOM (Surawski et al., 2016), despite their potential to return 2-27% burned C to the soil (Santin et al. 2020). While many studies have highlighted that the addition of PyOM to soil affects C and N

mineralization and can be influenced by the erosional redistribution of PyOM post-fire, empirical data across many ecosystems are lacking (Abney & Berhe, 2018; Bowring et al., 2022; Pingree & DeLuca, 2017; Whitman et al., 2014). A large fraction of PyOM is in a form of the highly stable C, commonly referred to as pyrogenic carbon (PyC). However, the quantity, form, and accessibility of thermally-transformed N in PyOM has been poorly quantified and characterized for prescribed fires (Ansley et al., 2006; Soong & Cotrufo, 2015). Therefore, leveraging prescribed burns in areas faced with WPE will provide critical insight into how single fires impact C and N cycling across a gradient of tree cover, and will highlight the potential capacity of PyOM to buffer losses of C and N in response to fire.

To assess the effect of prescribed burning on ecosystem C and N cycling in grasslands experiencing WPE, we use a 4,500-ha study region in the northern Great Plains (NGP) that has experienced WPE over the last 60+ years due to the rapid expansion *Pinus ponderosa* and *Juniperus spp.* (herein referred to as 'ponderosa' and 'juniper', respectively; Brookshire et al., 2020, Currey et al. 2022, Wood et al 2021). Notably, this period of WPE has coincided with a shift in fire activity from relatively frequent low-intensity grass fires to infrequent higher-intensity fires, due to decades of fire suppression (Reid & Fuhlendorf, 2011; Umbanhowar, 1996), but in the last decade management strategies have begun to include prescribed fire (DOI-DOA 20; Epstein et al., 2021). Prior to a prescribed fire we established 20 long-term monitoring plots and use a space-for-time and pre/post/control experimental design to quantify fire-induced woody mortality and the associated C and N loss from woody biomass, and determine the effect of the fire on soil concentrations of C

and N. Further, we use a satellite-derived spectral index to assess the severity of the prescribed burn (dMIRBI; Fernández et al., 2021) and to examine possible controls over the landscape distribution and production of PyOM. Finally, to assess the effect of PyOM on post-fire soil C processes, we performed a greenhouse experiment to examine the effect of ponderosa and juniper biochar on soil carbon dioxide (CO_2) flux rates. We expected greater mortality of the shrub-like juniper compared to the fire-adapted ponderosa pine, and therefore predicted that grasslands dominated by juniper would experience greater losses of C and N. Further, we hypothesized that burning in areas with greater woody cover would lead to increases in mineral soil PyOM due to the incorporation of partially consumed woody biomass and needle litter.

Materials and Methods

Site description

The study area, Unit D, is located in the central Montana region collectively known as the Missouri-Musselshell river breaks (47.436389 N, -108.148333 W). Unit D is located on a ~4,600 ha block of land managed by the Bureau of Land Management (BLM) and is directly adjacent to the Charles M. Russell National Wildlife Refuge area. The mean annual precipitation (MAP) and temperature (MAT) across the region is 358 mm and 8.4 °C, respectively. Our study site, south of the Missouri River, is in an unglaciated portion of the NGP where soils are mainly derived from Late Cretaceous Bear Paw Shale, which consists of bedrock with brackish and shallow marine origin and dispersed beds of bentonite clay (Jenson and Varnes, 1964). Soils are shallow entisols or vertisols with high clay contents

(~37%) and pH ranging from 6.7 in heavily woody areas to 7.1 in grass-dominated areas. Tracts of rough and broken land characterize the topography across much of the region and vegetation patterns are highly heterogeneous.

Between 1958- 2013 the region experienced extensive WPE at an annual rate of 0.12% yr^{-1} (Currey et al. 2022). Currently, *P. ponderosa* and *J. scopulorum* dominant the woody vegetation, although various *Juniperus* species are present, including *J. horizontalis* and *J. communis*, and hybridization is likely. In 2018, prior to the fire, we established twenty 20 x 20m plots that were accessed by foot and were distanced from established roads or footpaths. Plots were quasi-randomly chosen to maintain a semi-balanced mix of grassland, mixed grass-tree, and tree-dominant plots across a grass-woody gradient as described by Currey et al. 2022. Plots were then categorized into three woody-cover-based classifications that are used throughout this study: *grass* plots (< 33% woody cover, n = 3), *mixed* plots (33-66% woody cover, n = 9) and *tree* plots (> 66% woody cover, n = 8).

Aboveground biomass estimates

To estimate ponderosa aboveground biomass (AGB) C and N pools, we used species-specific allometric scaling of aboveground biomass and needle biomass from (D. Tinker et al., 2010. Scaling was applied to stems (n = 631) measured across all plots. Because we only cored four trees in each plot, we scaled dendrochronologically-derived biomass estimates to plot-scale by multiplying the biomass estimates by a correction factor calculated by dividing total plot basal area by cored tree basal area. Juniper AGB was calculated using canopy area allometry, where canopy area was estimated from across the

plots ocularly. We then calculated the proportion of wood versus needle biomass AGB using the relationship found in Ansley et al., 2012 and multiplied by the respective tissue C and N concentrations for species-specific C and N aboveground biomass pools. All plot scaled biomass estimates were then scaled up to the per-hectare scale. See Currey et al 2022 for additional details.

Dendrochronology

To determine the approximate age of ponderosa and juniper, and growth-rate of ponderosa, we collected cores or cross sections from ponderosa and juniper, respectively (Currey et al. 2022). Briefly, from each plot where ponderosa were present, we randomly sampled four ponderosa trees across a gradient of DBHs, extracting two opposing cores 30 cm from tree base using a 5mm increment borer. To assess tree growth, we used basal area increment analysis. Cores were scanned using a ~3000 dpi scanner and ring number and width was measured using the CooRecorder software program. In total, we examined ~150 cores from 77 ponderosa pine trees from 20 plots. Given that of junipers can have multiple stems, they were not cored for age analysis; instead, we destructively sampled 47 junipers at the root collar from just outside all plots. To determine the age of all junipers, stem cross-sections were counted twice from opposing edges.

Prescribed fire management

On May 14, 2018, the BLM led an extensive prescribed burn across Unit D using a combination of ground teams with drip torches and aerial support to promote ignition. The

prescribed fire was ignited at 9:50 and managed until 18:30. Fire activity significantly decreased starting at 14:15 when the smoke column laid down over the burn area and active smoldering was observed into the next day. BLM field observations on May 15th noted open timber stands with stem char and scorch heights up to 2 and 3 m, respectively, and greater burn activity in stands with greater juniper understory. The burn boundary for the event was acquired from www.mtbs.gov.

Fire severity

To determine the fire severity of the 2018 Unit D prescribed fire, we calculated the difference Mid-Infrared Burn Index (dMIRBI) spectral index of the area burned (map boundary obtained from the MTBS national database (https://www.mtbs.gov). The dMIRBI spectral index has been used in other savanna ecosystems (Tran et al., 2018; Trigg & Flasse, 2001) and has been shown to successfully detect changes in soil properties post-fire (Fernández et al., 2021). Pre- and post-fire images of Unit D for severity analysis were gathered from google earth engine. Using these images, spectral indices were calculated using data from Sentinel-2 satellite provided by the European Space Agency (acquired via Google Earth Engine). The Mid-Infrared Burn Index (MIRBI) was calculated using short-wave infrared band 1 (B11) and short-wave infrared band d (B12) using the following equation:

$$MIRBI = 10 * B11 - 9.8 * B12 \quad 1.$$

The burn severity index was calculated by subtracting the MIRBI pre-fire from the MIRBI post-fire using equation 2:

$$dMIRBI = MIRBI_{Pre-Fire} - MIRBI_{Post-Fire} \quad 1.$$

To assess the inter-fire severity within Unit D, we developed a classification system by dividing the burn severity index into four levels (Table 1) where Level 1 was unburned, Level 2 experienced low burn, Level 3 experienced medium burn, and Level 4 experienced high burn (Fernández et al., 2021).

Tree mortality assessment

Across all plots, every living stem with diameter at breast height (DBH) >10 cm was cataloged and tagged with an identification number before the fire. To assess tree mortality, plots were re-surveyed for living stems in May 2018. For each tree, the percentage of crown volume scorched were ocularly estimated, where crown foliage was defined by a change in color. Stems were considered deceased if 70-100% of the canopy was scorched (Sieg et al. 2006). In May 2019 trees were resurveyed to validate the initial mortality assessment by ensuring no crown regrowth.

C and N emission estimates

To calculate woody C emissions, we employed the widely-used "consumed biomass approach" that assumes all C from burned aboveground biomass is emitted (van der Werf et al. 2010). As such, for each plot, we multiplied the mortality of each species by the aboveground biomass estimates to estimate C emissions for woody and canopy needle biomass pools for both species. To calculate net C emissions by accounting for the thermally transformed carbon that ended up back in the soil, we then applied a correction

factor based on our soil PyC measurements (Santin et al., 2020; Surawski et al., 2016). To estimate total N emissions, we apply an approach similar to that of C emissions, since volatilization temperatures for C and N are similar (200 °C). Notably, our emission estimates are likely underestimated at the ecosystem scale as they do not include litter pool emissions.

Soil, surface PyOM, and woody tissue collection and processing

Mineral soil samples were collected across all 20 plots pre- and post-fire during April 2018 and May 2019, respectively. To isolate the mineral soil horizon, soil organic layers were removed prior to coring and mineral soil was sampled to a depth of 10 cm. To capture the heterogeneity of soil C and N, five soil cores were randomly sampled from each plot and composited into a single representative sample. Soils were oven-dried at 65 ºC for 24 hours, and dried samples were then milled to a fine powder for 12 hours in stainless steel jars on a slow-rolling tumbler. In total, 20 plots were used for all C and N analyses and 12 plots were used for % PyC analysis based on the availability of paired pre- and post-fire soil samples. To calculate spatial estimates of elemental soil pools, three soil bulk density cores were randomly extracted from each plot at a 0-10 cm mineral soil depth using a 5 cm slide hammer to avoid compaction. Bulk density soil cores were composited and dried at 105 ºC for 48 hours before being sieved at < 2 mm to remove roots and rocks before being massed.

To determine the potential of surface char to contribute to C and N concentrations in the mineral soil, post-fire we also collected and processed surface from 10 randomly selected plots. See supplemental methods for more information. To determine C and N

concentrations of foliar biomass, we collected and aggregated sunlit needles from the canopies of three ponderosa pines and junipers across five randomly selected plots. We made sure to collect foliar tissue from each of the three major juniper species when possible, to aggregate their collective chemistry. Ponderosa foliar samples were collected from similarly aged trees in the upper canopy using a shotgun to severe branches that were out of reach. Sunlit juniper foliar samples were collected by hand-clipping. Woody biomass C and N concentrations were determined from tree cores and cross-sections of five randomly selected ponderosa and juniper, respectively and ground using a rotary mill.

Soil and foliar chemical analysis

To determine total C and N concentrations of the soil, needle and woody biomass, and post-fire surface char, we used dry combustion. Soils and post-fire surface char were analyzed at Montana State University's Environmental Analytical Labratory with a Costech ESC 4010 elemental analyzer and Truspec CN analyzer (LECO, St Joseph, MI, USA), respectively. Needles were dried at 40 °C for 48 hrs and then hand milled in liquid nitrogen andd sent to Agvise Labratories (Northwoord, ND) for analysis. Woody biomass was air dried and ground using a rotary mill before being sent to Agvise laboratories for analysis.

PyC concentrations of soils were also analyzed using dry combustion. To isolate PyC in soil samples prior to analysis, we used the peroxide-weak nitric acid digestion protocol (Kurth et al., 2006). Briefly, replicate soil samples (~1.0 g) from each pre- and post-fire plot were individually added to a solution of 30% H_2O_2 and 1 M HNO_3 and heated

to 100 ºC for 16 hours. Samples were then visually inspected for evidence of any further reaction (i.e., effervescence) and allowed to react until effervescence subsided. Upon digestion completion, samples were filtered through a Whatman #2 filter, dried, and ground with mortar and pestle. Samples were then massed in aluminum tins for dry combustion. Duplicates were run for 10% of samples to ensure analytical precision.

Soil respiration measurements

To assess the effect of ponderosa and juniper biochar on soil respiration, we conducted a pilot greenhouse study at Montana State University in October 2020. Using the closed static chamber technique, CO_2 fluxes of juniper and ponderosa biochar were measured in replicated potted soils over a two-day experiment. Measurements were conducted using a cavity ringdown spectroscopy gas analyzer (CRDS, G2508, Picarro Inc., Santa Clara, CA, USA). See supplemental document for more details.

Statistical analysis

To evaluate the effects of fire on all soil elemental concentrations and pool size, we performed type II ANOVA using the 'Anova' function (lmerTest package; Kuznetsova et al. 2017), and post-hoc comparisons were made using pairwise Tukey HSD. Least square means and ± SE are reported. The year was used a fixed effect and plot as a random effect to account for repeated measurements for % C, %N, and PyC analyses. For pre/post/control analyses, fire treatment was used a fixed effect and plot used as random effects for individual comparison between months (e.g. April-May, April-September). Differences

between C and N- biomass and emission estimates were determined using Welch's two sample t-tests. To convert C, PyC, and N concentrations to a mass per unit area (pools Mg ha^{-1}), concentrations were multiplied by the plots bulk density and soil depth (10 cm). All model residuals were evaluated for normality and transformed as necessary to adhere to a normal distribution. Treatment significance was set *a priori* to $\alpha = 0.05$

Ordinary least square regression models were fit to examine how fire, topography, and WPF affected the pre-fire landscape distribution of PyC, woody mortality, PyC production, and changes in soil chemistry. Slope angle, northness, topographical position index (TPI: -1 indicates low points across the landscape and 1 shows high points), and percent clay were included as topographical variables for the model selection process. Vegetative predictors used included total woody cover (%), juniper cover (%), ponderosa cover (%), total weighted mortality (proportional plot-level tree mortality based on 2018 cover), ponderosa mortality (%), and juniper mortality (%). Models were refined using a selection criterion of AIC > two or greater, and if top models were not >2 AIC apart, the most parsimonious model was selected (dredge function in R). A hierarchical partitioning analysis was used to decompose the relative importance of model parameters with the Relaimpo package in R.

To calculate CO_2 fluxes, we first statistically and visually determined that each chamber exhibited a linear increase or decrease over the deployment time. Linear mixed models were then fit to assess whether the fixed effect of biochar addition accounted for variation in CO_2. The ambient air temperature was included as a fixed effect in all models to control for differences between days, and sample day crossed with replicate were

included as random effects. Due to the low individual sample numbers, the observations of Ponderosa (n= 3) and Juniper (n = 4) were combined for statistical comparison to the no biochar controls (n = 6). All analyses were performed in R (R Core Team 2021).

Results

Tree establishment and woody biomass-C growth rate

The mean year of establishment for ponderosa pine trees over >10 cm DBH was 1888 (range of 1702 - 1974), while the mean juniper establishment occurred much later in 1932 (range of 1908 – 1979; Fig 1A) across our 20 plots. The average total woody cover of all 20 plots pre-fire was 57% and the average woody cover of the 16 plots that burned was 60%. Across both juniper and ponderosa species, we estimate that total biomass-C has accumulated at a rate of 0.75 ± 0.23 Mg C ha^{-1} since 1950.

Fire severity, tree mortality, C and N biomass loss

Aerial imagery analysis and the dMIRBI index indicated that most of the fire was classified as low-medium burn severity scale (Fig 2). Roughly 9% of the unit was unburned, 59% displayed low fire severity, 31% medium fire severity, and < 1% experienced high severity fire impact (Table 1). Total woody mortality strongly correlated with fire severity (R^2 = 0.69, Fig 2). The woody mortality rate was ~33% for all living stems >10 cm DBH (p < 0.0001) across the 16 plots burned. Mortality was disproportionately driven by juniper stems which experienced ~90% mortality, and there was a significant decrease in mean juniper cover from 21% to 2 % (p < 0.0001). Ponderosa was more resilient to fire mortality

as we measured a ~36% decrease in living stems and a smaller reduction in mean ponderosa cover, from 39 to 25%. We documented a high percentage of sapling mortality as 98% of saplings did not survive. 4 out of the 20 plots were unburned and subsequently used as the control plots.

Pre-fire, 41 ± 5.3 Mg C ha^{-1} was stored in total aboveground woody biomass, with a greater fraction stored in ponderosa compared to juniper (p = 0.047; 26 ± 2.8 and 15 ± 2.2 Mg C ha^{-1}, respectively). Species morphology influenced the aboveground N storage with juniper containing higher foliar to woody N ratios (15:1) than ponderosa (6:1) on a per mass basis (kg N). We estimate that 43 % (18 ± 1.3 Mg C ha^{-1}) of total aboveground woody plant biomass-C was lost with similar losses from each species 10 ± 1.3 Mg C ha^{-1} from juniper and 6 ± 1.3 Mg C ha^{-1} from ponderosa (p < 0.19; Figure 4). Furthermore, before the fire, 1.2 ± 0.14 Mg N ha^{-1} was stored in aboveground woody biomass, with a disproportionate amount stored in juniper compared to ponderosa (p < 0.002; 0.81 ± 0.12 versus 0.37 ± 0.05 Mg N ha^{-1}). We estimate that 78% of woody- N was subject to emission loss (0.94 ± 0.15 Mg N ha^{-1}; Figure 4) with a greater proportion coming from juniper compared to ponderosa (p < 0.0009 ; 0.77 ± 0.15 versus 0.16 ± 0.05 Mg N ha^{-1}). Total C emissions were greater in plots with higher pre-fire ponderosa cover (p = 0.003; Figure 4c), but there was no relationship with pre-fire juniper cover (p = 0.41; Figure 4d). Conversely, total N emissions increased in plots with greater pre-fire juniper cover (p = < 0.0001; Figure 4d), while there was no relationship with pre-fire ponderosa cover (p = 0.80; Figure 4C).

Changes in soil chemistry

Concentrations of mineral soil (0-10 cm depth) % C and % N increased one-year after fire while P did not (Fig. 4). The increases in % C and % N increases were ubiquitous across both the burned and unburned controls (Supplemental Table 3). Prior to fire soil carbon ranged from 0.92 % to 2.6 % (mean = 1.5 ± 0.11 %), soil nitrogen ranged from 0.08 % to 0.16 % (mean = 0.11 ± 0.05 %). Mean concentrations of soil carbon increased by 33% to 2.0 ± 0.1 % C ($p < 0.0001$) and nitrogen increased by 26% to 0.15 ± 0.02 % N ($p < 0.0001$). After area scaling, total soil C pools increased by 5.3 ± 0.54 Mg C ha^{-1} from 13.0 ± 0.65 to 18.3 ± 0.65 Mg C ha^{-1}(Fig 6 ; $p < 0.0001$) and soil N pools increased by 0.30 ± 0.04 Mg N ha^{-1} from 1.0 ± 0.04 to 1.31± 0.04 (Fig 6; $p < 0.0001$). There was little evidence for a detectable change in total soil P concentrations ($p = 0.12$). Soil C:N ratios ($p = 0.008$) increased in the mineral soil after the fire.

We find strong evidence that it was the cumulative effects of both fire and WPE (pre-fire % cover) that led to increases in soil C (Fig 5; $p = 0.04$ and $p = 0.03$, respectively), where every 10% increase in woody cover led a 0.04% concentration increase in soil C post-fire. We also find strong evidence that the cumulative effects of WPE (mature stem density) and fire led to increases in soil N ($p = 0.03$ Supplemental Fig 5), where the presence of each ten mature stems (0.04 ha^{-1}) led to a 0.01 % increase in soil N post-fire.

PyC production, landscape distribution, and soil respiration

Pre-fire soil PyC concentrations increased by 33% from 0.30 ± 0.03 % PyC to 0.40 ± 0.04 % PyC post-fire at the 0-10 cm depth (Fig 4; $p = 0.0012$) and equates to an area scaled increase of 1.2 ± 0.3 Mg PyC ha^{-1}. Despite the increase in soil PyC, the relative proportion

of PyC to total soil carbon was not affected by fire (23 %; p = 0.42). The mean concentration of %C and %N in the post-fire surface PyOM samples were 20 % ± 4.0 and 0.77 % ± 0.13, respectively. The mean C: N ratio was 27.0 ± 3.0. Pre-fire soil PyC concentrations increased by 33% from 0.30 ± 0.03 % PyC to 0.40 ± 0.04 % PyC post-fire at the 0-10 cm depth (Fig 4 ; $p = 0.0012$), equating to an area scaled increase of 1.2 ± 0.3 Mg PyC ha^{-1}. Despite the increase in soil PyC, the relative proportion of PyC to total soil carbon was unaffected by fire (23 %; $p = 0.42$). The mean concentration of %C and %N in the post-fire surface PyOM samples were 20 ± 4.0 and 0.77 ± 0.13 %, respectively. The mean C: N ratio was 27.0 ± 3.0.

The key drivers for pre-fire landscape distribution of PyC were higher surface slope angles ($R^2 = 0.68$; $p = 0.0009$; Supplemental Figure 4.) and TPI (base of gullies/ravines; $p = 0.005$) with slope and TPI explaining 45 and 22 % of the variation, respectively. We found no direct evidence for significant landscape or vegetation predictors for PyC production. However, if we use the relationship between woody cover and the change in soil C from fire by applying the 23% fraction of total C that is PyC we can estimate a 0.01% increase in soil PyC with every 10% increase in woody cover. Finally, the cumulative addition of ponderosa and juniper biochar to an experimental sandy soil led to > 100% decrease in soil CO_2 flux compared to sand controls without biochar ($p = 0.05$; Supplemental Figure 3).

Discussion

Fire severity increases with woody expansion, but C and N emission losses are differentially driven by woody composition

Overall, the 2018 Unit D prescribed fire was classified as low-medium severity, but severity varied throughout the area burned. We found that fire severity was driven by woody mortality, supporting the hypothesis that WPE will drive increasingly severe fires in transitional grasslands (Fig 3B). We estimate that 27 Mg C ha^{-1} C and 0.85 Mg C ha^{-1} N were lost as volatilized woody biomass in response to the prescribed burn, and these estimates are line with studies in tropical savannas and boreal forests (Zhou et al., 2022;Grier et al. 1975, Little and Ohmann 1988).

Interestingly we found that woody mortality alone was not enough to explain shifts in biochemical processes in response to fire, and instead, woody species composition was a key driver of C and N pattern losses. We found that 1) ponderosa and juniper contributed equally to C losses and 2) pre-fire juniper cover best predicted N emission losses. Ponderosa are highly resistant to low-severity fire due to their thick bark and open crown and branching pattern (Fitzgerald, 2005), while juniper's thin bark, compact crown, and high volatile oil branch content makes them highly susceptible (Forest Service). As predicted, we observed a significant mortality in juniper post-fire (90%) compared to ponderosa (36%). Despite lower ponderosa mortality, ponderosa store significantly greater aboveground biomass than juniper, and we found that these greater biomasses are key factors driving C losses during fire. While pre-fire ponderosa cover was not a strong predictor of total C loss (Figure 4c) the fact that C emission losses were similar to juniper

despite 69% less mortality highlights the important role of ponderosa in aboveground C storage in WPE ecosystems. Juniper cover best predicted N losses as they contain significantly greater proportions of biomass N than ponderosa (Table 2) have a higher ratio of foliar to woody N observed for juniper (15:1) compared to ponderosa (6:1). We show that junipers serve as a major conduit through which N is lost during fire and we estimate they contributed 82% of the total woody N lost (0.77 Mg N ha of the total 0.94 Mg N ha).

Our estimates of C and N combustion loss might represent an overestimation compared to areas with greater grassy cover as the mean woody cover of the burned plots were 60%. Thus, these estimates likely reflect larger C losses associated with the historical accumulation of woody biomass-C compared to the smaller annual storage of AGB-C in grasses (~1 Mg C ha^{-1} yr; Meigs et al., 2009). Assuming the 0.75 Mg ha C mean growth rate from the previous 63 years, we estimate that it would take ~37 years to sequester the C lost from the fire. However, this estimate does not account for the complexity of C-fluxes during post-fire regrowth and compensatory effects from non-tree productivity (Meigs et al., 2009), and therefore may be an underestimate. Finally, emission losses of N are likely to take centuries to recover based on low atmospheric N deposition rates (Brookshire et al. 2020) and influence of the dominate N fixing species in the region, sweet clover (*Melilotus officinalis*), has been found to fix upwards of 12 kg N ha^{-1} yr^{-1} in non-agricultural settings and on a biennial basis (Lesica and Deluca, 2000).

Large C and N emission losses were offset by additions of soil C and N that were driven by PyOM incorporation

Although WPE and prescribed fire increased C and N emissions from transitional grasslands, we found that a single, low-intensity fire also led to one year increases in mineral soil C that buffered C emission losses by 30% (Fig 4a). We were surprised to observe that soil C concentrations also increased 29%, a high benchmark based on previous meta-analyses (Johnson & Curtis, 2001; Nave et al., 2011). We posit that PyOM-C inputs from combusted woody biomass explain the large observed increase in total mineral soil C post-fire. Indeed, a recent study found that the majority of PyOM-C was produced from mixed conifer fuel beds (e.g. needle and twig) compared to other vegetation fuel sources and types (Santin et al. 2020). Moreover, applying a back calculation from the C concentrations found in surface PyOM, we find additional support the large increase in C. Assuming a 0.5 cm layer of PyOM and ash post-fire with a bulk density of 0.62 g cm^3(Bodí et al., 2014), we estimate that 6.2 Mg C ha^{-1} could have been incorporated into the mineral layer, after applying the measured C concentration of surface char (20%; Supplemental methods). This increase is greater than what we observed (5.3 Mg C ha^{-1}) .

We find large increases in mineral soil N one year after fire that buffered N emissions by 33%. Similar to the increases in mineral soil C, these observations are high, but within the range of a meta-analysis (Johnson & Curtis, 2001). While increases in soil N are less frequently reported than losses, the high N concentration of surface PyOM (0.77%) is likely a reflection of consumed needle biomass due to its higher N concentrations than stem biomass (Table 2). In a recent global meta-analysis, Pellegrini et

al (2018) found that lower severity fire was associated with soil N increases in needle leaf forests. Thus, we suspect that the large one-year increase in total soil N was driven by the redistribution of the needle litter char into the soil, which was incompletely combusted and has high N content. Interestingly, fire severity and % woody mortality did not explain patterns of elemental soil changes (Fig 5 and Supplemental Fig 5). This suggests that stem mortality assessments are insufficient to explain soil chemical changes because the combustion of foliar material are the outsized drivers of PyOM incorporation into the soil.

One outstanding question that remains is how the newly incorporated soil PyOM will respond to future soil processes (i.e., C and N mineralization) in these ecosystems. One important factor to consider is that the C:N ratio (~27) of the char samples we collected is higher than the stoichiometric threshold that governs net N mineralization versus immobilization (20-25; Mooshammer et al., 2014). This suggests that despite increases in biologically available N immediately post-fire (Supplemental Table 1), long-term N mineralization rates will be slowed, and possibly affect future plant availability. To address the question of C mineralization, we experimentally tested how juniper and ponderosa char affected soil CO_2 soil fluxes by conducting a pilot greenhouse study and found that the addition of coniferous biochar decreased the soil CO_2 flux (Supplemental Figure 3). The observed negative priming effect suggests that the addition of coniferous PyOM could decrease the rate of microbial degradation of soil C pool following fire. However, despite these preliminary findings, our understanding of SOM-char interactions is still in its infancy and the observed decrease in microbial respiration may only be a transient (Whitman et al., 2014). Nevertheless, the availability of the thermally transformed C and

N for microbial processing and plant uptake is poorly understood and remains an area for future inquiry.

Prescribed fire produces a large quantity of a highly stable form of soil C (PyC) in conifer encroached grasslands

We find that a single, low-intensity fire led to the production of 1.2 Mg ha^{-1} of soil PyC in the mineral layer and represents a large fraction (23%) of the total soil C increase that we observed (Fig 4a). While 1.2 Mg ha^{-1} is lower than what was produced in the organic soil layer of another single prescribed fire study in western Montana (2.2 Mg PyC ha^{-1}; DeLuca et al., 2020), it is important to highlight that observed increases of PyC in this study occurred in the mineral layer where PyC is relatively protected from surface mobilization relative to the organic layer, and can therefore persist for long periods (Abiven & Santín, 2019; Rumpel et al. 2015). We posit that the short-term vertical transportation of PyC from the organic layer into the mineral layer may have been driven by the integration of the fine (< 2mm) PyC fraction via the temporary formation of cracks in the vertic soils found across the study site (Rumpel et al. 2015). Our PyC processing methods captured only the < 2 mm chemical fraction and excluded charcoal fragments > 2 mm which can account for upwards of 50% of the visibly detected charcoal (Nocentini et al., 2010). This suggests that the overall production of PyC was likely larger than we detected, but we would need additional chemical, thermal and observational methods to quantify the full PyC spectrum

Assessing the production of PyC from prescribed fire across this landscape aerially will be an important management tool moving forward. As such, we find PyC was

produced at a spatial gradient of 0.01% for every 10% increase in burned woody cover and offset total carbon emissions by 6%. Our biomass conversion estimates falls within the range of previous estimates of biomass to PyC conversion percentages in coniferous forests (1% to 20%; Lynch et al., 2004; Preston & Schmidt, 2006; D. B. Tinker & Knight, 2000). Despite the ubiquitous increases in PyC, the proportion of PyC to total soil C did not change, emphasizing that our method of PyC determination likely captured only a fraction of the PyC added to the soil. Indeed, PyC is exceedingly difficult to quantify absolutely because it exists across a spectrum of thermally altered material (Bird et al., 2015).

Implications

The ubiquitous increases in PyC across both burned and unburned control sites point to the influence of horizontal erosion as a powerful driver of the short-term (< 1 year) redistribution across the landscape. However, we found that the abundance of soil PyC pre-fire was best explained by surface slope angle and topographical position (TPI), suggesting horizontal erosional transport and deposition may explain long-term PyC distribution across the landscape. Indeed, plots located on steep slopes and/or at the base of ravines and gullies were characterized as having the greatest concentrations of soil PyC.

Understanding how increases in woody cover in grasslands influence and respond to fire are critical for predicting future changes to processes in these transitional ecosystems. Our findings highlight that C and N emission losses are strongly influenced by community composition under low-medium fire severity. Importantly, the combustion of juniper has a disproportionately large impact on N loss from the system due to greater

%N biomass concentration, greater foliar to total biomass ratio, and high susceptibility to combustion during low severity fire. While C recovery could take decades (~37 years), N recovery will require substantially more time, likely on the order of centuries, although this is dependent on N-fixer succession and atmospheric N deposition inputs.

Our findings also highlight that low frequency and severity fires increase soil C and N with increasing conifer expansion. While there is large uncertainty as to how PyOM will influence future soil organic matter processes, we find field and greenhouse evidence that prescribed burns may lead to more stable soil carbon stocks as they reduce the fuel for the future and also increase soil C stability via increased inaccessibility via PyC inputs. (Pellegrini et al., 2021).

While PyC production is relatively low compared to C emission losses in grassland-savanna ecosystems, the long-term stability of PyC makes it an important C sink over time. As such, while the short-term effect of a single prescribed fire leads to large emission C loss, infrequent and low-severity fires may infact promote C sequestration over time. Here, we provide a PyC production rate that can be estimated based on woody plant biomass and can be used in combination with remote sensing to spatially estimate PyC production in areas of WPE. We note that there is strong erosional control over the redistribution of PyC where vertical transportation into the mineral layer occurs within one year, and over the long-term, PyC accumulation is driven by horizontal transportation.

Taken together, this study constrains the spatiotemporal variability of fire effects on C and N cycling in grassland-savannas, with important implications for land managers conducting prescribed burns and defining parametrizations in global fire models. This work

highlights the instability of aboveground woody C storage even in response to low severity fire and underpins the importance of understanding long-term C and N dynamics of regional ecosystems before undertaking afforestation efforts for climate mitigation.

Acknowledgements

This research was supported by a grants from the U.S. Bureau of Land Management (agreement number L16AS00082), the Murdock Trust (Reference number 201812566) and . The authors would like to thank Matt Comer for his insights and guidance in establishing the field plots and general knowledge of the region. We gratefully acknowledge Tory Dille, Evan Bilbrey, Hannah Duff, and Shealyn Malone for assistance with field sample collection and processing.

Authors' contributions

J.B., conceived the project and secured funding. JB, JG and BC established the field plots, JG and B.C. processed field samples and analyzed the data with interpretation assistance from JB. JG conducted the greenhouse experiment and drafted the initial manuscript. All co-authors revised, read, and approved the final manuscript.

Conflict of Interest

The authors declare that they have no conflict of interest

References cited

Abiven, S., & Santín, C. (2019). Editorial: From Fires to Oceans: Dynamics of Fire-Derived Organic Matter in Terrestrial and Aquatic Ecosystems. *Frontiers in Earth Science*, *7*. https://www.frontiersin.org/article/10.3389/feart.2019.00031

Abney, R. B., & Berhe, A. A. (2018). Pyrogenic Carbon Erosion: Implications for Stock and Persistence of Pyrogenic Carbon in Soil. *Frontiers in Earth Science*, *6*. https://doi.org/10.3389/feart.2018.00026

Ansley, R. J., Mirik, M., Surber, B. W., & Park, S. C. (2012). Canopy Area and Aboveground Mass of Individual Redberry Juniper (Juniperus pinchotii) Trees. *Rangeland Ecology & Management*, *65*(2), 189–195. https://doi.org/10.2111/REM-D-11-00112.1

Barger, N. N., Archer, S. R., Campbell, J. L., Huang, C., Morton, J. A., & Knapp, A. K. (2011). Woody plant proliferation in North American drylands: A synthesis of impacts on ecosystem carbon balance. *Journal of Geophysical Research: Biogeosciences*, *116*(G4). https://doi.org/10.1029/2010JG001506

Bird, M. I., Wynn, J. G., Saiz, G., Wurster, C. M., & McBeath, A. (2015). The Pyrogenic Carbon Cycle. *Annual Review of Earth and Planetary Sciences*, *43*(1), 273–298. https://doi.org/10.1146/annurev-earth-060614-105038

Boby, L. A., Schuur, E. A. G., Mack, M. C., Verbyla, D., & Johnstone, J. F. (2010). Quantifying fire severity, carbon, and nitrogen emissions in Alaska's boreal forest. *Ecological Applications*, *20*(6), 1633–1647. https://doi.org/10.1890/08-2295.1

Bodí, M. B., Martin, D. A., Balfour, V. N., Santín, C., Doerr, S. H., Pereira, P., Cerdà, A., & Mataix-Solera, J. (2014). Wildland fire ash: Production, composition and eco-hydro-geomorphic effects. *Earth-Science Reviews*, *130*, 103–127. https://doi.org/10.1016/j.earscirev.2013.12.007

Bowring, S. P. K., Jones, M. W., Ciais, P., Guenet, B., & Abiven, S. (2022). Pyrogenic carbon decomposition critical to resolving fire's role in the Earth system. *Nature Geoscience*, *15*(2), 135–142. https://doi.org/10.1038/s41561-021-00892-0

Brookshire, E. N. J., Stoy, P. C., Currey, B., & Finney, B. (2020). The greening of the Northern Great Plains and its biogeochemical precursors. *Global Change Biology*, *26*(10), 5404–5413. https://doi.org/10.1111/gcb.15115

DeLuca, T. H., Gundale, M. J., Brimmer, R. J., & Gao, S. (2020). Pyrogenic Carbon Generation From Fire and Forest Restoration Treatments. *Frontiers in Forests and Global Change*, *3*. https://doi.org/10.3389/ffgc.2020.00024

Dore, S., Kolb, T. E., Montes-Helu, M., Sullivan, B. W., Winslow, W. D., Hart, S. C., Kaye, J. P., Koch, G. W., & Hungate, B. A. (2008). Long-term impact of a stand-replacing fire on ecosystem CO2 exchange of a ponderosa pine forest. *Global Change Biology*, *14*(8), 1801–1820. https://doi.org/10.1111/j.1365-2486.2008.01613.x

Epstein, K., Wood, D., Roemer, K., Currey, B., Duff, H., Gay, J., Goemann, H., Loewen, S., Milligan, M., Wendt, J., Brookshire, E. N. J., Maxwell, B., McNew, L., McWethy, D., Stoy, P., & Haggerty, J. (2021). Toward an urgent yet deliberate conservation strategy: Sustaining social-ecological systems in rangelands of the Northern Great Plains, Montana. *Ecology and Society*, *26*(1). https://doi.org/10.5751/ES-12141-260110

Fernández, C., Fernández-Alonso, J. M., Vega, J. A., Fontúrbel, T., Llorens, R., & Sobrino, J. A. (2021). Exploring the use of spectral indices to assess alterations in soil properties in pine stands affected by crown fire in Spain. *Fire Ecology*, *17*(1), 2. https://doi.org/10.1186/s42408-020-00089-7

Fitzgerald. (2005). *Fire Ecology of Ponderosa Pine and Rebuilding of Fire-Resilient Ponderosa Pine Ecosystems*. United States Forest Service.

Harden, J. W., Mack, M., Veldhuis, H., & Gower, S. T. (2002). Fire dynamics and implications for nitrogen cycling in boreal forests. *Journal of Geophysical Research: Atmospheres*, *107*(D3), WFX 4-1-WFX 4-8. https://doi.org/10.1029/2001JD000494

Hiers, J. K., O'Brien, J. J., Varner, J. M., Butler, B. W., Dickinson, M., Furman, J., Gallagher, M., Godwin, D., Goodrick, S. L., Hood, S. M., Hudak, A., Kobziar, L. N., Linn, R., Loudermilk, E. L., McCaffrey, S., Robertson, K., Rowell, E. M., Skowronski, N., Watts, A. C., & Yedinak, K. M. (2020). Prescribed fire science: The case for a refined research agenda. *Fire Ecology*, *16*(1), 11. https://doi.org/10.1186/s42408-020-0070-8

Hobbie, S. E. (2015). Plant species effects on nutrient cycling: Revisiting litter feedbacks. *Trends in Ecology & Evolution*, *30*(6), 357–363. https://doi.org/10.1016/j.tree.2015.03.015

Jenson and Varnes. (1964). Geology of the Fort Peck area, Garfield, McCone, and Valley Counties, Montana. *USGS*. https://pubs.er.usgs.gov/publication/pp414F

Johnson, D. W., & Curtis, P. S. (2001). Effects of forest management on soil C and N storage: Meta analysis. *Forest Ecology and Management*, *140*(2), 227–238. https://doi.org/10.1016/S0378-1127(00)00282-6

Johnson, D. W., Susfalk, R. B., Dahlgren, R. A., & Klopatek, J. M. (1998). Fire is more important than water for nitrogen fluxes in semi-arid forests. *Environmental Science & Policy*, *1*(2), 79–86. https://doi.org/10.1016/S1462-9011(98)00008-2

Kuhlbusch, T. A. J. (1998). Black Carbon and the Carbon Cycle. *Science*, *280*(5371), 1903–1904. https://doi.org/10.1126/science.280.5371.1903

Kurth, V. J., MacKenzie, M. D., & DeLuca, T. H. (2006). Estimating charcoal content in forest mineral soils. *Geoderma*, *137*(1), 135–139. https://doi.org/10.1016/j.geoderma.2006.08.003

Lehmann, J., Skjemstad, J., Sohi, S., Carter, J., Barson, M., Falloon, P., Coleman, K., Woodbury, P., & Krull, E. (2008). Australian climate–carbon cycle feedback reduced by soil black carbon. *Nature Geoscience*, *1*(12), 832–835. https://doi.org/10.1038/ngeo358

Liao, C., Peng, R., Luo, Y., Zhou, X., Wu, X., Fang, C., Chen, J., & Li, B. (2008). Altered ecosystem carbon and nitrogen cycles by plant invasion: A meta-analysis. *New Phytologist*, *177*(3), 706–714. https://doi.org/10.1111/j.1469-8137.2007.02290.x

Lynch, J. A., Clark, J. S., & Stocks, B. J. (2004). Charcoal production, dispersal, and deposition from the Fort Providence experimental fire: Interpreting fire regimes from charcoal records in boreal forests. *Canadian Journal of Forest Research*, *34*(8), 1642–1656. https://doi.org/10.1139/x04-071

MacKenzie, M. D., DeLuca, T. H., & Sala, A. (2004). Forest structure and organic horizon analysis along a fire chronosequence in the low elevation forests of western Montana. *Forest Ecology and Management*, *203*(1), 331–343. https://doi.org/10.1016/j.foreco.2004.08.003

McLauchlan, K. K., Higuera, P. E., Miesel, J., Rogers, B. M., Schweitzer, J., Shuman, J. K., Tepley, A. J., Varner, J. M., Veblen, T. T., Adalsteinsson, S. A., Balch, J. K., Baker, P., Batllori, E., Bigio, E., Brando, P., Cattau, M., Chipman, M. L., Coen, J., Crandall, R., … Watts, A. C. (2020). Fire as a fundamental ecological process:

Research advances and frontiers. *Journal of Ecology*, *108*(5), 2047–2069. https://doi.org/10.1111/1365-2745.13403

Meigs, G. W., Donato, D. C., Campbell, J. L., Martin, J. G., & Law, B. E. (2009). Forest Fire Impacts on Carbon Uptake, Storage, and Emission: The Role of Burn Severity in the Eastern Cascades, Oregon. *Ecosystems*, *12*(8), 1246–1267. https://doi.org/10.1007/s10021-009-9285-x

Mooshammer, M., Wanek, W., Hämmerle, I., Fuchslueger, L., Hofhansl, F., Knoltsch, A., Schnecker, J., Takriti, M., Watzka, M., Wild, B., Keiblinger, K. M., Zechmeister-Boltenstern, S., & Richter, A. (2014). Adjustment of microbial nitrogen use efficiency to carbon:nitrogen imbalances regulates soil nitrogen cycling. *Nature Communications*, *5*(1), 3694. https://doi.org/10.1038/ncomms4694

Nave, L. E., Vance, E. D., Swanston, C. W., & Curtis, P. S. (2011). Fire effects on temperate forest soil C and N storage. *Ecological Applications*, *21*(4), 1189–1201. https://doi.org/10.1890/10-0660.1

Nocentini, C., Certini, G., Knicker, H., Francioso, O., & Rumpel, C. (2010). Nature and reactivity of charcoal produced and added to soil during wildfire are particle-size dependent. *Organic Geochemistry*, *41*(7), 682–689. https://doi.org/10.1016/j.orggeochem.2010.03.010

Pellegrini, A. F. A., Ahlström, A., Hobbie, S. E., Reich, P. B., Nieradzik, L. P., Staver, A. C., Scharenbroch, B. C., Jumpponen, A., Anderegg, W. R. L., Randerson, J. T., & Jackson, R. B. (2018). Fire frequency drives decadal changes in soil carbon and nitrogen and ecosystem productivity. *Nature*, *553*(7687), 194–198. https://doi.org/10.1038/nature24668

Pellegrini, A. F. A., Caprio, A. C., Georgiou, K., Finnegan, C., Hobbie, S. E., Hatten, J. A., & Jackson, R. B. (2021). Low-intensity frequent fires in coniferous forests transform soil organic matter in ways that may offset ecosystem carbon losses. *Global Change Biology*, *27*(16), 3810–3823. https://doi.org/10.1111/gcb.15648

Pellegrini, A. F. A., Harden, J., Georgiou, K., Hemes, K. S., Malhotra, A., Nolan, C. J., & Jackson, R. B. (2021). Fire effects on the persistence of soil organic matter and long-term carbon storage. *Nature Geoscience*, 1–9. https://doi.org/10.1038/s41561-021-00867-1

Pellegrini, A. F. A., Hobbie, S. E., Reich, P. B., Jumpponen, A., Brookshire, E. N. J., Caprio, A. C., Coetsee, C., & Jackson, R. B. (2020). Repeated fire shifts carbon

and nitrogen cycling by changing plant inputs and soil decomposition across ecosystems. *Ecological Monographs*, *90*(4), e01409. https://doi.org/10.1002/ecm.1409

Pellegrini, A. F. A., Refsland, T., Averill, C., Terrer, C., Staver, A. C., Brockway, D. G., Caprio, A., Clatterbuck, W., Coetsee, C., Haywood, J. D., Hobbie, S. E., Hoffmann, W. A., Kush, J., Lewis, T., Moser, W. K., Overby, S. T., Patterson, W. A., Peay, K. G., Reich, P. B., … Jackson, R. B. (2021). Decadal changes in fire frequencies shift tree communities and functional traits. *Nature Ecology & Evolution*, *5*(4), 504–512. https://doi.org/10.1038/s41559-021-01401-7

Pingree, M. R. A., & DeLuca, T. H. (2017). Function of Wildfire-Deposited Pyrogenic Carbon in Terrestrial Ecosystems. *Frontiers in Environmental Science*, *5*. https://doi.org/10.3389/fenvs.2017.00053

Preston, C. M., & Schmidt, M. W. I. (2006). Black (pyrogenic) carbon: A synthesis of current knowledge and uncertainties with special consideration of boreal regions. *Biogeosciences*, *3*(4), 397–420. https://doi.org/10.5194/bg-3-397-2006

Reich, P. B., Peterson, D. W., Wedin, D. A., & Wrage, K. (2001). Fire and Vegetation Effects on Productivity and Nitrogen Cycling Across a Forest–Grassland Continuum. *Ecology*, *82*(6), 1703–1719. https://doi.org/10.1890/0012-9658(2001)082[1703:FAVEOP]2.0.CO;2

Ryan, K. C., Knapp, E. E., & Varner, J. M. (2013). Prescribed fire in North American forests and woodlands: History, current practice, and challenges. *Frontiers in Ecology and the Environment*, *11*(s1), e15–e24. https://doi.org/10.1890/120329

Santin, C., Doerr, S. H., Jones, M. W., Merino, A., Warneke, C., & Roberts, J. M. (2020). The Relevance of Pyrogenic Carbon for Carbon Budgets From Fires: Insights From the FIREX Experiment. *Global Biogeochemical Cycles*, *34*(9), e2020GB006647. https://doi.org/10.1029/2020GB006647

Santín, C., Doerr, S. H., Kane, E. S., Masiello, C. A., Ohlson, M., Rosa, J. M. de la, Preston, C. M., & Dittmar, T. (2016). Towards a global assessment of pyrogenic carbon from vegetation fires. *Global Change Biology*, *22*(1), 76–91. https://doi.org/10.1111/gcb.12985

Scholes, R., & Archer, S. (2003). Tree-Grass Interactions in Savannas. *Annual Review of Ecology and Systematics*, *28*, 517–544. https://doi.org/10.1146/annurev.ecolsys.28.1.517

Sieg, Carolyn, Joel D. McMillin, James F. Fowler, Kurt K. Allen, José F. Negron, Linda L. Wadleigh, John A. Anhold, Ken E. Gibson, Best Predictors for Postfire Mortality of Ponderosa Pine Trees in the Intermountain West, *Forest Science*, Volume 52, Issue 6, December 2006, Pages 718–728, https://doi.org/10.1093/forestscience/52.6.718

Surawski, N. C., Sullivan, A. L., Roxburgh, S. H., Meyer, C. P. M., & Polglase, P. J. (2016). Incorrect interpretation of carbon mass balance biases global vegetation fire emission estimates. *Nature Communications*, *7*(1), 11536. https://doi.org/10.1038/ncomms11536

Tilman, D., Reich, P., Phillips, H., Menton, M., Patel, A., Vos, E., Peterson, D., & Knops, J. (2000). Fire Suppression and Ecosystem Carbon Storage. *Ecology*, *81*(10), 2680–2685. https://doi.org/10.1890/0012-9658(2000)081[2680:FSAECS]2.0.CO;2

Tinker, D. B., & Knight, D. H. (2000). Coarse Woody Debris following Fire and Logging in Wyoming Lodgepole Pine Forests. *Ecosystems*, *3*(5), 472–483. https://doi.org/10.1007/s100210000041

Tinker, D., Stakes, G. K., & Arcano, R. M. (2010). Allometric Equation Development, Biomass, and Aboveground Productivity in Ponderosa Pine Forests, Black Hills, Wyoming. *Western Journal of Applied Forestry*, *25*(3), 112–119. https://doi.org/10.1093/wjaf/25.3.112

Tran, B. N., Tanase, M. A., Bennett, L. T., & Aponte, C. (2018). Evaluation of Spectral Indices for Assessing Fire Severity in Australian Temperate Forests. *Remote Sensing*, *10*(11), 1680. https://doi.org/10.3390/rs10111680

Trigg, S., & Flasse, S. (2001). An evaluation of different bi-spectral spaces for discriminating burned shrub-savannah. *International Journal of Remote Sensing*, *22*(13), 2641–2647. https://doi.org/10.1080/01431160110053185

van der Werf, G. R., Randerson, J. T., Giglio, L., van Leeuwen, T. T., Chen, Y., Rogers, B. M., Mu, M., van Marle, M. J. E., Morton, D. C., Collatz, G. J., Yokelson, R. J., & Kasibhatla, P. S. (2017). Global fire emissions estimates during 1997–2016. *Earth System Science Data*, *9*(2), 697–720. https://doi.org/10.5194/essd-9-697-2017

van der Werf, G. R., Randerson, J. T., Giglio, L., Collatz, G. J., Mu, M., Kasibhatla, P. S., Morton, D. C., DeFries, R. S., Jin, Y., & van Leeuwen, T. T. (2010). Global fire emissions and the contribution of deforestation, savanna, forest, agricultural,

and peat fires (1997–2009). *Atmospheric Chemistry and Physics*, *10*(23), 11707–11735. https://doi.org/10.5194/acp-10-11707-2010

Vermeire, L. T., Heitschmidt, R. K., & Rinella, M. J. (2009). Primary Productivity and Precipitation-Use Efficiency in Mixed-Grass Prairie: A Comparison of Northern and Southern US Sites. *Rangeland Ecology & Management*, *62*(3), 230–239. https://doi.org/10.2111/07-140R2.1

Whitman, T., Enders, A., & Lehmann, J. (2014). Pyrogenic carbon additions to soil counteract positive priming of soil carbon mineralization by plants. *Soil Biology and Biochemistry*, *73*, 33–41. https://doi.org/10.1016/j.soilbio.2014.02.009

Zhou, Y., Singh, J., Butnor, J. R., Coetsee, C., Boucher, P. B., Case, M. F., Hockridge, E. G., Davies, A. B., & Staver, A. C. (2022). Limited increases in savanna carbon stocks over decades of fire suppression. *Nature*, *603*(7901), 445–449. https://doi.org/10.1038/s41586-022-04438-1

Figures

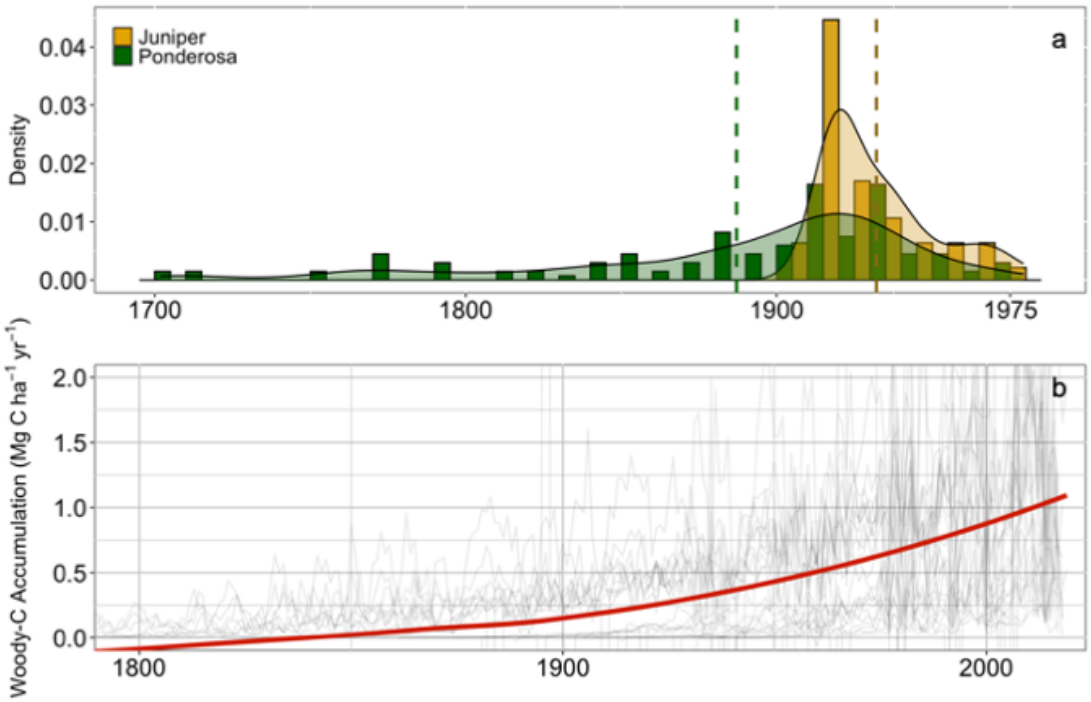


Figure 1. a) Establishment distribution of ponderosa and juniper across our plots in Unit D the Musselshell Missouri River Breaks regions of Central Montana. Dashed lines represent mean establishment dates for each species. b) Red trendline denotes the mean woody carbon accumulation of (juniper + ponderosa) across Unit D. Shaded areas represent individual plot (n=23) growth rates used to calculate the mean. Note scale difference on the x-axis.

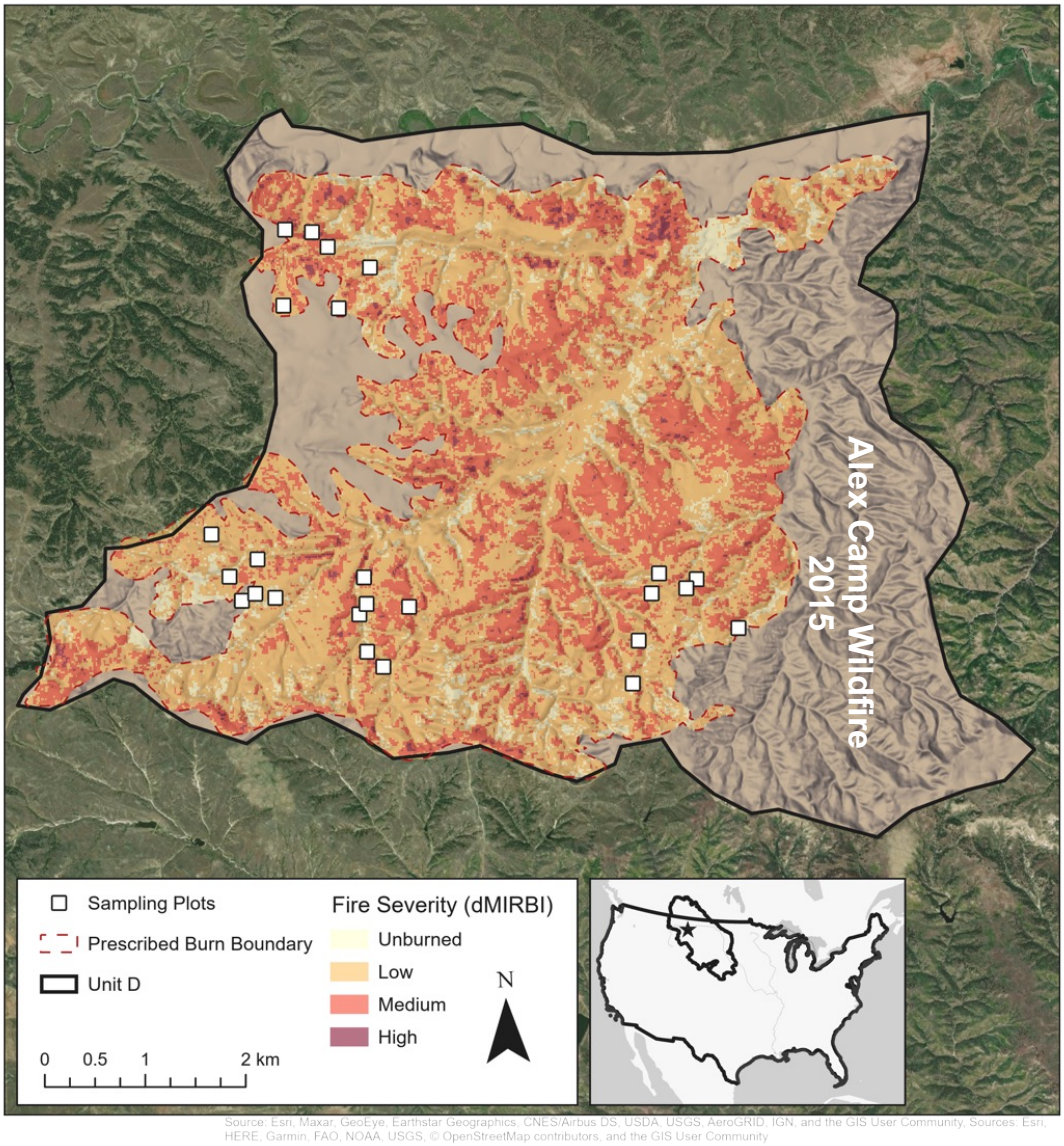


Figure 2. Burn severity derived using the dMIRBI spectral index from the 2018 Bureau of Land Management (BLM) prescribed fire in Unit D. Unit D is located in the Musselshell Missouri River Breaks regions of Central Montana and is roughly 4,500 ha. White squares represent the 0.25 ha sampling plots established and used for this study. Inset star shows the location of the site within the North American Northern Great Plains boundary. Brown areas outside of the red burn boundary were areas not impacted by the prescribed fire within Unit D. The Alex Camp boundary was from a wildfire that burned a portion of Unit D in 2015. See Table 1. for binning criteria used to classify burn severity.

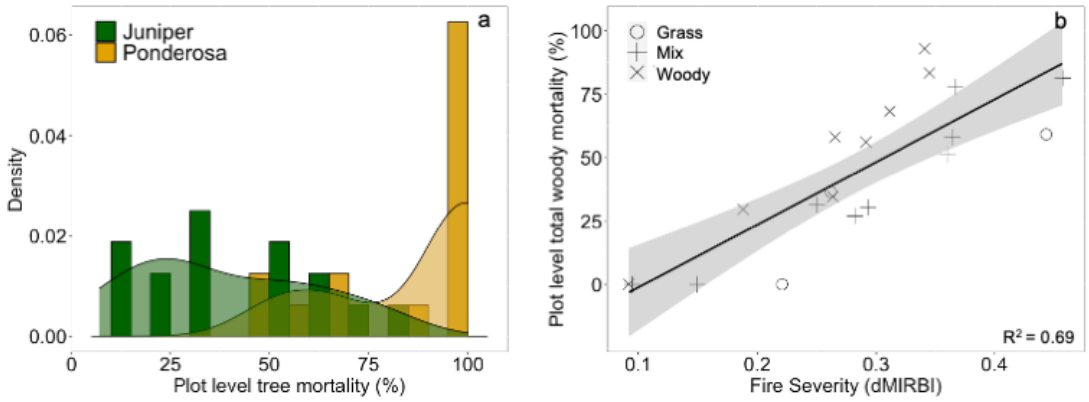


Figure 3. a) Distribution of plot level mortality (%) by species b) The linear relationship of the total mortality (weighted by the pre-fire proportion of woody cover in each plot) and severity (dMIRBI spectral index) across the plots from Fig 1. Shapes represent the plot level vegetation designation cover classified by percent woody cover.

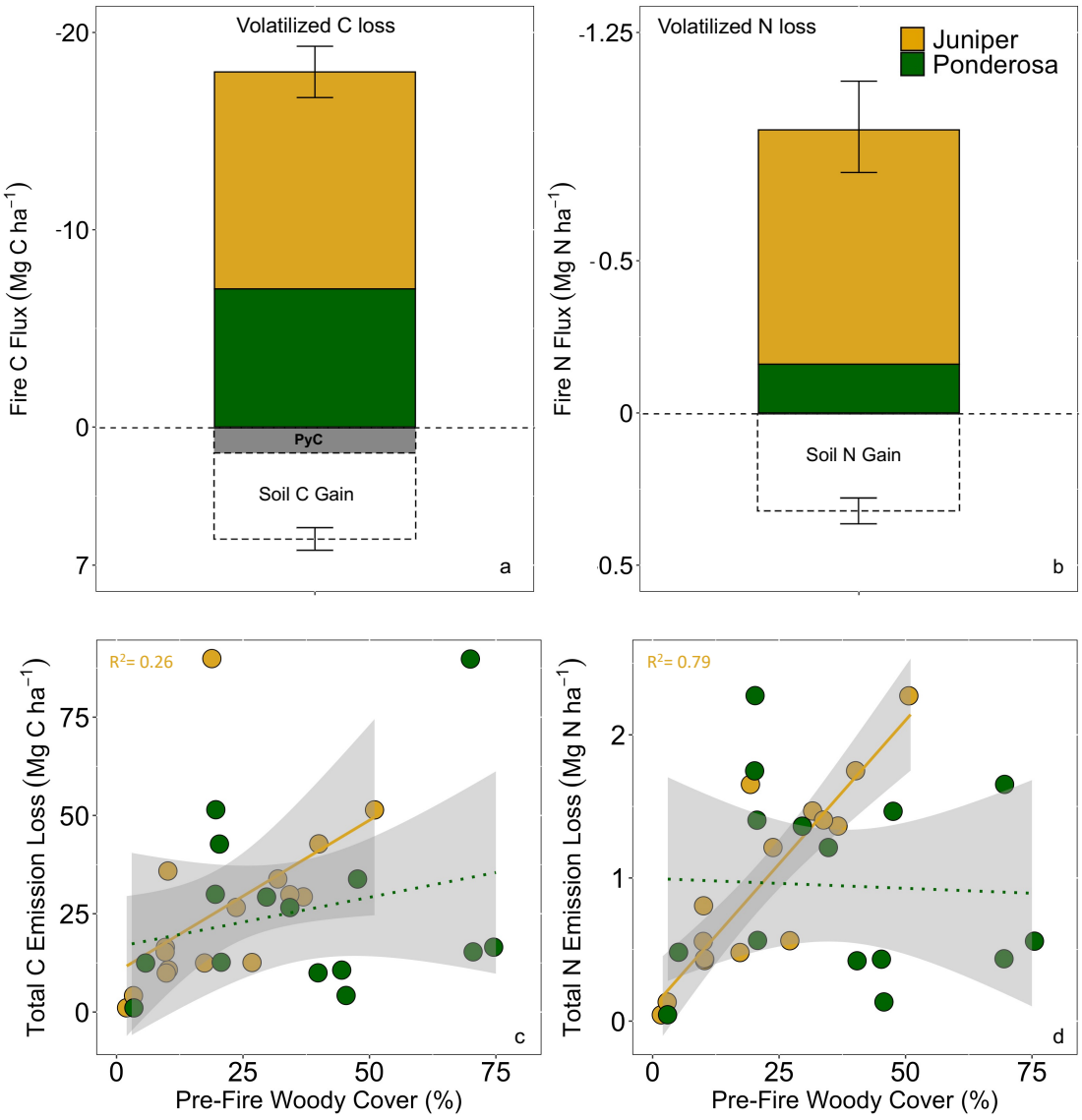


Figure 4. Area scaled carbon (a) and nitrogen (b) flux estimates from the plots that burned in the 2018 prescribed fire (n = 16 plots). The grey shaded area in (a) indicates the proportion of soil pyrogenic carbon (PyC) gain. Error bars represent SE of the overall volatile emissions or soil gain. Relationship between plot carbon and nitrogen emission loss and pre-fire cover of juniper and ponderosa in the burned plots. Color in (c) and (d) indicates individual regression of the 16 plots and the respective woody cover by species. Solid lines denote a significant trend at ($\alpha = 0.05$). Note the different y-axis scales in all plots.

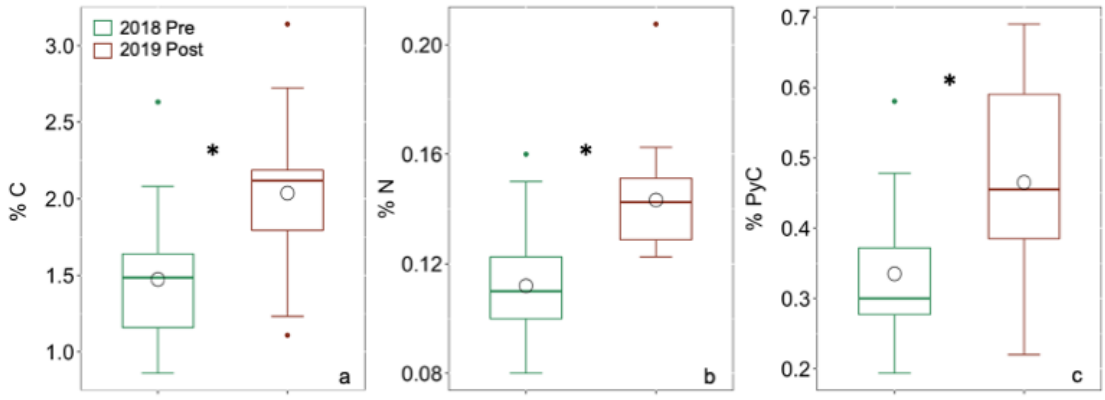


Figure 5. Pre and post fire differences of soil C, N, and pyrogenic carbon (PyC) concentrations (0 – 10 cm) across the 16 burned plots. Black circles represent ordinary least square means. Box plots * denote statistical significance at ($\alpha = 0.05$).

Tables

Table 1. Severity classification and % area affected in Unit D from the 2018 prescribed fire. Severity was measured using the Difference mid-infrared burn index **(**dMIRBI) spectral index acquired from the Sentinel-2 satellite. No burn zone cutoff was defined by highest index observed across our 4 control plots.

Classification	**dMIRBI index**	**% Area of Unit D**
No burn	> 0.14	9
Level 1 (low)	0.14 - 0.36	59
Level 2 (medium)	0.36 – 0.60	31
Level 3 (high)	< 0.60	> 1

Table 2. Woody vegetation biomass chemistry and total pre-fire aboveground biomass pools (kg ha^{-1}). Values are means ± SE from across the 20 plots. Juniper chemistry is an aggregation of the three major species across our study system.

	%C	%N	C:N	AGB C-Pool	AGB N-Pool
Juniper					
Wood	50.0	0.10	506	6080 ± 900	48.3 ± 7.4
Needle	51.3	1.06	48.6	8960 ± 1325	760 ± 110
Ponderosa pine					
Wood	51.2	0.03	2290	22300 ± 4175	52.3 ± 9.8
Needle	49.3	1.02	49.6	3800 ± 575	315 ± 48

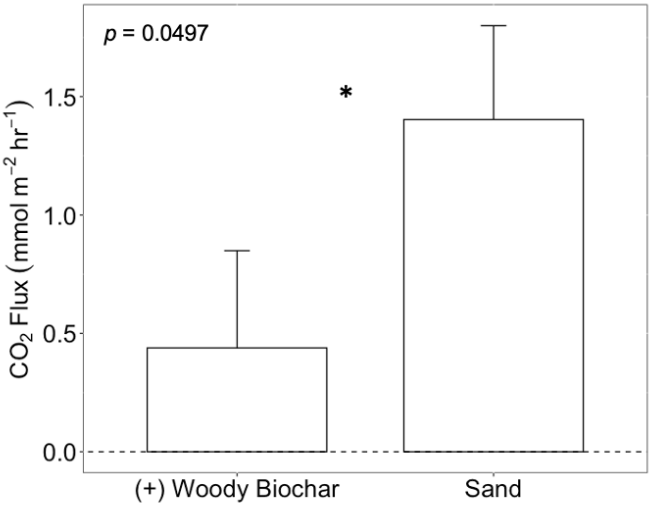
Supplemental Figures



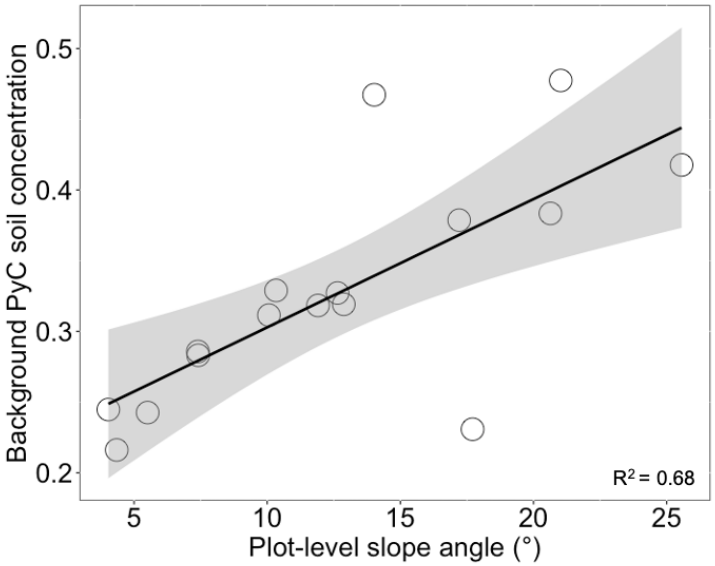
Supplemental Figure 1. Aerial image of a largely unburned portion of Unit D (2020) where WPE is occurring in the Musselshell-Missouri River breaks region of Central Montana.



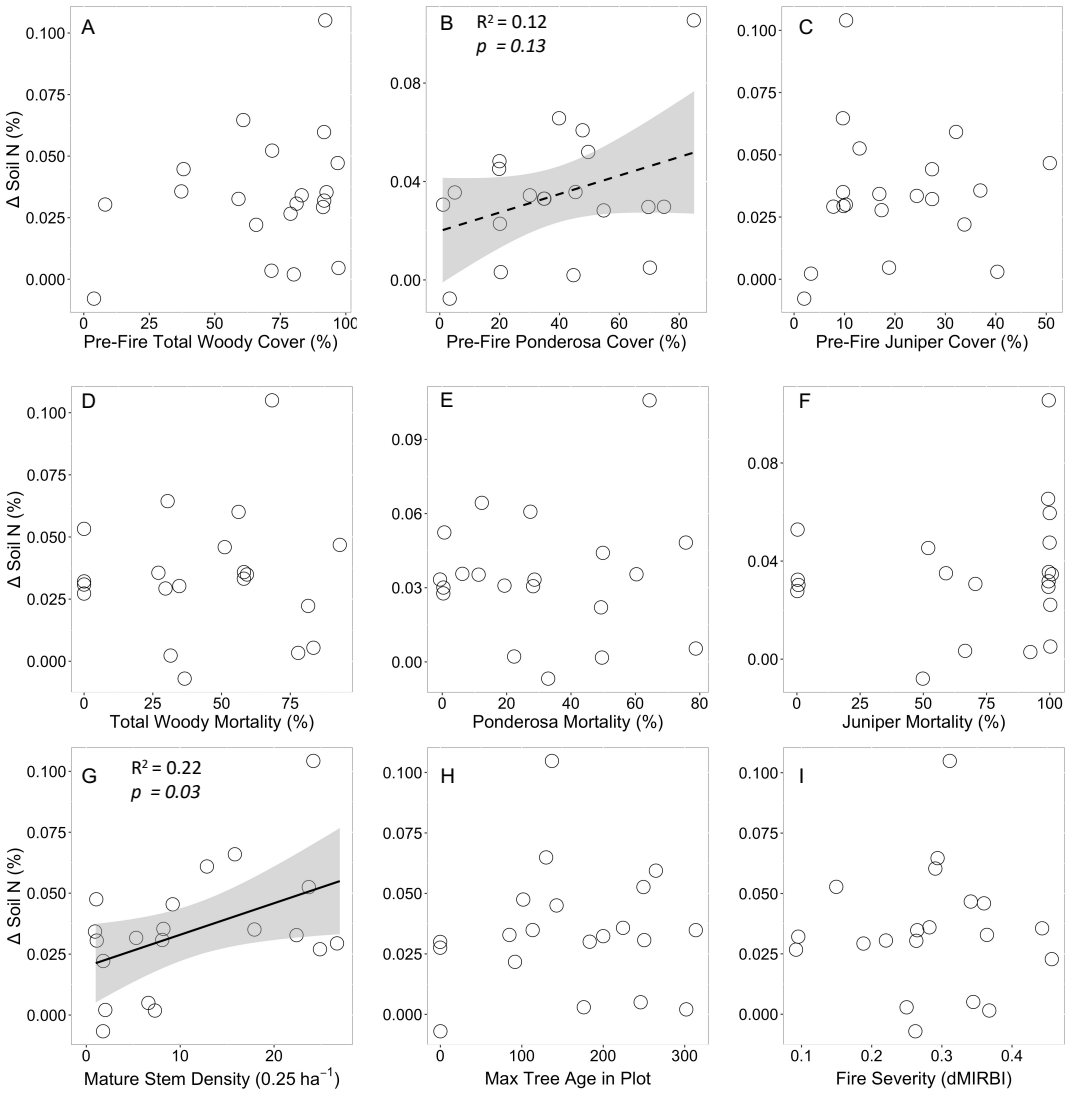
Supplemental Figure 2. Pre- and post-burn photos (April 2018 and May 2019) from one of the plots in Unit D.



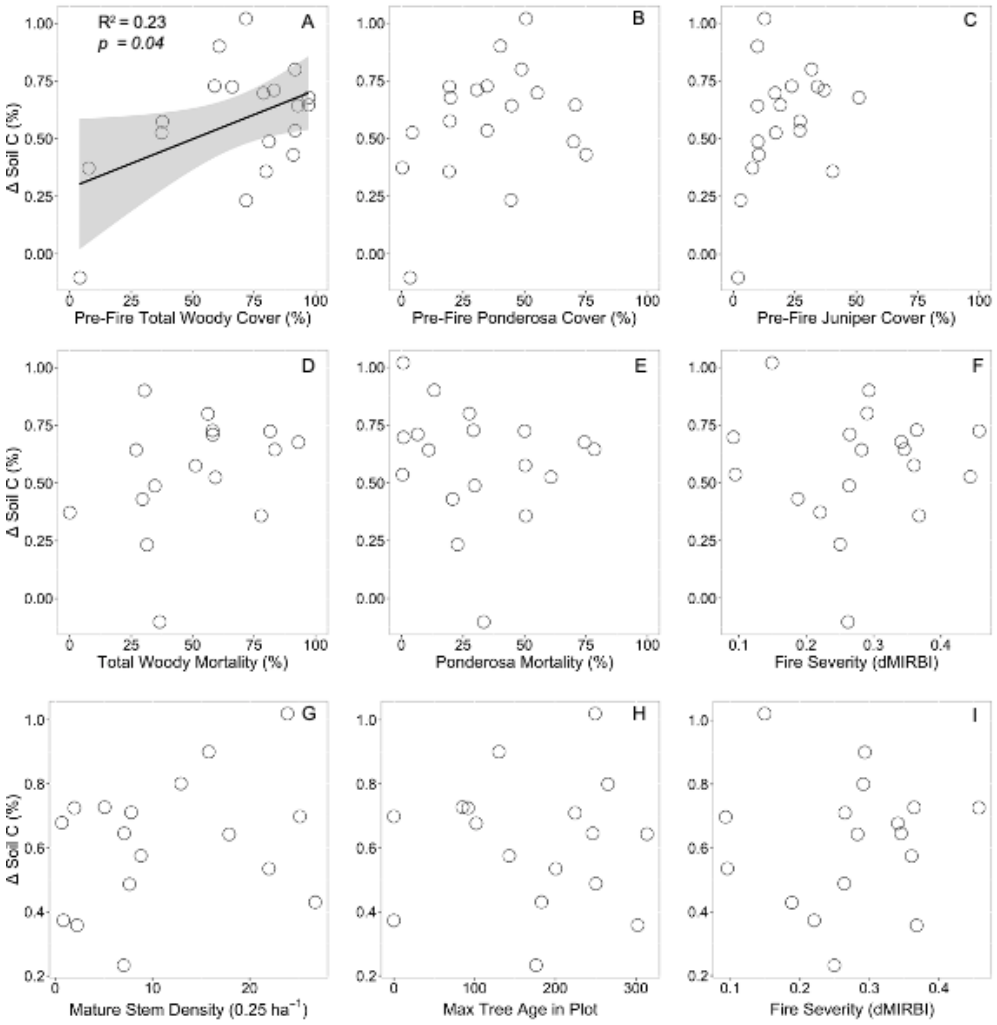
Supplemental Figure 3. Cumulative CO_2 fluxes of woody biochar (ponderosa n =4 and juniper n = 3) amended sandy-loam soils and sandy-loam controls (90% sand and 10% loam mix; n =7). Values are least squared means (+ SE), * denotes significant difference at ($\alpha = 0.05$).



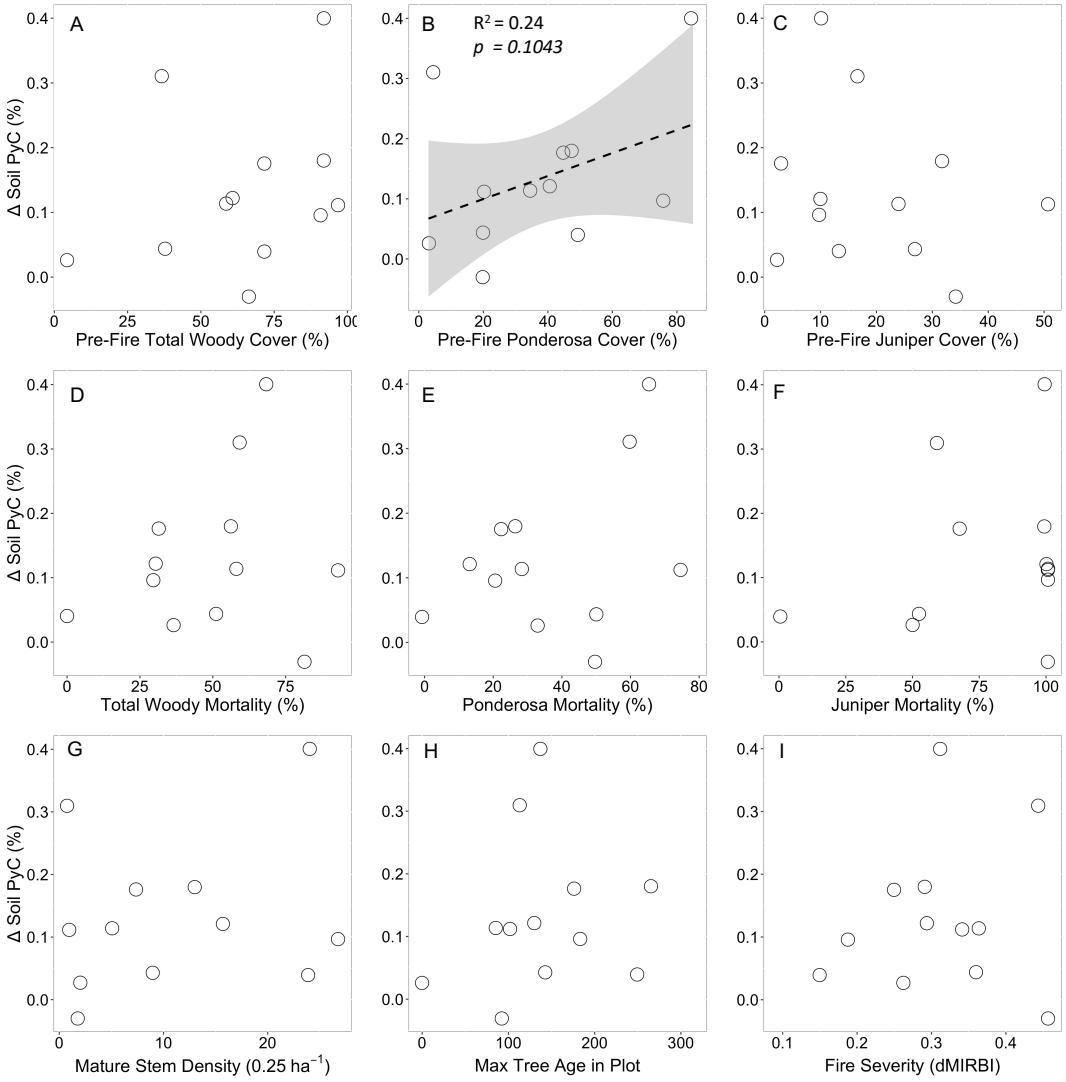
Supplemental Figure 4. Relationship between pre-fire soil PyC (0-10 cm soil depth) and surface slope angle. Relationship between PyC and model residuals (fixed additive effects of slope and TPI) and slope. Solid trend line denotes significant ordinary least squares relationship at ($\alpha = 0.05$).



Supplemental Figure 5. Ordinary least square regressions between the pre and post fire change in mineral soil N concentrations (0-10 cm) and woody expansion (% cover, stem density, max tree age) and fire related (mortality and fire severity) explanatory variables. Soli trend line denote significant linear trend at ($\alpha = 0.05$).



Supplemental Figure 7. Ordinary least square regressions between the pre and post fire change in mineral soil C concentrations (0-10 cm) and woody expansion (% cover, stem density, max tree age) and fire related (mortality and fire severity) explanatory variables. Soli trend line denote significant linear trend at ($\alpha = 0.05$).



Supplemental Figure 7. Relationship between pre-fire PyC (0-10 cm soil depth) and slope. Model residuals of the fixed additive effects of Slope and TPI to show their strong control over the distribution of soil PyC.

Supplementary Tables

Table 1. KCL extractable NO_3-N, NH_4-N, and NH_4:NO_3 (g kg^{-1} dry soil) pre and post fire at 0-10 cm soil depth. Values are modeled means (±SE), with values in April 2018 representing pre-burn conditions

April-18 (Pre-fire)		**May-18**	**Sept-18**
	NH_4-N		
	Burned	2.01 ± 0.23	3.79 ± 0.62
1.05 ± 0.2	Unburned Controls	1.34 ± 0.46	0.97 ± 1.33
	p-value	0.41	0.001
	NO_3-N		
	Burned	0.10 ± 0.02	3.14 ± 0.39
0.14 ± 0.05	Unburned Control	0.08 ± 0.03	0.38 ± 0.81
	p-value	0.85	0.012
	NH_4:NO_3		
	Burned	15.5 ± 3.9	1.7 ± 0.4
6.7 ± 1.8	Unburned Controls	16.6 ± 8.7	4.9 ± 2.4
	p-value	0.99	0.14

Supplemental Table 2. Bray's extractable PO_4-P (ug g^{-1} dry soil) pre and post-fire. . Values are modeled means (±SE), p-values represent the post-hoc pairwise comparison between the burned and unburned controls at ($\alpha = 0.05$)..

April-18 (pre-fire)		**May-18**	**Sept-18**
	Burned	3.79 ± 0.43	5.43 ± 0.34
3.09 ± 0.31	Unburned Controls	3.08 ± 0.33	4.53 ± 0.49
	p-value	0.1568	0.1427

Table 3. One-year differences in soil concentrations (0-10 cm) of % C, % N, % P, and % PyC before and after fire across the burned and unburned plots in . Values are least square means and ± SE

April-2018 (pre-fire)		**May-2019**
	Soil %C, n = 20	
	Burned	2.01 ± 0.13
1.47 ± 0.12	Unburned Controls	1.98 ± 0.23
	Soil %N, n = 20	
	Burned	0.15 ± 0.005
0.11 ± 0.005	Unburned Controls	0.14 ± 0.01
	Soil %P, n = 20	
	Burned	0.05 ± 0.001
0.05 ± 0.001	Unburned Controls	0.06 ± 0.003
	Soil % PyC, n = 12	
	Burned	0.46 ± 0.04
0.33 ± 0.03	Unburned Controls	0.51 ± 0.13

CHAPTER FOUR

GLOBAL DISTRIBUTION AND CLIMATE SENSITIVITY OF THE TROPICAL MONTANE FOREST NITROGEN CYCLE

Contribution of Authors and Co-Authors

Manuscript in Chapter 4

Author: Justin D. Gay
Contributions: Conducted the global meta-analysis, analyzed and interpreted the data, and wrote the first draft of the manuscript

Co-Author: Bryce Currey
Contributions: Assisted in analyzing and interpreting data, and revised the manuscript

Co-Author: Jack Brookshire
Contributions: Conceived the project, collected field samples, assisted in data analysis and interpretation, and revised the manuscript.

Manuscript Information

Justin D. Gay, Bryce Currey, ENJ Brookshire
Nature Communications

Status of Manuscript:
____ Prepared for submission to a peer-reviewed journal
__X__ Officially submitted to a peer-reviewed journal
____ Accepted by a peer-reviewed journal
____ Published in a peer-reviewed journal

Springer
Submitted February 15, 2022
In revision April 4, 2022

144

GLOBAL DISTRIBUTION AND CLIMATE SENSITIVITY OF THE TROPICAL MONTANE FOREST NITROGEN CYCLE

J.D Gay[1], B. Currey[1], ENJ Brookshire[1]

[1]Land Resources and Environmental Science. Montana State University. 334 Leon Johnson Hall. P.O. Box 173120. Bozeman, MT 59717-3120, USA

Abstract

Tropical forests are pivotal to global climate and biogeochemical cycles, yet the geographic distribution of nutrient limitation to plants and microbes across the biome is unresolved. One long-standing generalization is that tropical montane forests are nitrogen (N)-limited whereas lowland forests tend to be N-rich. However, empirical tests of this hypothesis have yielded equivocal results. Here we evaluate the topographic signature of the ecosystem-level tropical N cycle by examining climatic and geophysical controls of surface soil N content and stable isotopes (^{15}N) from elevational gradients distributed across tropical mountains globally. We document steep increases in soil N content and declining $\delta^{15}N$ with increasing elevation, consistent with decreased microbial N processing and lower gaseous N losses. Temperature explained much of the change, with the declines in soil N concentrations and density (kg N m^2) having apparent temperature sensitivities (Q_{10}) of 1.93. Although montane forests make up 11% of forested tropical land area, we estimate they harbor twice the soil N density of lowland forests and account for > 16% of the tropical forest soil N pool. Our findings support the existence of widespread microbial N limitation across tropical montane forest ecosystems and high sensitivity to climate warming.

Introduction

Tropical mountains give rise to some of the most striking climatic and ecological gradients on Earth. Over relatively small distances, elevational gradients in tropical mountains recapitulate latitudinal shifts in temperature[1] and thus provide a natural laboratory for understanding environmental control of ecosystem function and effects of global change[2,3]. One outstanding question is how climate warming will affect soil nutrient cycles that constrain productivity and carbon storage in tropical montane forests[4–6]. In contrast to most of the lowland tropics, tropical montane forests can accumulate large pools of N in soil organic matter (SOM)[7] yet are often considered to be limited by the availability of inorganic N[8–10]. Observations and models predict that warming in tropical mountains will enhance primary production[4,11–13] but also increase losses of soil carbon[3,14]. Increases in microbial N mineralization could further stimulate plant growth but also increase N losses, including emissions of the heat-trapping gas nitrous oxide (N_2O). However, the degree to which organically-bound N will continue to constrain both processes is uncertain.

Despite decades of research showing slower microbial N processing in montane than lowland tropical forest soils[7,15,16], it remains unclear how climate variation shapes the balance of N inputs and losses that determine the long-term stability of the soil N pool. The elevational distributions of these fluxes (e.g., biological N fixation, gaseous and hydrologic losses) are poorly quantified for tropical montane forests globally. For example, while soil N_2O emissions have been shown to decline with increasing elevation in some montane forests[17,18], consistent with lower N availability, observations of large hydrologic losses of

N from other montane forests[19,20] suggest high N availability at the ecosystem level. Furthermore, the size and geographic distribution of tropical montane forests and their soil N pools are poorly constrained. Although global inventories show larger soil N pools in tropical mountains than lowlands[21–23], these estimates are highly uncertain due to limited sampling in forested mountainous terrain[23]. Tropical mountains are distributed across distinct biogeographical regions and a wide range of lithologies and precipitation[24,25], making generalization difficult. For example, erosion in steep terrain can rejuvenate rock-derived nutrients[26], including N[27], but also limit N accumulation, especially in geologically young mountains[28,29]. In addition, regional and elevational variation in precipitation can constrain primary production, SOM decomposition and nutrient availability[2,30,31]. Therefore, disentangling climate versus other biophysical drivers is essential for understanding potential warming effects on the N cycle in tropical montane forests.

Here, we address these uncertainties by analyzing data on soil N and its natural abundance isotope (^{15}N) collected across tropical elevational transects globally. We focus our analysis on shallow (0-20 cm) mineral soils as these have shorter SOM residence times and higher climate sensitivity compared to deeper soil[32] and represent the vast majority of samples collected globally. We use $\delta^{15}N$ as an integrative measure of ecosystem-level N cycling as the relative abundance of ^{15}N to ^{14}N in mineral soils records the long-term imprint of microbial processing and N bioavailability[33]. In biologically active soils, higher (isotopically enriched) $\delta^{15}N$ values indicate increased availability of N to plants and microbes and proportionally larger fractionating losses of N (i.e., via gaseous losses)[31,33,34].

While previous global analyses[31,35,36] show higher soil $\delta^{15}N$ in warmer and lower precipitation climates, it is unclear how this applies to humid tropical mountains where precipitation shows no globally consistent pattern with elevation[2,25]. Leveraging elevational gradient data, we determine key environmental drivers of the soil N cycle in montane forests and use statistical and geospatial modeling to map its global distribution.

Results and Discussion

Elevational patterns of soil N and $\delta^{15}N$

We compiled a database of soil samples from 324 humid forest sites distributed across sixteen elevational gradients (Fig. 1 a; Supplementary Figs. 1and 2) and from lowland tropical forests[36] across the major tropical land areas (Neotropics, Africa, Asia-Pacific). The sites span a large range of elevation (0 – 3660 m.a.s.l), climate (7 –30°C, MAT; 1200 –8000 mm, MAP), and a diversity of rock types and lithologic ages (Supplementary Table 1). We first used mixed-effects models to isolate the effect of elevation from any effects of biogeographic region or individual transect location (Supplementary Table 2). This revealed large increases in soil N content with increasing elevation across tropical mountains worldwide, although there was considerable regional spread in the data at higher elevations (Fig 2a). Soil organic carbon (SOC) also increased with elevation (Supplementary Fig. 3), more so than N, resulting in increasing C:N ratios with greater elevation (Fig. 2b). Across the global elevational range, soil C:N ratios cross the stoichiometric threshold that governs net N mineralization versus immobilization (C:N

~20-25)[37], consistent with microbial N limitation and slower bioavailable N cycling in montane compared to lowland forests[5,38].

Elevational patterns in $\delta^{15}N$ further support lower N bioavailability and gaseous losses with increasing elevation. Globally, $\delta^{15}N$ decreases by about 2‰ for every 1 km increase in elevation (Fig 2c). The range of soil $\delta^{15}N$ (-0.3 - 10.1‰) and its change with elevation is similar to that documented for soil $\delta^{15}N$ across global latitudinal climate gradients[35,36]. Additionally, our findings mirror the inverse relationship between the C:N stoichiometry of SOM and its $\delta^{15}N$ enrichment observed globally[36,39]. Across elevational gradients, $\delta^{15}N$ declines nonlinearly with increasing soil N content (Fig 2d) and C:N ratios (Supplementary Fig. 4), such that lowland forest soils are characterized by uniformly low %N and enriched in $\delta^{15}N$ while montane forests have high %N and low $\delta^{15}N$ This pattern is consistent with a topographic shift from net microbial mineralization to immobilization and lower fractionating loss (e.g., denitrification) as a primary regulator of N accumulation in tropical montane forests.

Drivers of tropical soil N content and $\delta^{15}N$

To determine drivers of %N and $\delta^{15}N$, we combined globally gridded data sets of climate, geophysical, and soil properties with transect and lowland data in mixed-effects models. Across all transects, MAT decreases by 5.1 +/- 0.07 C for every 1 km rise in elevation (Supplementary Fig. 5). Hierarchical partitioning analysis (Supplementary Table 3) determined MAT to be the most important driver of soil N content, explaining 25% of the

geographic distribution, followed by MAT:MAP interaction (18%), SOC (18%), tropical region (Africa, Neotropics, Asia-Pacific; 18%), MAP (12%), and slope (8%). For $\delta^{15}N$, the model similarly identified MAT as the most important driver (42%), followed by MAP (26%), tropical region (19%), and SOC (12%). These results are consistent with continental and global-scale analyses describing the importance of climate and SOC in governing the spatial distribution of the N cycle and its isotopic imprint[33,36,40], with $\delta^{15}N$ generally decreasing with increasing MAP and SOC. MAP is highly variable across tropical regions (Supplementary Fig. 1), but has no coherent relationship with elevation, soil N, or $\delta^{15}N$ across our sites (Supplementary Figs 6 and 7). In contrast, the uniformity of the positive MAT- $\delta^{15}N$ and negative MAT-N relationships across the global diversity of tropical mountain environments points to temperature as a main control of microbial N transformations that isotopically discriminate against $\delta^{15}N$.

We next examined the temperature sensitivity of soil N concentrations and the soil N pool by deriving the apparent Q_{10} (i.e., the decrease in N concentrations and pools with a 10°C increase in temperature) using exponential fitting to the elevational variation in MAT (Fig. 3). Consistent with non-linearly coupled changes in N concentrations with elevation, our analysis yielded apparent Q_{10} values of ~1.9 for their change with ambient temperature. This value is consistent with that found for soil enzyme activities (V_{max} 1.5-2) measured across tropical elevational gradients[3,41] and results from litter decomposition[30] and soil nitrogen mineralization studies[42] across tropical forests. The global convergence of temperature sensitivities for soil N contents suggests a strong kinetic underpinning of the

inverse relationship between soil N accumulation and fractionating loss pathways (i.e., gaseous versus hydrological), consistent with decreasing microbial denitrification with increasing tropical elevation[17,18]. However, such space-for-time analyses cannot determine microbial temperature sensitivity at a given elevation/ambient temperature[14], nor account for potential acclimation to past or future temperatures[41]. For instance, temperature sensitivities of microbial processes tend to be higher in colder environments[43,44], suggesting greater temperature sensitivity of microbial N turnover in montane forests than indicated by our gradient analysis.

Global distribution of tropical montane forest soil N pools and $\delta^{15}N$

Based on differences in parameters of elevational changes in N and $\delta^{15}N$, we developed geospatial models combining climate, topography (Supplementary Table 4), and tree cover data to map the pantropical distribution of soil N pools and $\delta^{15}N$ (Fig. 1d-i; Methods). We first calculated soil N pools (0- 20 cm) across our sites by spatially coupling soil N data with globally gridded maps of bulk density (Methods; Supplementary Fig. 8). Across all sites, soil N pools (0-20 cm) are nearly twice as large in montane (1.5 (geometric standard deviation 0.7-3.1) kg N m^{-2}) than in lowland forests (0.85 (0.4-1.6) kg N m^{-2}, $t(49) = 4.146$, $p = < 0.001$).

Drivers explaining the spatial distribution of soil N pools were similar to that for %N except that SOC emerged as a more important explanatory variable (30%; Supplementary Table 3), followed by geographic region (20%), MAT (19%), MAP (15%), and MAT:MAP

interaction (15%). The global model reproduces observed N pools across individual elevational gradients but tends to underestimate the largest montane N pools (Supplementary Fig. 9), suggesting our results are conservative. Despite montane forests accounting for only 4.3% (2.1×10^6 km^2) of tropical land area and 49% of tropical mountainous terrain (Supplementary Tables 5 and 6), we estimate they account for an outsized proportion (16.5%; 1.9 ± 0.9 Pg N) of the global tropical forest soil N pool (11.6 ± 8.2 Pg N; Supplementary Table 7).

Accurate estimates of soil N and its environmental drivers are critical for benchmarking coupled C-N cycles in terrestrial ecosystem models. Although existing global maps also show higher soil N in montane relative to lowland tropical forests, the size and geographic distribution of the montane soil N pool are poorly constrained due to low sampling density[21,23]. For example, soil N concentrations in our montane data set are 1.6 times higher than simulated by a recent globally gridded data product[23] for the same sites (Supplemental Fig 10). Our models also reveal significant geographic variation in the contribution of montane forests to tropical soil N pools (Supplementary Table 5) not captured in existing estimates. For instance, 22% of Asia-Pacific forests are montane, comprising over half of global montane forests, and constitute a large (31%) fraction of the global montane N pool. However, soils in Neotropical montane forests tend to have higher N contents (Fig. 2a) and thus harbor the largest fraction (43%) of the global montane soil N pool. Because lowland forests constituted a small proportion of our data set, our estimates of lowland soil N pools and $\delta^{15}N$ and their environmental drivers are less certain. Nevertheless, our model

estimates of the global tropical soil N pool are similar to previous estimates[21] and confirm large N pools and relatively low $\delta^{15}N$ across extensive SOC-rich wetland and peatland areas[45] of western Amazonia, the upper Congo, and southern Borneo (Fig. 1b, c; Supplementary Fig. 1). Despite low data representation across lowland forests, our model results are consistent with previous models showing SOC to be a strong predictor of N stocks, but also indicate a fundamental shift to temperature control with increasing elevation.

The prominent role of elevational climate variation in regulating the tropical soil N cycle offers insight into existing conceptual theory. Despite decades of thought that plant growth in montane forests is predominantly limited by N, recent syntheses of tropical fertilization experiments[46] find no global tendency for trees to be more N limited at higher than lower elevations, and observations of large leaching losses of bioavailable N from some montane forests[19,20] suggests N richness at the ecosystem scale[47]. Broad geographic evidence for increasing N constraints to microbial but not vegetative activity with elevation suggests some degree of decoupling in the plant-microbe N cycle that may also be subject to change with increased temperature. Although our analysis accounts for broad variation in biophysical drivers, other factors could contribute to the observed patterns in soil N. For example, some tropical mountains are characterized by elevational increases in ectomycorrhizal trees that can access soil organic N directly, and are associated with higher SOM accumulation, C:N ratios, and lower N availability[48]. In addition, erosional supply of geologic N is higher in mountainous terrain[27] and could contribute to enhanced N storage.

However, our isotopic evidence is most consistent with increasing microbial N limitation at higher elevations[38] and a shift in the proportion of N lost from highly fractionating (e.g., denitrification) to less fractionating (e.g., hydrologic leaching) processes[31].

Our results identify a large and potentially vulnerable pool of soil nitrogen across tropical montane forests. Montane forests are increasingly subject to the direct effects of agricultural expansion and from deforestation-driven amplification of warming[49]. Warming is occurring at a faster rate in mountains than other tropical land areas[50], potentially jeopardizing these large stocks of soil organic N via enhanced microbial processing. While our findings reveal emergent climate sensitivities of the soil microbial N cycle, any net ecosystem-level warming effects will depend on the climate sensitives of multiple N sources, sinks and their interaction, including biological N fixation and plant uptake. The degree to which N availability will limit warming-induced enhancement of montane forest productivity, or alternately result in enhanced N losses to water and the atmosphere, will depend on how microbial N turnover and supply keep pace with increasing demand.

Methods

Data assembly

We conducted an extensive web-based search for studies reporting mineral soil (< 20 cm depth) total N (% N) and $\delta^{15}N$ from mature humid tropical forests (MAP > 1200, latitude

± 23.5° N and S of the equator) where samples were collected along a continuous elevational transect. $\delta^{15}N$ is reported as ‰ = [($R_{sample}/R_{standard}$)-1] x 1000, where R = $^{15}N:^{14}N$ of the sample and the standard, with the standard as the background atmospheric ratio of $^{15}N:^{14}N$. In total, 16 independent elevational gradient transects were identified for a total of 185 soil %N and 168 soil $\delta^{15}N$ observations. Five transects included both bulk soil $\delta^{15}N$ and % N (Costa Rica[19,51], Trinidad[52], Borneo[53], Australia[44]), four transects reported only $\delta^{15}N$ (the Democratic Republic of the Congo[54], Rwanda[24], Ecuador[17,24]), and seven reported only % N (Cameroon[55], Colombia[7], Costa Rica[15], Hawaii[56], Peru[5], Papua New Guinea[57,58]; Supplemental Table 1). Two of the sixteen transects were established as part of previous sampling campaigns at Volcan Orosi in Costa Rica[19] and the Northern Range of Trinidad[52]. Here, we collected and composited four mineral soil samples (0-20 cm) from 33 and 37 locations distributed across elevation. We included an additional 85 lowland sites from a global soil %N and $\delta^{15}N$ dataset[36] previously aggregated at ~0.1° latitude. While reported sampling depths varied across studies, we excluded all soils >30 cm depth and those classified as organic horizons (Oi, Oa, Oe). However, we cannot rule out the possibility that some studies incorporated organic soils in cases where sampling procedures were not described in detail. Further, it is possible that differences in analytical methods for the determination of N (e.g., Kjeldahl digestion, Dumas combustion) may have influenced our analysis. Geolocation data was requisite for all %N and $\delta^{15}N$ values to extract gridded ancillary data. For studies that provided a map figure with no sampling geolocation data, coordinates were derived by georeferencing map figures and extracting the coordinates from the map (Supplemental Fig. 2). For studies without open-source raw

data or summary tables, figures were digitized to extract values with *Plot Digitizer* (version 2.6.8.).

Quantifying tropical montane forest extent

Montane terrain was defined using a six-tier geospatial classification framework[59] combining slope, elevation, and local elevation range (LER) using a ~1 km cell resolution global DEM (USGS GTOPO30). LER is calculated as the difference between the maximum and minimum elevation within a 5 km radius of each grid cell to identify areas of low elevation but high relief (i.e., rugged topography). Montane land surfaces are pixels with an elevation > 2500 meters above sea level (m.a.s.l.), surfaces between 1500-2499 m.a.s.l. with slopes > 2°, and surfaces between 1000-1499 m.a.s.l. with slopes > 5° or an LER of > 300 m. Between 300-999 m.a.s.l., montane classification is restricted to LER values > 300 m. All terrain < 300 m.a.s.l. is classified as non-mountain or lowland. To restrict output to forested areas, we created a pantropical forest mask using 2010 global tree cover[60] and classified pixels with > 10 % tree cover and MAP > 1200 mm as humid tropical forest. Each sampling point in our soil chemistry dataset was then mapped onto this forest layer and classified as montane or lowland. All geospatial analyses were conducted using R (v4.0.3, R Core Team 2020) and ESRI ArcGIS Pro (ESRI 2019).

Drivers of soil N and $\delta^{15}N$

We fit linear mixed-effect regression models using maximum likelihood (lme4 and lmerTest packages in R) to examine relationships between C:N, %N, and $\delta^{15}N$ and

elevation across the 16 transects. A transect-specific identifier variable was used as a random effect in all models to account for violations of independence from sampling within individual transects. 95% confidence intervals were calculated using Monte-Carlo simulations for all figures containing transect-derived data in which model error was randomly simulated around mean response values 1000 times using the standard deviation from which the inner 95% was calculated. Response and predictor variables that did not exhibit normal distributions were log-transformed ($\log_e$) before statistical analyses. All statistical analyses were conducted in R (v4.0.3, R Core Team 2020) with packages cited in supplemental information. Significance was set a priori to $\alpha = 0.05$.

Linear mixed-effects regression models were fit to identify the main drivers in the distribution of tropical forest soil $\delta^{15}N$ and N pools by using biophysical parameters previously shown to influence N cycling processes (m.a.s.l., MAT, MAP, Slope angle, % clay, SOC)[28,36,40]. N pools were calculated by multiplying reported soil N concentrations and modeled bulk density for 0-20 cm (250m resolution)[22]. Although MAT and elevation exhibit strong multicollinearity, both were initially included in the full model to determine their relative explanatory power, although model selection subsequently removed m a.s.l from all models. Model refinement was conducted using a selection criterion of Δ AIC > 2 or greater (*dredge* function in R). We next used a hierarchical partitioning analysis to decompose the relative importance of $\delta^{15}N$ and %N model parameters in the respective regression models with the *Relaimpo* package in R. Model variance is reported using the $R^2_{(GLMM)}$ summary statistic and include both the $R^2_{(c)}$ (variance explained by the entire model) and $R^2_{(m)}$ (variance explained by the fixed effect; MuMin package in R).

To evaluate the temperature sensitivity of the soil N cycle, we calculated an apparent Q_{10} by fitting an exponential function of soil N concentrations and N pools (kg m^2) to the elevational distribution of MAT. Because $\delta^{15}N$ does not scale proportionally since it is on a per mil scale a Q_{10} was not fit. Least-square estimates of the regression parameters for all nonlinear models and significance tests for the exponential term were derived from the *nlstools* package in R.

$$(\text{N pool}) = 6.545^{0.066 \cdot \text{MAT}} \quad \text{equation 1}$$

$$(\%\text{N}) = 3.158^{0.066 \cdot \text{MAT}} \quad \text{equation 2}$$

and then using results to calculate Q_{10}:

$$(\%N_2/\%N_1)^{\frac{10}{MAT_2\text{-}MAT_1}} \quad \text{equation 3}$$

where $\%N_1$ and $\%N_2$ values represent the bulk soil %N (or N pool) from the curve fit with a MAT of 10 °C (25-15 °C) from Eq. 1 and 2.

Mapping soil N pools and $\delta^{15}N$

To create pantropical maps of $\delta^{15}N$ and N pools (Figure 1d – 1i), we multiplied model coefficients from our statistical models with respective gridded variables, including a binary gridded layer of each tropical region at ~1 km resolution. Pantropical N pools were

then calculated by summing mapped N pool data for the entire tropics, tropical montane, and lowland forests. Uncertainty around our estimates was derived from the multiplication of model SE and the 95% confidence interval critical t-distribution value (t^*) which is a function of model degrees of freedom.

$$\text{Upper/Lower CI} = \text{N pool} \pm t^* \cdot \text{SE} \qquad \text{equation 4}$$

$\delta^{15}N$ model results were compared to observed values based on the respective modeled values extracted from the sampled geographic coordinates along the transects. The gridded global N pool model was calculated based on %N values from the observed transect and lowland forest datasets and modeled bulk density. These were then compared to the observed N pool values from the sampled geographic coordinates along the transects. Model error was assessed using root mean squared error (RMSE; Supplementary Fig. 9). Finally, we compared our observations of soil %N to those simulated at 250 m resolution by SoilGrids 2.0 (ref 23) for the same montane coordinates (Supplementary Fig. 10).

References cited

1. Humboldt, A. von & Bonpland, A. Analysis of the geography of plants. (1805).

2. Malhi, Y. *et al.* Introduction: Elevation gradients in the tropics: laboratories for ecosystem ecology and global change research. *Global Change Biology* **16**, 3171–3175 (2010).

3. Nottingham, A. T. *et al.* Climate warming and soil carbon in tropical forests: Insights from an elevation gradient in the Peruvian Andes. *BioScience* **65**, 906–921 (2015).

4. Malhi, Y. *et al.* The variation of productivity and its allocation along a tropical elevation gradient: a whole carbon budget perspective. *New Phytologist* **214**, 1019–1032 (2017).

5. Nottingham, A. T. *et al.* Soil microbial nutrient constraints along a tropical forest elevation gradient: a belowground test of a biogeochemical paradigm. *Biogeosciences* **12**, 6071–6083 (2015).

6. Nottingham, A. T. *et al.* Microbes follow Humboldt: temperature drives plant and soil microbial diversity patterns from the Amazon to the Andes. *Ecology* **99**, 2455–2466 (2018).

7. Jenny, H., Bingham, F. & Padillasaravia, B. Nitrogen and organic matter contents of equatorial soils of Colombia, South-America. *Soil Science* **66**, 173–186 (1948).

8. Tanner, E., Vitousek, P. & Cuevas, E. Experimental investigation of nutrient limitation of forest growth on wet tropical mountains. *Ecology* **79**, 10–22 (1998).

9. Vitousek, P. M., Matson, P. A. & Turner, D. R. Elevational and age gradients in Hawaiian montane rainforest: foliar and soil nutrients. *Oecologia* **77**, 565–570 (1988).

10. Vitousek, P. M. & Sanford, R. L. Nutrient Cycling in Moist Tropical Forest. *Annual Review of Ecology and Systematics* **17**, 137–167 (1986).

11. Krishnaswamy, J., John, R. & Joseph, S. Consistent response of vegetation dynamics to recent climate change in tropical mountain regions. *Global change biology* **20**, 203–215 (2014).

12. Duque, A. *et al.* Mature Andean forests as globally important carbon sinks and future carbon refuges. *Nature Communications* **12**, 2138 (2021).

13. Fadrique, B. *et al.* Widespread but heterogeneous responses of Andean forests to climate change. *Nature* **564**, 207–212 (2018).

14. Nottingham, A. T. *et al.* Microbial responses to warming enhance soil carbon loss following translocation across a tropical forest elevation gradient. *Ecology Letters* **0**,.

15. Marrs, R. H., Proctor, J., Heaney, A. & Mountford, M. D. Changes in soil nitrogen-mineralization and nitrification along an altitudinal transect in tropical rain forest in Costa Rica. *The Journal of Ecology* 466–482 (1988).

16. Grubb, P. J. Control of forest growth and distribution on wet tropical mountains: with special reference to mineral nutrition. *Annual Review of Ecology and Systematics* **8**, 83–107 (1977).

17. Wolf, K., Veldkamp, E., Homeier, J. & Martinson, G. O. Nitrogen availability links forest productivity, soil nitrous oxide and nitric oxide fluxes of a tropical montane forest in southern Ecuador. *Global Biogeochemical Cycles* **25**, (2011).

18. Barthel, M. *et al.* Low N2O and variable CH4 fluxes from tropical forest soils of the Congo Basin. *Nat Commun* **13**, 330 (2022).

19. Brookshire, E. N. J., Hedin, L. O., Newbold, J. D., Sigman, D. M. & Jackson, J. K. Sustained losses of bioavailable nitrogen from montane tropical forests. *Nat. Geosci.* **5**, 123–126 (2012).

20. Rütting, T. *et al.* Leaky nitrogen cycle in pristine African montane rainforest soil. *Global Biogeochemical Cycles* **29**, 1754–1762 (2015).

21. Batjes, N. H. Total carbon and nitrogen in the soils of the world. *European journal of soil science* **47**, 151–163 (1996).

22. Hengl, T. *et al.* SoilGrids250m: Global gridded soil information based on machine learning. *PLoS one* **12**, e0169748 (2017).

23. Poggio, L. *et al.* SoilGrids 2.0: producing soil information for the globe with quantified spatial uncertainty. *SOIL* **7**, 217–240 (2021).

24. Bauters, M. *et al.* Parallel functional and stoichiometric trait shifts in South American and African forest communities with elevation. *Biogeosciences* **14**, 5313–5321 (2017).

25. Dalling, J. W., Heineman, K., González, G. & Ostertag, R. Geographic, environmental and biotic sources of variation in the nutrient relations of tropical montane forests. *Journal of Tropical Ecology* **32**, 368–383 (2016).

26. Porder, S., Vitousek, P., Chadwick, O., Chamberlain, C. & Hilley, G. Uplift, erosion, and phosphorus limitation in terrestrial ecosystems. *Ecosystems* **10**, 158–170 (2007).

27. Houlton, B. Z., Morford, S. L. & Dahlgren, R. A. Convergent evidence for widespread rock nitrogen sources in Earth's surface environment. *Science* **360**, 58–62 (2018).

28. Hilton, R. G., Galy, A., West, A. J., Hovius, N. & Roberts, G. G. Geomorphic control on the delta N-15 of mountain forests. *Biogeosciences* **10**, 1693–1705 (2013).

29. Vitousek, P. M., Van Cleve, K., Balakrishnan, N. & Mueller-Dombois, D. Soil development and nitrogen turnover in montane rainforest soils on Hawai'i. *Biotropica* 268–274 (1983).

30. Taylor, P. G. *et al.* Temperature and rainfall interact to control carbon cycling in tropical forests. *Ecology Letters* **20**, 779–788 (2017).

31. Houlton, B. & Bai, E. Imprint of denitrifying bacteria on the global terrestrial biosphere. *Proceedings of the National Academy of Sciences of the United States* **106**, 21713–21716 (2009).

32. Shi, Z. *et al.* The age distribution of global soil carbon inferred from radiocarbon measurements. *Nature Geoscience* **13**, 555–559 (2020).

33. Craine, J. M. *et al.* Ecological interpretations of nitrogen isotope ratios of terrestrial plants and soils. *Plant and Soil* 1–26 (2015).

34. Martinelli, L. *et al.* Nitrogen stable isotopic composition of leaves and soil: Tropical versus temperate forests. *Biogeochemistry* **46**, 45–65 (1999).

35. Amundson, R. *et al.* Global patterns of the isotopic composition of soil and plant nitrogen. *Global Biogeochemical Cycles* **17**, (2003).

36. Craine, J. M. *et al.* Convergence of soil nitrogen isotopes across global climate gradients. *Scientific reports* **5**, (2015).

37. Mooshammer, M. *et al.* Adjustment of microbial nitrogen use efficiency to carbon:nitrogen imbalances regulates soil nitrogen cycling. *Nat Commun* **5**, (2014).

38. Camenzind, T., Hättenschwiler, S., Treseder, K. K., Lehmann, A. & Rillig, M. C. Nutrient limitation of soil microbial processes in tropical forests. *Ecological Monographs* **88**, 4–21 (2018).

39. Mariotti, A., Pierre, D., Vedy, J. C., Bruckert, S. & Guillemot, J. The abundance of natural nitrogen 15 in the organic matter of soils along an altitudinal gradient (Chablais, Haute Savoie, France). *CATENA* **7**, 293–300 (1980).

40. Sena-Souza, J. P., Houlton, B. Z., Martinelli, L. A. & Nardoto, G. B. Reconstructing continental-scale variation in soil δ15N: a machine learning approach in South America. *Ecosphere* **11**, e03223 (2020).

41. Nottingham, A. T., B\aa\aath, E., Reischke, S., Salinas, N. & Meir, P. Adaptation of soil microbial growth to temperature: Using a tropical elevation gradient to predict future changes. *Global change biology* **25**, 827–838 (2019).

42. Liu, Y. *et al.* A global synthesis of the rate and temperature sensitivity of soil nitrogen mineralization: latitudinal patterns and mechanisms. *Global Change Biology* **23**, 455–464 (2017).

43. Davidson, E. A. & Janssens, I. A. Temperature sensitivity of soil carbon decomposition and feedbacks to climate change. *Nature* **440**, 165–173 (2006).

44. Zimmermann, M. & Bird, M. I. Temperature sensitivity of tropical forest soil respiration increase along an altitudinal gradient with ongoing decomposition. *Geoderma* **187–188**, 8–15 (2012).

45. Page, S. E., Rieley, J. O. & Banks, C. J. Global and regional importance of the tropical peatland carbon pool. *Global change biology* **17**, 798–818 (2011).

46. Wright, S. J. Plant responses to nutrient addition experiments conducted in tropical forests. *Ecological Monographs* **89**, e01382 (2019).

47. Brookshire, E. N. J., Gerber, S., Menge, D. N. L. & Hedin, L. O. Large losses of inorganic nitrogen from tropical rainforests suggest a lack of nitrogen limitation. *Ecol. Lett.* **15**, 9–16 (2012).

48. Bâ, A. M., McGuire, K. L. & Diédhiou, A. G. *Ectomycorrhizal symbioses in tropical and neotropical forests*. (CRC press, 2014).

49. Zeng, Z. *et al.* Deforestation-induced warming over tropical mountain regions regulated by elevation. *Nature Geoscience* 1–7 (2020).

50. Nogués-Bravo, D., Araújo, M. B., Errea, M. P. & Martínez-Rica, J. P. Exposure of global mountain systems to climate warming during the 21st Century. *Global Environmental Change* **17**, 420–428 (2007).

51. Weintraub, S. R., Cole, R. J., Schmitt, C. G. & All, J. D. Climatic controls on the isotopic composition and availability of soil nitrogen across mountainous tropical forest. *Ecosphere* **7**, e01412 (2016).

52. Brookshire, E. N. J. & Thomas, S. A. Ecosystem Consequences of Tree Monodominance for Nitrogen Cycling in Lowland Tropical Forest. *PLoS ONE* **8**, e70491 (2013).

53. Kitayama, K. & Iwamoto, K. Patterns of natural 15N abundance in the leaf-to-soil continuum of tropical rain forests differing in N availability on Mount Kinabalu, Borneo. *Plant and Soil* **229**, 203–212 (2001).

54. Bauters, M. *et al.* Contrasting nitrogen fluxes in African tropical forests of the Congo Basin. *Ecological Monographs* **89**, e01342 (2019).

55. Proctor, J., Edwards, I. D., Payton, R. W. & Nagy, L. Zonation of forest vegetation and soils of Mount Cameroon, West Africa. *Plant Ecology* **192**, 251–269 (2007).

56. Vitousek, P. M., Matson, P. A. & Turner, D. R. Elevational and Age Gradients in Hawaiian Montane Rainforest: Foliar and Soil Nutrients. *Oecologia* **77**, 565–570 (1988).

57. Grubb, P. J. & Stevens, P. F. *The forests of the Fatima Basin and Mt Kerigomna, Papua New Guinea with a review of montane and subalpine rainforests in Papuasia*. (Canberra, ACT: Dept. of Human Geography, Research School of Pacific Studies …, 2017).

58. Dieleman, W. I. J., Venter, M., Ramachandra, A., Krockenberger, A. K. & Bird, M. I. Soil carbon stocks vary predictably with altitude in tropical forests: Implications for soil carbon storage. *Geoderma* **204–205**, 59–67 (2013).

59. Kapos, V., Rhind, J., Edwards, M., Price, M. F. & Ravilious, C. Developing a map of the world's mountain forests. in *Forests in sustainable mountain development: a state of knowledge report for 2000. Task Force on Forests in Sustainable Mountain Development.* 4–19 (CABI, 2000). doi:10.1079/9780851994468.0004.

60. Sexton, J. O. *et al.* Global, 30-m resolution continuous fields of tree cover: Landsat-based rescaling of MODIS vegetation continuous fields with lidar-based estimates of error. *International Journal of Digital Earth* **6**, 427–448 (2013).

61. Pan, Y., Birdsey, R. A., Phillips, O. L. & Jackson, R. B. The structure, distribution, and biomass of the world's forests. *Annual Review of Ecology, Evolution, and Systematics* **44**, 593–622 (2013).

Figures

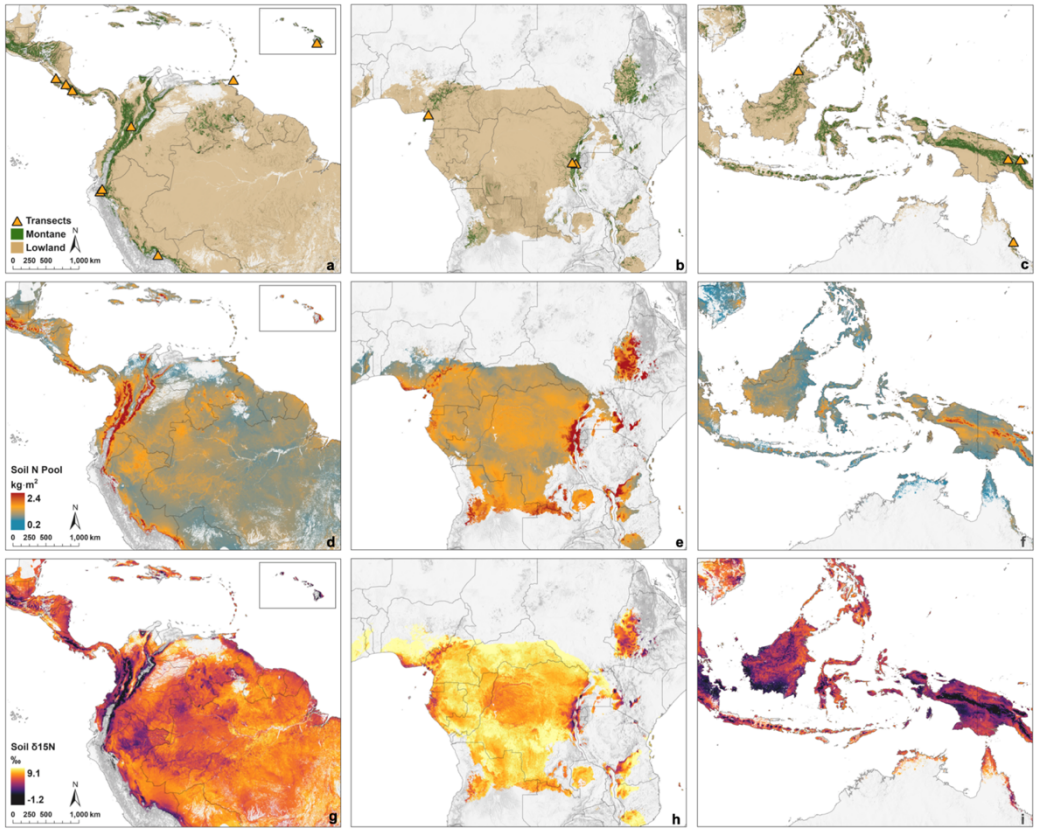


Fig. 1 | Global distribution of tropical montane forests, soil N pools, and $\delta^{15}N$. Extent of montane and lowland tropical forests and locations of elevational gradient transects (**a-c**). The distribution of surface mineral soil (0-20 cm) N pools (**d-f**) and $\delta^{15}N$ (**g-i**) based on linear mixed-effects models (Supplementary Table 3). Panels display area-equivalent forest extent for regions containing elevational transects. Areas shaded in dark grey are classified as non-humid tropical forest.

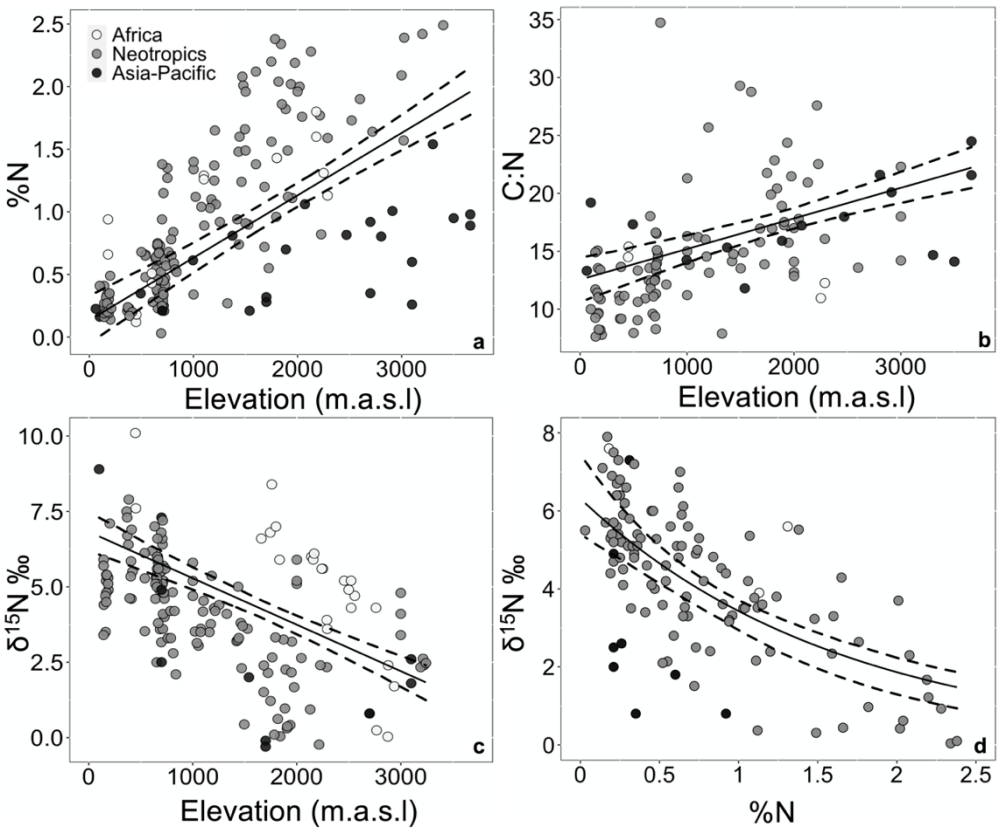


Fig. 2 | Elevational distribution of soil N content, C:N ratios, and $\delta^{15}N$ across tropical montane forests. The change in soil %N (**a**), C:N (**b**), and $d^{15}N$ (**c**) with increasing elevation were determined using linear mixed effects models with elevation as the fixed effect and transect identity nested within tropical region as a random effect (Supplementary Table 2). (**d**) negative exponential relationship between soil $d^{15}N$ and %N. Model 95% confidence intervals (dashed lines) were estimated using Monte-Carlo simulations.

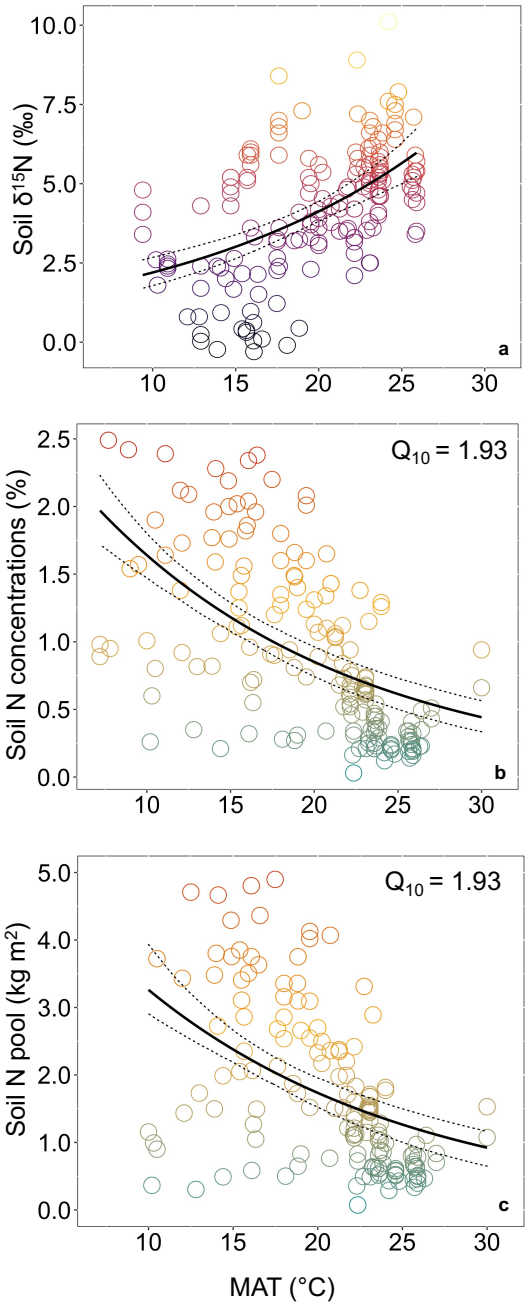
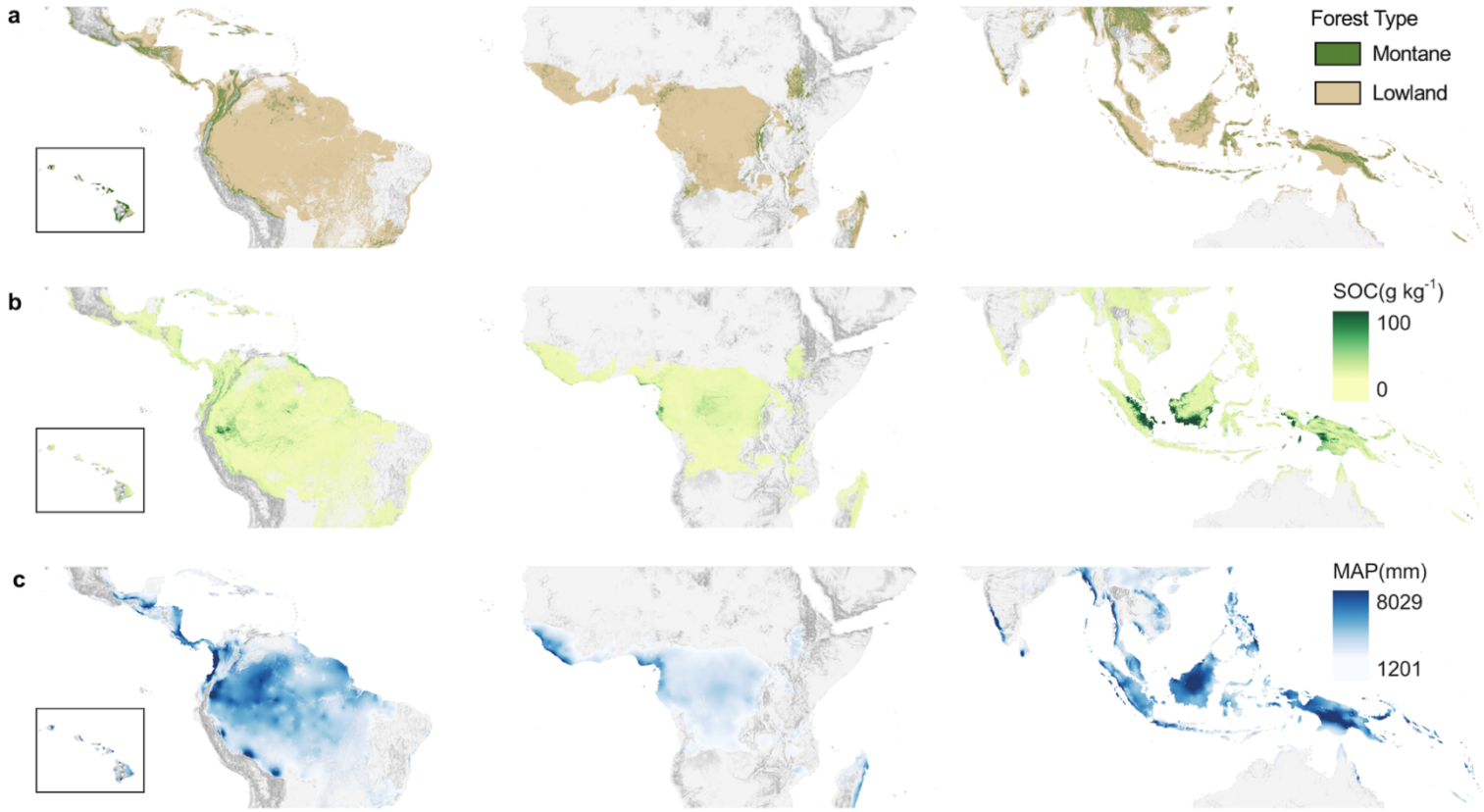
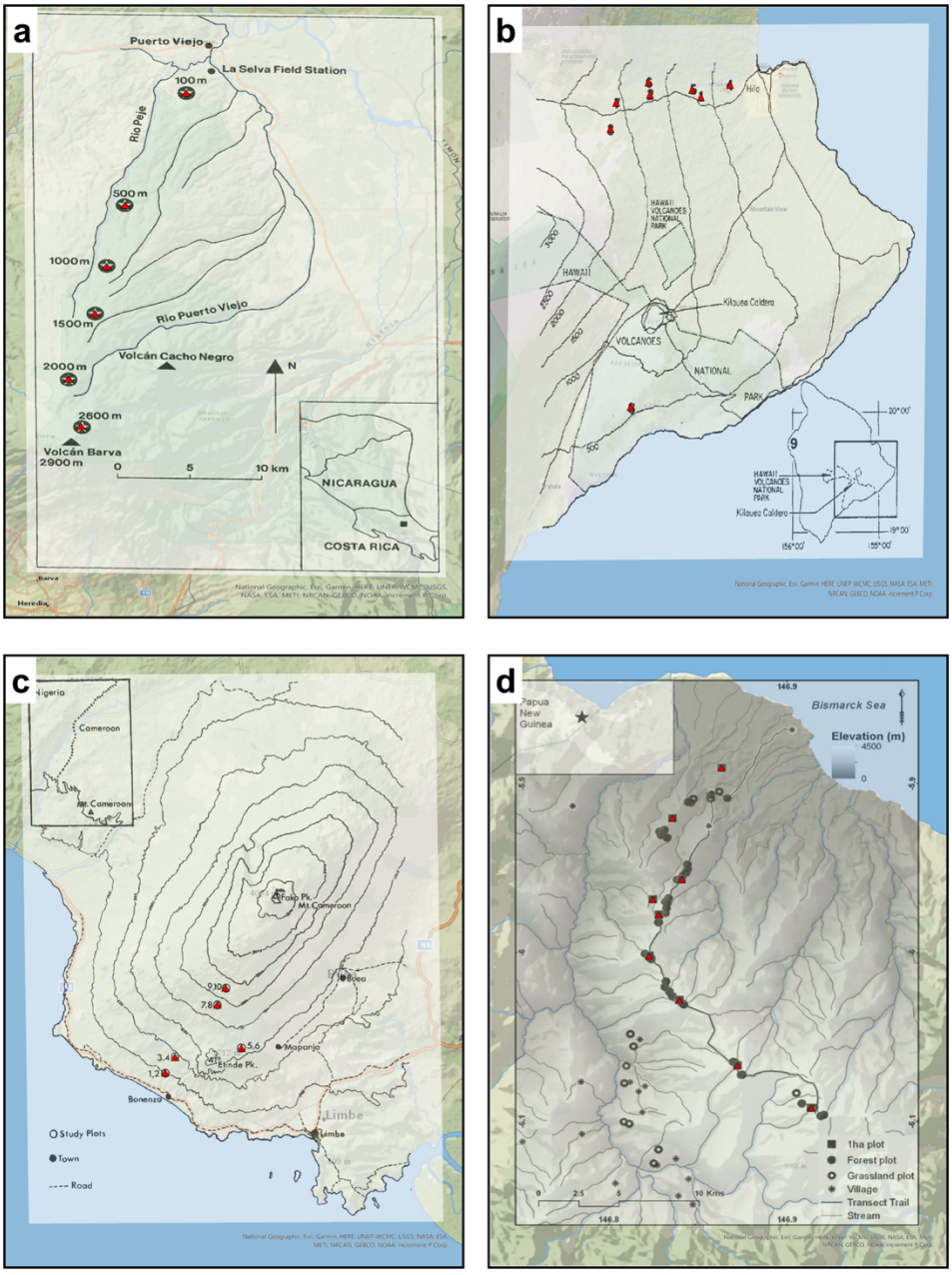


Fig. 3 | Temperature sensitivity of tropical montane forest N. Curves were fit using non-linear regression of soil N concentrations (b) and area scaled N pools (c) against MAT across all elevational transects. Temperature sensitivities (Q_{10}) were then determined for (b) and (c) using regression model results (Methods). Since $\delta^{15}N$ (a) is reported on a non-proportional scale (per mil ‰) a Q_{10} could not be derived. Color scales denote soil N metrics that align with Fig 1.

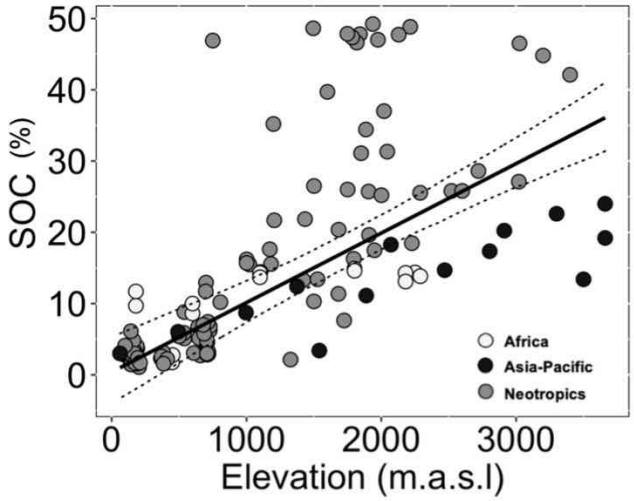
Supplemental Figures



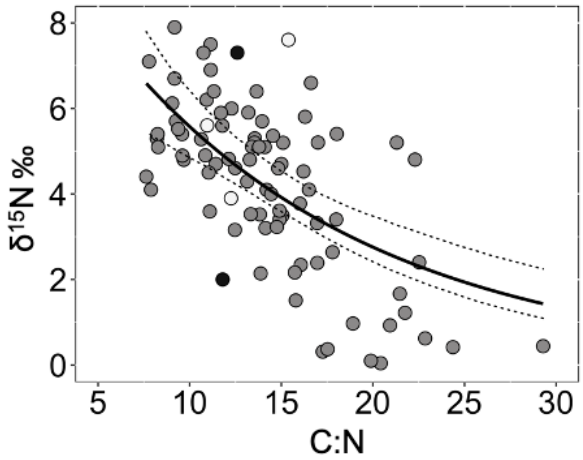
Supplementary Figure 1. Tropical forest cover extent, soil organic carbon (SOC), and MAP. Grey areas are classified as non-forested ecosystems. Hawaii inset not to scale.



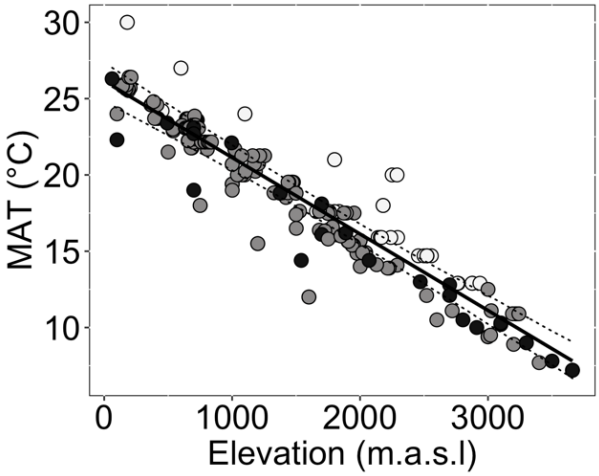
Supplementary Fig. 2. Georeferenced maps of sampling locations for studies that did not provide coordinate data. a) Heaney and Proctor, 1990; Costa Rica. b) Vitousek et al., 1988; Island of Hawai'i. c) Proctor et al., 2007; Cameroon. d) Dieleman et al., 2013; Papua New Guinea. Red triangles indicate extracted coordinate locations. Base map from National Geographic and ESRI.



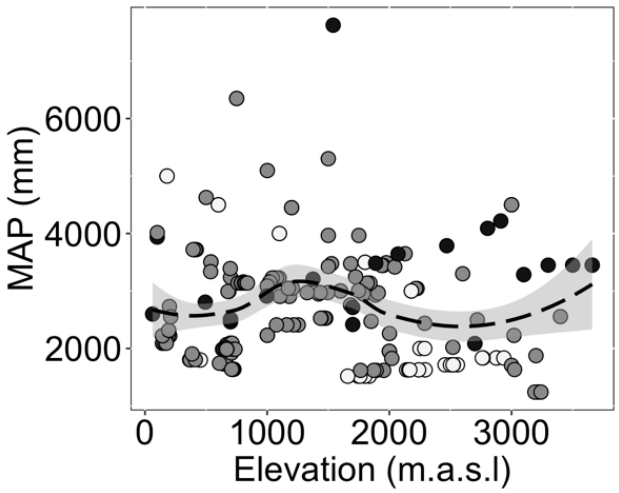
Supplementary Fig. 3. Relationship between soil organic carbon (%) and elevation across the transects. Trend line represents the global mean where SOC increases with elevation (P = <0.0001, R^2m = 0.30, R^2C = 0.74; ±95% CI). Color indicates tropical region. The slope is the calculated fixed effect from a linear mixed model with transect location nested within region.



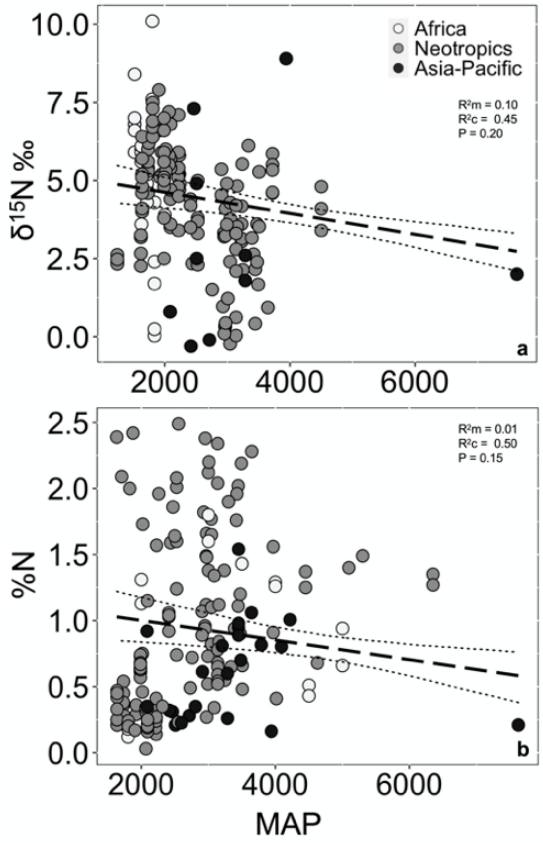
Supplementary Fig. 4. Nonlinear relationship between bulk soil ^{15}N and soil C:N. A negative exponential curve was fit $y = 10.803 * \exp^{(-0.065* x)}$ (exponential term, $p <$ 0.0001) with 95% confidence intervals derived from Monte-Carlo simulations. Color indicates tropical region.



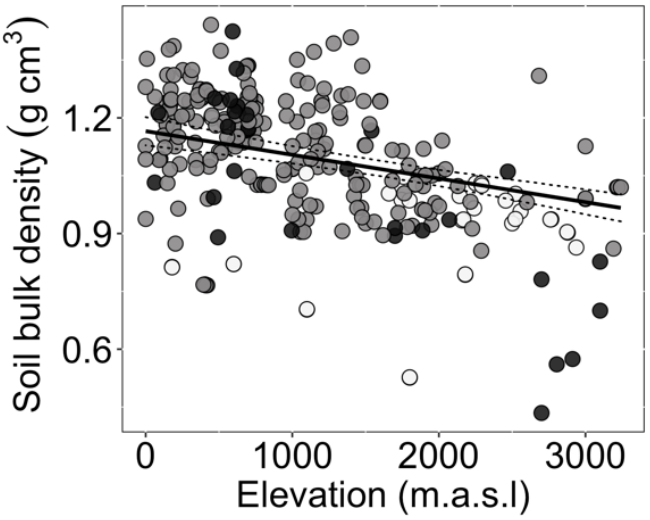
Supplementary Fig. 5. Elevational change in temperature across tropical montane forests. Trend line displays a significant relationship (P = <0.0001, R^2m = 0.81, R^2c = 0.98 ; ±95% CI) between decreasing mean annual temperatures and increasing elevation across the transects (5.1 °C km^{-1} lapse rate). Colors indicate tropical region. The slope is the calculated fixed effect from a linear mixed model with transect location nested within region as the random effect.



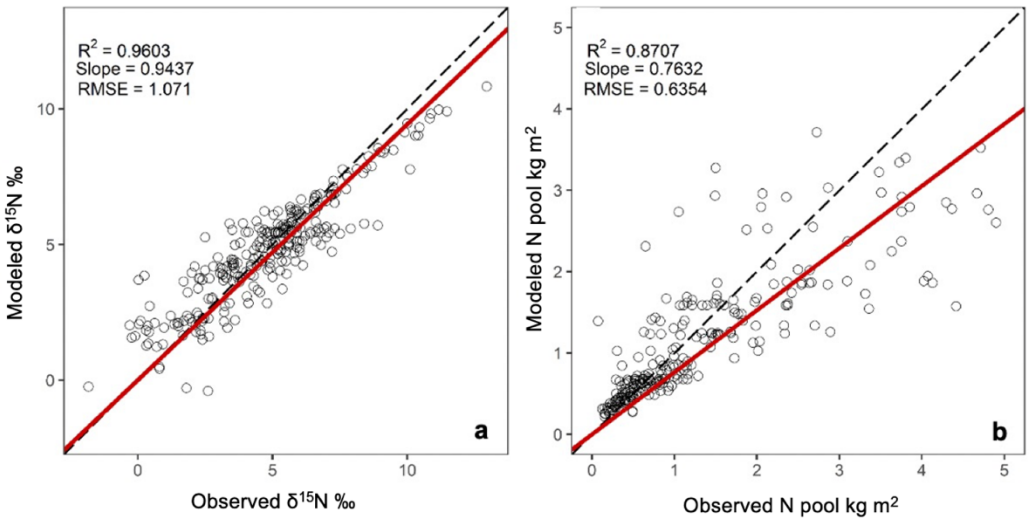
Supplementary Fig. 6. Relationship between mean annual precipitation (mm) and elevation across tropical montane forests. Data were fit with a smoothed LOESS line. Colors indicate region.



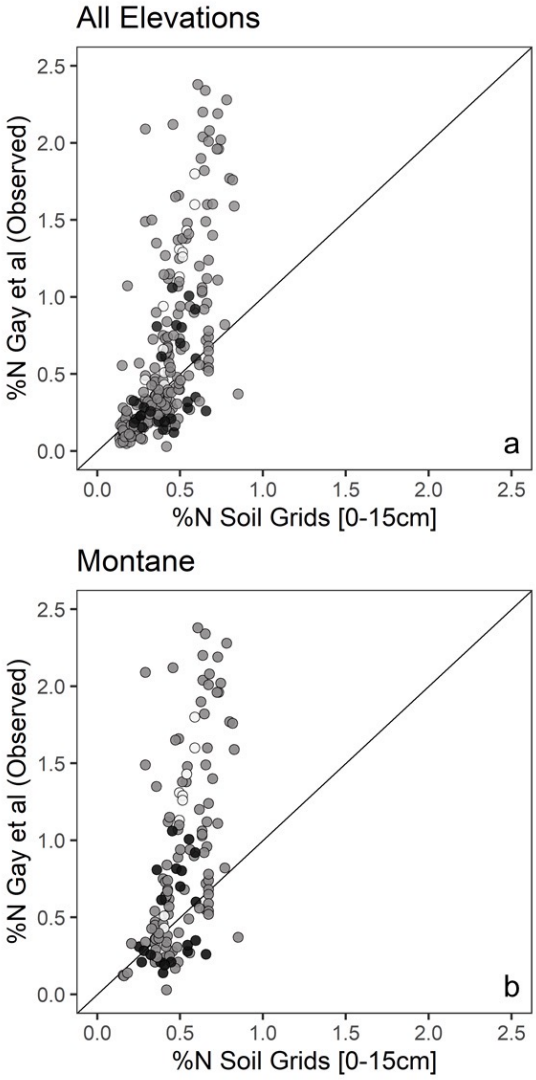
Supplementary Fig. 7. Relationships between soil ^{15}N (a), N (b), and mean annual precipitation (mm) across the elevational transects. Dashed trend lines denote non-significant linear relationships $P > 0.05$ with ±95% CI. Shade indicates region, with white indicating Africa, grey indicating the Neotropics, and black indicating Pacific-Asia. The slope is the calculated fixed effect from a linear mixed model with transect location nested within region as the random effect.



Supplementary Fig. 8. Changes in soil bulk density (g cm^3) across the elevational transects. Trend line displays the global mean relationship (P = < 0.0001, R^2m = 0.11, R^2c = 0.64; ±95% CI) between decreasing bulk density (to 20 cm soil depth) and increasing elevation 95%. Color indicates tropical region. The slope is the calculated fixed effect from a linear mixed model with transect location nested within region.



Supplementary Fig. 9. Observed vs. modeled data comparison for a) $\delta^{15}N$ (‰) and b) N pools (kg N m^2). The black dashed line depicts a 1:1 line, and the red line is the slope of the modeled vs. observed data. Observed N pool data were derived from the product of measured soil %N and gridded bulk density data. Modeled data are results from global linear mixed-effects models for the original sampling locations.



Supplementary Fig. 10. Observed versus SoilGrid 2.0 soil N. Each point shows the observed and simulated (SoilGrids 2.0) soil N concentration for all tropical soil (a) and (b) montane elevational gradient site coordinates.

Supplemental Tables

Supplementary Table 1. Biophysical properties of elevational gradients. In soil type and bedrock columns, L represents values for the lowest elevation sampling point along the transect, while M represents mid-elevation, and H represents the highest elevation. References refer to main text references. * Bruijnzeel et al. *Tropical Montane Cloud Forests Science for Conservation and Management*. Cambridge University Press,2011

	$\delta^{15}N$ (‰)	%N	Elevation	MAT (ºC)	MAP (mm)	Soil Type	Bedrock	Cloud Forest Elevation(m)*
Australia[44]	2-8.9	0.16-0.31	100 - 1540	22.3-14.4	3939-7625	L: Loam H: Loamy-sand	Metamorphic sedimentary H: granite	1000-3500
Borneo[53]	-0.3- 4.9	0.21-1.9	700 - 3100	23.1-10.2	2300-2300	L: Oxisol H: Histosol/spodosol	Sedimentary/patchy ultrabasic H: Granite (>3000m)	1500-3500
Cameroon[55]	*N/A*	0.43-1.8	180 - 2180	30-18.9	3000-5000	L:Acrudoxic Hapludands M: Vitric Hapludands H: Thaptic Hulvudands	Recent basaltic lava flows overlying Holocene olivine basalt	1000-3500
Colombia[7]	*N/A*	0.09-1.1	16 - 2994	29.9-11.9	1200-8000	*Not Reported*	*Not Reported*	1800-3500
Costa Rica[19]	2.1-7	0.03-2.08	634 - 1479	23-19.5	1987-3139	Ultisols/Inceptisols	Pleistocene to Holocene basalts	1800-3500
Costa Rica[51]	-0.23-6.1	0.27-2.38	537 - 2289	23-13.9	2438-3648	Ultisols/Humults	Miocene-era igneous	1800-3500
Costa Rica[15]	N/A	0.41-1.96	100 - 2600	24-10.5	2260-5096	L: Entisol H: Andisols	Plio-Pleistocene basalt and andesite	1800-3500
DRC[54]	3.9-10.1	N/A	448-2289	24.2-20	1800-2000	L: Ferralsols H: Ferralsols/Acrisols	Basalt	2000-3500
Ecuador[17]	2.3-5.8	N/A	394 - 3241	23.7-10.9	1241-3720	L: Inceptisols H: Planosols/Histosols	M: Jurassic Granite L: and H: Paleozoic metamorphic shist/sandstone	>400
Ecuador[24]	3.4-5.2	N/A	1001 - 3000	19.4-9.4	1950-4500	Andisols	Lahar/red bed volcaniclastics/granitic	>400
Hawaii[56]	*N/A*	1.25-2.12	750 -1600	18-12	3000-6350	Histosols	3100 y/o basalt flow	1000-3000
Papua-New Guinea[57]	*N/A*	0.89-1.54	3330 - 3660	9.0-7.2	3450	Inceptisol	Pliocene Granodiorite	2000-3500
Papua-New Guinea[58]	*N/A*	0.22-1.06	62-2912	26.3-10	2598-4218	L: Hapludolls/Rendolls M: Troporthents H: Cryorthents	L: Limestone over alluvial deposits H: Limestone	2000-3500
Peru[5]	N/A	0.23-2.49	194 - 3400	26.4-7.7	1633-3967	L:Haplic Alisols/Cambisols M: Cambisols H: Umbrisols	Paleozoic meta sedimentary mudstone M: Granite intrusions	1800-3500
Rwanda[22]	0.03-8.4	N/A	1659-2937	17.6-12.9	1518-1835	Inceptisols/ultisol/entisol	Shale and quartz	2000-3500
Trinidad[50]	3.4-7.9	0.14-0.54	142-727	25.8-23.5	1638-2238	Ultisols	Meta-sedimentary phyllites from Cretaceous and Jurassic and Mesozoic metamorphic	>660

Supplementary Table 2. Linear mixed model results (Figure 2a, 2b, 2c) for N cycling indices (fixed effects) across the elevational transects. Transect ID is nested within tropical region as the random effects.

Response	Effect	Coeff.	SE	P-value	$R^2_{(m)}$	$R^2_{(c)}$
%N	m.a.s.l	0.0005	0.000041	<0.0001	0.30	0.78
$\delta^{15}N$	m.a.s.l	-0.0015	0.00017	<0.0001	0.30	0.70
C:N	m.a.s.l	0.00017	0.000035	<0.0001	0.19	0.62

Supplementary Table 3. Hierarchical partitioning results for drivers of tropical soil %N, N pools and $\delta^{15}N$. Fixed effect coefficients, estimated marginal and conditional R^2, and relative importance metric (lmg) for global $\delta^{15}N$ and N pool distributions across tropical forest soils. Lmg metric is normalized to sum to 100%. Region lmg describes the overall explanatory value of all three regions and is not broken down to each categorical level.

Response	Effect	Coeffs.	SE	P-value	$R^2_{(m)}$	$R^2_{(c)}$	Lmg(%)
N pool	MAT	-0.81	0.23	0.0006	0.30	0.64	20
	MAP	-1.84	0.65	0.005			15
	SOC	0.24	0.1	0.02			31
	MAT*MAP	0.09	0.03	0.001			14
	Region						20
	Region: Africa	15.85	5.26	0.002			
	Region: Neotropics	15.56	5.62	0.38			
	Region: Asia Pacific	15.09	5.59	0.04			
$\delta^{15}N$	MAT	0.23	0.04	< 0.0001	0.40	0.82	42
	MAP	-1.06	0.37	0.04			26
	SOC	-1.0	0.33	0.001			12
	Region						20
	Region: Africa	11.26	3.0	0.002			
	Region: Neotropics	10.06	1.76	0.33			
	Region: Asia Pacific	7.22	1.64	0.004			
%N	MAT	-0.78	0.23	0.0007	0.45	0.71	25
	MAP	-1.7	0.63	0.007			12
	MAT*MAP	0.09	0.03	0.001			18
	SOC	0.36	0.10	0.0002			18
	Slope	0.11	0.04	0.015			8
	Region						19
	Region: Africa	13.85	5.14	0.007			
	Region: Neotropics	13.42	4.82	0.19			
	Region: Asia Pacific	12.84	4.79	0.005			

Supplementary Table 4. Montane classification criteria and their binned tropical land area estimates. Numeric values in Description column are elevation in (m.a.s.l) and LER is the local elevational range.

Categories	Description	Raster Cells	Area Coverage (km^2)	Proportion of Montane Tropics (%)
Level 1	< 1000 and LER > 300	1,321,090	1,098,647	25.80
Level 2	1000-1500 and slope > 5° slope angle *or* LER > 300 m	1,152,823	958,712	22.50
Level 3	1500-2500 and slope > 2°	1,429,402	1,188,721	27.90
Level 4	2500-3500	517,098	430,030	10.10
Level 5	3500-4500	559,921	465,642	10.94
Level 6	> 4500	137,249	114,139	2.68

Supplementary Table 5. Global and regional extent of tropical montane forest. All areas in km^2. Percentages in parentheses indicate the proportion of the total area of that row. Percentages in brackets represent the proportion of the indicated global area.

Region	Total Area		Forest	%	Montane	%	Montane Forest	%	
Global	49,456,052		20,064,281	(40.6)	4,412,463	(8.9)	2,150,464	(4.4)	
		% Of Global							**% Of Global Montane Forest**
Neotropics	15,083,978	[30.5]	9,556,500	(63.4)	1,989,714	(13.2)	684,021	(4.5)	[31.8]
Africa	24,654,851	[49.9]	6,067,746	(24.6)	1,204,124	(4.9)	364,898	(1.5)	[17.0]
Asia Pacific	9,717,223	[19.7]	4,440,035	(45.7)	1,218,625	(12.5)	1,101,545	(11.3)	[51.2]

Supplementary Table 6. Previously reported tropical forest extent. *Tropical montane cloud forest extent

Citation	Montane forest extent	Total tropical forest (M km^2)
Pan et al 2013	3.51 million km^2	13.5
Wright 2019	12% (tropical mountains)	11
Kapos et al 2000	~2 million km^2	
FAO 2020	1.79 million km^2	19.9
Mulligan 2010*	2.21 million km^2	15.7

Supplementary Table 7. Total mineral soil N pool for global tropical forests (Pg N ± 95% confidence interval; 0-20 cm). Values in parentheses indicate the percent of the total N pool for that region (row). Percentages in brackets represent the proportion of the indicated global pool. N Pool estimates are summed from global models used to create Figure 1

Region	Total N pool		Montane N pool	%		Lowland N pool	%	
Global	11.56 ± 8.20		1.90 ± 0.86	(16.5)		9.65 ± 7.34	(83.5)	
		% of Global			**% of Global Montane**			**% of Global Lowland**
Neotropics	5.25 ± 3.90	[45.4]	0.82 ± 0.27	(15.6)	[43.2]	4.43 ± 3.63	(84.4)	[45.9]
Africa	4.41 ± 2.48	[38.2]	0.50 ± 0.15	(11.3)	[26.3]	3.91 ± 2.34	(88.7)	[40.5]
Asia Pacific	1.90 ± 1.81	[16.4]	0.59 ± 0.44	(30.9)	[31.1]	1.31 ± 1.38	(69.1)	[13.6]

CHAPTER FIVE

SYNTHESIS

Eugene Odum highlighted the importance of scale in ecology by postulating that thinking at an ecosystem level unifies ecologists, and other scientists alike, as it is the basic unit of structure and function with which humanity operates and must ultimately deal with (Odum, 1964). So, while ecology is a discipline that addresses the complex biological organization of the Earth through the confinement of the laws of thermodynamics, it is not just a biological or environmental science; it is a human science. Thus, it is critical to identify emergent biogeochemical patterns and feedback in response to anthropogenic global change, and also to understand how these responses scale to the ecosystem level.

This dissertation has been inspired through observation, experimentation, and reflection on how human activity — both directly and indirectly — affects the biogeochemical fluxes of carbon and nitrogen in natural and managed ecosystems. This work demonstrates the complex interactions among carbon and nitrogen cycling in terrestrial ecosystems and highlights that one cannot be considered without considering the other. Specifically, this work expands our understanding of how the terrestrial carbon sink is responding to anthropogenic global change and how its management may be leveraged as a tool to mitigate climate change.

Taken together, the results of Chapters 1 and 2 highlights the potential for meaningful management practices in the UMRB that can accomplish both stakeholder goals of agronomic production and the reduction of woody plants *and* contribute positively to C sequestration when considered at the proper time scale. Furthermore, Chapter 1

highlights management practices that promote the high retention of N, whereas in Chapter 2 evaluating the N cycling dynamics was more complex due to the large losses of N from interactions between fire and the plant community and the subsequent production of PyOM. Chapter 3 highlights the climate sensitivity of the soil N cycle across tropical montane forests, a large and potentially vulnerable pool whose response to global changes will strongly influence future montane forest C sequestration potential. Ultimately, the work presented in this dissertation underscores the importance of taking a coupled view of both the C and N cycles when evaluating how anthropogenic global change is impacting the ability of terrestrial ecosystems to sequester C *and* the land management strategies we employ to increase C sequestration.

References Cited

Abiven, S., & Santín, C. (2019). Editorial: From Fires to Oceans: Dynamics of Fire-Derived Organic Matter in Terrestrial and Aquatic Ecosystems. *Frontiers in Earth Science*, *7*. https://www.frontiersin.org/article/10.3389/feart.2019.00031

Abney, R. B., & Berhe, A. A. (2018). Pyrogenic Carbon Erosion: Implications for Stock and Persistence of Pyrogenic Carbon in Soil. *Frontiers in Earth Science*, *6*. https://doi.org/10.3389/feart.2018.00026

Alvarez, A. L., Weyers, S. L., Goemann, H. M., Peyton, B. M., & Gardner, R. D. (2021). Microalgae, soil and plants: A critical review of microalgae as renewable resources for agriculture. *Algal Research*, *54*, 102200. https://doi.org/10.1016/j.algal.2021.102200

Amundson, R., Austin, A., Schuur, E., Yoo, K., Matzek, V., Kendall, C., Uebersax, A., Brenner, D., & Baisden, W. (2003). Global patterns of the isotopic composition of soil and plant nitrogen. *GLOBAL BIOGEOCHEMICAL CYCLES*, *17*(1). https://doi.org/10.1029/2002GB001903

Ansley, R. J., Mirik, M., Surber, B. W., & Park, S. C. (2012). Canopy Area and Aboveground Mass of Individual Redberry Juniper (Juniperus pinchotii) Trees. *Rangeland Ecology & Management*, *65*(2), 189–195. https://doi.org/10.2111/REM-D-11-00112.1

Asner, G. P., Seastedt, T. R., & Townsend, A. R. (1997). The Decoupling of Terrestrial Carbon and Nitrogen Cycles. *BioScience*, *47*(4), 226–234. JSTOR. https://doi.org/10.2307/1313076

Bâ, A. M., McGuire, K. L., & Diédhiou, A. G. (2014). *Ectomycorrhizal symbioses in tropical and neotropical forests*. CRC press.

Bai, E., Li, S., Xu, W., Li, W., Dai, W., & Jiang, P. (2013). A meta-analysis of experimental warming effects on terrestrial nitrogen pools and dynamics. *New Phytologist*, *199*(2), 441–451. https://doi.org/10.1111/nph.12252

Baik, E., Sanchez, D. L., Turner, P. A., Mach, K. J., Field, C. B., & Benson, S. M. (2018). Geospatial analysis of near-term potential for carbon-negative bioenergy in the United States. *Proceedings of the National Academy of Sciences*, *115*(13), 3290–3295. https://doi.org/10.1073/pnas.1720338115

Bao, X., Carris, L. M., Huang, G., Luo, J., Liu, Y., & Castlebury, L. A. (2010). Tilletia puccinelliae, a new species of reticulate-spored bunt fungus infecting Puccinellia distans. *Mycologia*, *102*(3), 613–623. https://doi.org/10.3852/09-135

Bao, Y., Dolfing, J., Guo, Z., Chen, R., Wu, M., Li, Z., Lin, X., & Feng, Y. (2021). Important ecophysiological roles of non-dominant Actinobacteria in plant residue decomposition, especially in less fertile soils. *Microbiome*, *9*(1), 84. https://doi.org/10.1186/s40168-021-01032-x

Barger, N. N., Archer, S. R., Campbell, J. L., Huang, C., Morton, J. A., & Knapp, A. K. (2011). Woody plant proliferation in North American drylands: A synthesis of impacts on ecosystem carbon balance. *Journal of Geophysical Research: Biogeosciences*, *116*(G4). https://doi.org/10.1029/2010JG001506

Barthel, M., Bauters, M., Baumgartner, S., Drake, T. W., Bey, N. M., Bush, G., Boeckx, P., Botefa, C. I., Dériaz, N., Ekamba, G. L., Gallarotti, N., Mbayu, F. M., Mugula, J. K., Makelele, I. A., Mbongo, C. E., Mohn, J., Mandea, J. Z., Mpambi, D. M., Ntaboba, L. C., … Six, J. (2022). Low N2O and variable CH4 fluxes from tropical forest soils of the Congo Basin. *Nature Communications*, *13*(1), 330. https://doi.org/10.1038/s41467-022-27978-6

Batjes, N. H. (1996). Total carbon and nitrogen in the soils of the world. *European Journal of Soil Science*, *47*(2), 151–163.

Bauer, R., Lutz, M., Begerow, D., Piątek, M., Vánky, K., Bacigálová, K., & Oberwinkler, F. (2008). Anther smut fungi on monocots. *Mycological Research*, *112*(11), 1297–1306. https://doi.org/10.1016/j.mycres.2008.06.002

Bauters, M., Verbeeck, H., Demol, M., Bruneel, S., Taveirne, C., Heyden, D. V. der, Cizungu, L., & Boeckx, P. (2017). Parallel functional and stoichiometric trait shifts in South American and African forest communities with elevation. *Biogeosciences*, *14*(23), 5313–5321.

Bauters, M., Verbeeck, H., Rütting, T., Barthel, M., Bazirake Mujinya, B., Bamba, F., Bodé, S., Boyemba, F., Bulonza, E., & Carlsson, E. (2019). Contrasting nitrogen fluxes in African tropical forests of the Congo Basin. *Ecological Monographs*, *89*(1), e01342.

Berardi, D., Brzostek, E., Blanc-Betes, E., Davison, B., DeLucia, E. H., Hartman, M. D., Kent, J., Parton, W. J., Saha, D., & Hudiburg, T. W. (2020). 21st-century biogeochemical modeling: Challenges for Century-based models and where do

we go from here? *GCB Bioenergy*, *12*(10), 774–788. https://doi.org/10.1111/gcbb.12730

Bird, M. I., Wynn, J. G., Saiz, G., Wurster, C. M., & McBeath, A. (2015). The Pyrogenic Carbon Cycle. *Annual Review of Earth and Planetary Sciences*, *43*(1), 273–298. https://doi.org/10.1146/annurev-earth-060614-105038

Bleby, T. M., Aucote, M., Kennett-Smith, A. K., Walker, G. R., & Schachtman, D. P. (1997). Seasonal water use characteristics of tall wheatgrass [Agropyron elongatum (Host) Beauv.] in a saline environment. *Plant, Cell & Environment*, *20*(11), 1361–1371. https://doi.org/10.1046/j.1365-3040.1997.d01-29.x

Boby, L. A., Schuur, E. A. G., Mack, M. C., Verbyla, D., & Johnstone, J. F. (2010). Quantifying fire severity, carbon, and nitrogen emissions in Alaska's boreal forest. *Ecological Applications*, *20*(6), 1633–1647. https://doi.org/10.1890/08-2295.1

Bodí, M. B., Martin, D. A., Balfour, V. N., Santín, C., Doerr, S. H., Pereira, P., Cerdà, A., & Mataix-Solera, J. (2014). Wildland fire ash: Production, composition and eco-hydro-geomorphic effects. *Earth-Science Reviews*, *130*, 103–127. https://doi.org/10.1016/j.earscirev.2013.12.007

Bossio, D. A., Cook-Patton, S. C., Ellis, P. W., Fargione, J., Sanderman, J., Smith, P., Wood, S., Zomer, R. J., von Unger, M., Emmer, I. M., & Griscom, B. W. (2020). The role of soil carbon in natural climate solutions. *Nature Sustainability*, 1–8. https://doi.org/10.1038/s41893-020-0491-z

Bowles, T. M., Jackson, L. E., Loeher, M., & Cavagnaro, T. R. (2017). Ecological intensification and arbuscular mycorrhizas: A meta-analysis of tillage and cover crop effects. *Journal of Applied Ecology*, *54*(6), 1785–1793. https://doi.org/10.1111/1365-2664.12815

Bowring, S. P. K., Jones, M. W., Ciais, P., Guenet, B., & Abiven, S. (2022). Pyrogenic carbon decomposition critical to resolving fire's role in the Earth system. *Nature Geoscience*, *15*(2), 135–142. https://doi.org/10.1038/s41561-021-00892-0

Brookshire, E. N. J., Gerber, S., Menge, D. N. L., & Hedin, L. O. (2012). Large losses of inorganic nitrogen from tropical rainforests suggest a lack of nitrogen limitation RID H-3819-2011. *Ecology Letters*, *15*(1), 9–16. https://doi.org/10.1111/j.1461-0248.2011.01701.x

Brookshire, E. N. J., Hedin, L. O., Newbold, J. D., Sigman, D. M., & Jackson, J. K. (2012). Sustained losses of bioavailable nitrogen from montane tropical forests. *Nature Geoscience*, *5*(2), 123–126. https://doi.org/10.1038/NGEO1372

Brookshire, E. N. J., Stoy, P. C., Currey, B., & Finney, B. (2020). The greening of the Northern Great Plains and its biogeochemical precursors. *Global Change Biology*, *26*(10), 5404–5413. https://doi.org/10.1111/gcb.15115

Brookshire, E. N. J., & Thomas, S. A. (2013). Ecosystem Consequences of Tree Monodominance for Nitrogen Cycling in Lowland Tropical Forest. *PLoS ONE*, *8*(7), e70491. https://doi.org/10.1371/journal.pone.0070491

Burgess, M. H., Miller, P. R., & Jones, C. A. (2012). Pulse Crops Improve Energy Intensity and Productivity of Cereal Production in Montana, USA. *Journal of Sustainable Agriculture*, *36*(6), 699–718. https://doi.org/10.1080/10440046.2012.672380

Camenzind, T., Hättenschwiler, S., Treseder, K. K., Lehmann, A., & Rillig, M. C. (2018). Nutrient limitation of soil microbial processes in tropical forests. *Ecological Monographs*, *88*(1), 4–21.

Carvalho, J. L. N., Hudiburg, T. W., Franco, H. C. J., & DeLucia, E. H. (2017). Contribution of above- and belowground bioenergy crop residues to soil carbon. *GCB Bioenergy*, *9*(8), 1333–1343. https://doi.org/10.1111/gcbb.12411

Castro, J. de S., Calijuri, M. L., Assemany, P. P., Cecon, P. R., de Assis, I. R., & Ribeiro, V. J. (2017). Microalgae biofilm in soil: Greenhouse gas emissions, ammonia volatilization and plant growth. *Science of The Total Environment*, *574*, 1640–1648. https://doi.org/10.1016/j.scitotenv.2016.08.205

Cederlund, H., Wessén, E., Enwall, K., Jones, C. M., Juhanson, J., Pell, M., Philippot, L., & Hallin, S. (2014). Soil carbon quality and nitrogen fertilization structure bacterial communities with predictable responses of major bacterial phyla. *Applied Soil Ecology*, *84*, 62–68. https://doi.org/10.1016/j.apsoil.2014.06.003

Certini, G. (2005). Effects of fire on properties of forest soils: A review. *Oecologia*, *143*(1), 1–10. https://doi.org/10.1007/s00442-004-1788-8

Christiansen, J. R., Outhwaite, J., & Smukler, S. M. (2015). Comparison of CO2, CH4 and N2O soil-atmosphere exchange measured in static chambers with cavity ring-down spectroscopy and gas chromatography. *Agricultural and Forest Meteorology*, *211–212*, 48–57. https://doi.org/10.1016/j.agrformet.2015.06.004

Congreves, K. A., Otchere, O., Ferland, D., Farzadfar, S., Williams, S., & Arcand, M. M. (2021). Nitrogen Use Efficiency Definitions of Today and Tomorrow. *Frontiers in Plant Science*, *12*, 912. https://doi.org/10.3389/fpls.2021.637108

Córdova, S. C., Olk, D. C., Dietzel, R. N., Mueller, K. E., Archontouilis, S. V., & Castellano, M. J. (2018). Plant litter quality affects the accumulation rate, composition, and stability of mineral-associated soil organic matter. *Soil Biology and Biochemistry*, *125*, 115–124. https://doi.org/10.1016/j.soilbio.2018.07.010

Cotrufo, M. F., Ranalli, M. G., Haddix, M. L., Six, J., & Lugato, E. (2019). Soil carbon storage informed by particulate and mineral-associated organic matter. *Nature Geoscience*, 1–6. https://doi.org/10.1038/s41561-019-0484-6

Craine, J. M., Brookshire, E. N. J., Cramer, M. D., Hasselquist, N. J., Koba, K., Marin-Spiotta, E., & Wang, L. (2015). Ecological interpretations of nitrogen isotope ratios of terrestrial plants and soils. *Plant and Soil*, 1–26.

Craine, J. M., Elmore, A. J., Wang, L., Augusto, L., Baisden, W. T., Brookshire, E. N. J., Cramer, M. D., Hasselquist, N. J., Hobbie, E. A., Kahmen, A., & others. (2015). Convergence of soil nitrogen isotopes across global climate gradients. *Scientific Reports*, *5*. http://www.nature.com/srep/2015/150206/srep08280/full/srep08280.html?WT.ec_id=SREP-704-20150210

Dalling, J. W., Heineman, K., González, G., & Ostertag, R. (2016). Geographic, environmental and biotic sources of variation in the nutrient relations of tropical montane forests. *Journal of Tropical Ecology*, *32*(5), 368–383.

Davidson, E. A., & Janssens, I. A. (2006). Temperature sensitivity of soil carbon decomposition and feedbacks to climate change. *Nature*, *440*(7081), 165–173.

de Graaff, M.-A., Jastrow, J. D., Gillette, S., Johns, A., & Wullschleger, S. D. (2014). Differential priming of soil carbon driven by soil depth and root impacts on carbon availability. *Soil Biology and Biochemistry*, *69*, 147–156. https://doi.org/10.1016/j.soilbio.2013.10.047

DeLuca, T. H., Gundale, M. J., Brimmer, R. J., & Gao, S. (2020). Pyrogenic Carbon Generation From Fire and Forest Restoration Treatments. *Frontiers in Forests and Global Change*, *3*. https://doi.org/10.3389/ffgc.2020.00024

Dieleman, W. I. J., Venter, M., Ramachandra, A., Krockenberger, A. K., & Bird, M. I. (2013). Soil carbon stocks vary predictably with altitude in tropical forests:

Implications for soil carbon storage. *Geoderma*, *204–205*, 59–67. https://doi.org/10.1016/j.geoderma.2013.04.005

Dirks, A. C., & Jackson, R. D. (2020). Community Structure of Arbuscular Mycorrhizal Fungi in Soils of Switchgrass Harvested for Bioenergy. *Applied and Environmental Microbiology*, *86*(19). https://doi.org/10.1128/AEM.00880-20

Dolan, K. A., Stoy, P. C., & Poulter, B. (2020). Land management and climate change determine second-generation bioenergy potential of the US Northern Great Plains. *GCB Bioenergy*, *12*(7), 491–509. https://doi.org/10.1111/gcbb.12686

Dore, S., Kolb, T. E., Montes-Helu, M., Sullivan, B. W., Winslow, W. D., Hart, S. C., Kaye, J. P., Koch, G. W., & Hungate, B. A. (2008). Long-term impact of a stand-replacing fire on ecosystem CO2 exchange of a ponderosa pine forest. *Global Change Biology*, *14*(8), 1801–1820. https://doi.org/10.1111/j.1365-2486.2008.01613.x

Duque, A., Peña, M. A., Cuesta, F., González-Caro, S., Kennedy, P., Phillips, O. L., Calderón-Loor, M., Blundo, C., Carilla, J., Cayola, L., Farfán-Ríos, W., Fuentes, A., Grau, R., Homeier, J., Loza-Rivera, M. I., Malhi, Y., Malizia, A., Malizia, L., Martínez-Villa, J. A., … Feeley, K. J. (2021). Mature Andean forests as globally important carbon sinks and future carbon refuges. *Nature Communications*, *12*(1), 2138. https://doi.org/10.1038/s41467-021-22459-8

Edgar, R. C. (2010). Search and clustering orders of magnitude faster than BLAST. *Bioinformatics*, *26*(19), 2460–2461. https://doi.org/10.1093/bioinformatics/btq461

Elhady, A., Giné, A., Topalovic, O., Jacquiod, S., Sørensen, S. J., Sorribas, F. J., & Heuer, H. (2017). Microbiomes associated with infective stages of root-knot and lesion nematodes in soil. *PLOS ONE*, *12*(5), e0177145. https://doi.org/10.1371/journal.pone.0177145

Engel, R. E., Miller, P. R., McConkey, B. G., & Wallander, R. (2017). Soil Organic Carbon Changes to Increasing Cropping Intensity and No-Till in a Semiarid Climate. *Soil Science Society of America Journal*, *81*(2), 404–413. https://doi.org/10.2136/sssaj2016.06.0194

Engel, R., Jones, C., & Wallander, R. (2011). Ammonia Volatilization from Urea and Mitigation by NBPT following Surface Application to Cold Soils. *Soil Science Society of America Journal*, *75*(6), 2348–2357. https://doi.org/10.2136/sssaj2011.0229

Epstein, H. E., Lauenroth, W. K., Burke, I. C., & Coffin, D. P. (1997). Productivity Patterns of C3 and C4 Functional Types in the U.s. Great Plains. *Ecology*, *78*(3), 722–731. https://doi.org/10.1890/0012-9658(1997)078[0722:PPOCAC]2.0.CO;2

Epstein, K., Wood, D., Roemer, K., Currey, B., Duff, H., Gay, J., Goemann, H., Loewen, S., Milligan, M., Wendt, J., Brookshire, E. N. J., Maxwell, B., McNew, L., McWethy, D., Stoy, P., & Haggerty, J. (2021). Toward an urgent yet deliberate conservation strategy: Sustaining social-ecological systems in rangelands of the Northern Great Plains, Montana. *Ecology and Society*, *26*(1). https://doi.org/10.5751/ES-12141-260110

Fadrique, B., Báez, S., Duque, Á., Malizia, A., Blundo, C., Carilla, J., Osinaga-Acosta, O., Malizia, L., Silman, M., & Farfán-Ríos, W. (2018). Widespread but heterogeneous responses of Andean forests to climate change. *Nature*, *564*(7735), 207–212.

Fajardy, M., & Dowell, N. M. (2017). Can BECCS deliver sustainable and resource efficient negative emissions? *Energy & Environmental Science*, *10*(6), 1389–1426. https://doi.org/10.1039/C7EE00465F

Fay, P. A., Prober, S. M., Harpole, W. S., Knops, J. M. H., Bakker, J. D., Borer, E. T., Lind, E. M., MacDougall, A. S., Seabloom, E. W., Wragg, P. D., Adler, P. B., Blumenthal, D. M., Buckley, Y. M., Chu, C., Cleland, E. E., Collins, S. L., Davies, K. F., Du, G., Feng, X., … Yang, L. H. (2015). Grassland productivity limited by multiple nutrients. *Nature Plants*, *1*(7), 1–5. https://doi.org/10.1038/nplants.2015.80

Fernández, C., Fernández-Alonso, J. M., Vega, J. A., Fontúrbel, T., Llorens, R., & Sobrino, J. A. (2021). Exploring the use of spectral indices to assess alterations in soil properties in pine stands affected by crown fire in Spain. *Fire Ecology*, *17*(1), 2. https://doi.org/10.1186/s42408-020-00089-7

Fernández-Martínez, M., Vicca, S., Janssens, I. A., Sardans, J., Luyssaert, S., Campioli, M., Chapin III, F. S., Ciais, P., Malhi, Y., Obersteiner, M., Papale, D., Piao, S. L., Reichstein, M., Rodà, F., & Peñuelas, J. (2014). Nutrient availability as the key regulator of global forest carbon balance. *Nature Climate Change*, *4*(6), 471–476. https://doi.org/10.1038/nclimate2177

Fierer, N., Allen, A. S., Schimel, J. P., & Holden, P. A. (2003). Controls on microbial CO2 production: A comparison of surface and subsurface soil horizons. *Global Change Biology*, *9*(9), 1322–1332. https://doi.org/10.1046/j.1365-2486.2003.00663.x

Firestone, M., & Davidson, E. (1989). Microbiological Basis of NO and N2O Production and Consumption in Soil. *Exchange of Trace Gases between Terrestrial Ecosystems and the Atmosphere, 47*.

Fitzgerald. (2005). *Fire Ecology of Ponderosa Pine and Rebuilding of Fire-Resilient Ponderosa Pine Ecosystems*. United States Forest Service.

Friedlingstein, P., O'Sullivan, M., Jones, M. W., Andrew, R. M., Hauck, J., Olsen, A., Peters, G. P., Peters, W., Pongratz, J., Sitch, S., Le Quéré, C., Canadell, J. G., Ciais, P., Jackson, R. B., Alin, S., Aragão, L. E. O. C., Arneth, A., Arora, V., Bates, N. R., … Zaehle, S. (2020). *Global Carbon Budget 2020* [Preprint]. Data, Algorithms, and Models. https://doi.org/10.5194/essd-2020-286

Goemann, H. M., Gay, J. D., Mueller, R. C., Brookshire, E. N. J., Miller, P., Poulter, B., & Peyton, B. M. 2021. Aboveground and belowground responses to cyanobacterial biofertilizer supplement in a semi-arid, perennial bioenergy cropping system. *GCB Bioenergy*, *n/a*(n/a). https://doi.org/10.1111/gcbb.12892

Graven, H. D., Keeling, R. F., Piper, S. C., Patra, P. K., Stephens, B. B., Wofsy, S. C., Welp, L. R., Sweeney, C., Tans, P. P., Kelley, J. J., Daube, B. C., Kort, E. A., Santoni, G. W., & Bent, J. D. (2013). Enhanced Seasonal Exchange of CO2 by Northern Ecosystems Since 1960. *Science*, *341*(6150), 1085–1089. https://doi.org/10.1126/science.1239207

Griscom, B. W., Adams, J., Ellis, P. W., Houghton, R. A., Lomax, G., Miteva, D. A., Schlesinger, W. H., Shoch, D., Siikamäki, J. V., Smith, P., Woodbury, P., Zganjar, C., Blackman, A., Campari, J., Conant, R. T., Delgado, C., Elias, P., Gopalakrishna, T., Hamsik, M. R., … Fargione, J. (2017). Natural climate solutions. *Proceedings of the National Academy of Sciences*, *114*(44), 11645–11650. https://doi.org/10.1073/pnas.1710465114

Grubb, P. J. (1977). Control of forest growth and distribution on wet tropical mountains: With special reference to mineral nutrition. *Annual Review of Ecology and Systematics*, *8*(1), 83–107.

Grubb, P. J., & Stevens, P. F. (2017). *The forests of the Fatima Basin and Mt Kerigomna, Papua New Guinea with a review of montane and subalpine rainforests in Papuasia*. Canberra, ACT: Dept. of Human Geography, Research School of Pacific Studies ….

Gruber, N., & Galloway, J. N. (2008). An Earth-system perspective of the global nitrogen cycle. *Nature*, *451*(7176), 293–296. https://doi.org/10.1038/nature06592

Guenet, B., Gabrielle, B., Chenu, C., Arrouays, D., Balesdent, J., Bernoux, M., Bruni, E., Caliman, J.-P., Cardinael, R., Chen, S., Ciais, P., Desbois, D., Fouche, J., Frank, S., Henault, C., Lugato, E., Naipal, V., Nesme, T., Obersteiner, M., … Zhou, F. (2021). Can N2O emissions offset the benefits from soil organic carbon storage? *Global Change Biology*, *27*(2), 237–256. https://doi.org/10.1111/gcb.15342

Halvorson, A. D., Wienhold, B. J., & Black, A. L. (2002). Tillage, Nitrogen, and Cropping System Effects on Soil Carbon Sequestration. *Soil Science Society of America Journal*, *66*(3), 906–912. https://doi.org/10.2136/sssaj2002.9060

Hanson et al. (2020). Is growing switchgrass economically feasible? *University of Wyoming Extension*. https://www.wyoextension.org/agpubs/pubs/B-1360-1-switchgrass-web.pdf

Hanson, P. J., Edwards, N. T., Garten, C. T., & Andrews, J. A. (2000). Separating root and soil microbial contributions to soil respiration: A review of methods and observations. *Biogeochemistry*, *48*(1), 115–146. https://doi.org/10.1023/A:1006244819642

Harden, J. W., Mack, M., Veldhuis, H., & Gower, S. T. (2002). Fire dynamics and implications for nitrogen cycling in boreal forests. *Journal of Geophysical Research: Atmospheres*, *107*(D3), WFX 4-1-WFX 4-8. https://doi.org/10.1029/2001JD000494

Harmoney, K. R. (2015). Cool-Season Grass Biomass in the Southern Mixed-Grass Prairie Region of the USA. *BioEnergy Research*, *8*(1), 203–210. https://doi.org/10.1007/s12155-014-9514-9

Hartman, W. H., Ye, R., Horwath, W. R., & Tringe, S. G. (2017). A genomic perspective on stoichiometric regulation of soil carbon cycling. *The ISME Journal*, *11*(12), 2652–2665. https://doi.org/10.1038/ismej.2017.115

Heaton, E., Voigt, T., & Long, S. P. (2004). A quantitative review comparing the yields of two candidate C4 perennial biomass crops in relation to nitrogen, temperature and water. *Biomass and Bioenergy*, *27*(1), 21–30. https://doi.org/10.1016/j.biombioe.2003.10.005

Helgason, B. L., Walley, F. L., & Germida, J. J. (2010). No-till soil management increases microbial biomass and alters community profiles in soil aggregates. *Applied Soil Ecology*, *46*(3), 390–397. https://doi.org/10.1016/j.apsoil.2010.10.002

Hendrickson, J. R., Schmer, M. R., & Sanderson, M. A. (2013). Water Use Efficiency by Switchgrass Compared to a Native Grass or a Native Grass Alfalfa Mixture. *BioEnergy Research*, *6*(2), 746–754. https://doi.org/10.1007/s12155-012-9290-3

Hengl, T., Mendes de Jesus, J., Heuvelink, G. B., Ruiperez Gonzalez, M., Kilibarda, M., Blagotić, A., Shangguan, W., Wright, M. N., Geng, X., & Bauer-Marschallinger, B. (2017). SoilGrids250m: Global gridded soil information based on machine learning. *PLoS One*, *12*(2), e0169748.

Hetrick, B. A. D., Kitt, D. G., & Wilson, G. T. (2011). Mycorrhizal dependence and growth habit of warm-season and cool-season tallgrass prairie plants. *Canadian Journal of Botany*. https://doi.org/10.1139/b88-193

Hiers, J. K., O'Brien, J. J., Varner, J. M., Butler, B. W., Dickinson, M., Furman, J., Gallagher, M., Godwin, D., Goodrick, S. L., Hood, S. M., Hudak, A., Kobziar, L. N., Linn, R., Loudermilk, E. L., McCaffrey, S., Robertson, K., Rowell, E. M., Skowronski, N., Watts, A. C., & Yedinak, K. M. (2020). Prescribed fire science: The case for a refined research agenda. *Fire Ecology*, *16*(1), 11. https://doi.org/10.1186/s42408-020-0070-8

Hilton, R. G., Galy, A., West, A. J., Hovius, N., & Roberts, G. G. (2013). Geomorphic control on the delta N-15 of mountain forests. *Biogeosciences*, *10*(3), 1693–1705. https://doi.org/10.5194/bg-10-1693-2013

Hobbie, S. E. (1992). Effects of plant species on nutrient cycling. *Trends in Ecology & Evolution*, *7*(10), 336–339. https://doi.org/10.1016/0169-5347(92)90126-V

Houlton, B., & Bai, E. (2009). Imprint of denitrifying bacteria on the global terrestrial biosphere. *PROCEEDINGS OF THE NATIONAL ACADEMY OF SCIENCES OF THE UNITED STATES OF*, *106*(51), 21713–21716. https://doi.org/10.1073/pnas.0912111106

Houlton, B. Z., Morford, S. L., & Dahlgren, R. A. (2018). Convergent evidence for widespread rock nitrogen sources in Earth's surface environment. *Science*, *360*(6384), 58–62.

Hu, J., Yang, J. Y., Li, J., Gao, T., Yang, G. W., & Ren, H. Y. (2018). First report of Ustilago avenae causing loose smut of oat (Avena sativa) in Shandong China. *Journal of Plant Pathology*, *100*(1), 123–123. https://doi.org/10.1007/s42161-018-0016-z

Humboldt, A. von, & Bonpland, A. (1805). *Analysis of the geography of plants*.

Jackson, R. B., Canadell, J., Ehleringer, J. R., Mooney, H. A., Sala, O. E., & Schulze, E. D. (1996). A global analysis of root distributions for terrestrial biomes. *Oecologia*, *108*(3), 389–411. https://doi.org/10.1007/BF00333714

JENNY, H., BINGHAM, F., & PADILLASARAVIA, B. (1948). NITROGEN AND ORGANIC MATTER CONTENTS OF EQUATORIAL SOILS OF COLOMBIA, SOUTH-AMERICA. *SOIL SCIENCE*, *66*(3), 173–186.

Jenson and Varnes. (1964). Geology of the Fort Peck area, Garfield, McCone, and Valley Counties, Montana. *USGS*. https://pubs.er.usgs.gov/publication/pp414F

Jian, J., Steele, M. K., Day, S. D., Quinn Thomas, R., & Hodges, S. C. (2018). Measurement strategies to account for soil respiration temporal heterogeneity across diverse regions. *Soil Biology and Biochemistry*, *125*, 167–177. https://doi.org/10.1016/j.soilbio.2018.07.003

John, A. A., Jones, C. A., Ewing, S. A., Sigler, W. A., Bekkerman, A., & Miller, P. R. (2017). Fallow replacement and alternative nitrogen management for reducing nitrate leaching in a semiarid region. *Nutrient Cycling in Agroecosystems*, *108*(3), 279–296. https://doi.org/10.1007/s10705-017-9855-9

Johnson, D. W., & Curtis, P. S. (2001). Effects of forest management on soil C and N storage: Meta analysis. *Forest Ecology and Management*, *140*(2), 227–238. https://doi.org/10.1016/S0378-1127(00)00282-6

Johnson, D. W., Susfalk, R. B., Dahlgren, R. A., & Klopatek, J. M. (1998). Fire is more important than water for nitrogen fluxes in semi-arid forests. *Environmental Science & Policy*, *1*(2), 79–86. https://doi.org/10.1016/S1462-9011(98)00008-2

Kallenbach, C. M., Grandy, A. S., Frey, S. D., & Diefendorf, A. F. (2015). Microbial physiology and necromass regulate agricultural soil carbon accumulation. *Soil Biology and Biochemistry*, *91*, 279–290. https://doi.org/10.1016/j.soilbio.2015.09.005

Kapos, V., Rhind, J., Edwards, M., Price, M. F., & Ravilious, C. (2000). Developing a map of the world's mountain forests. In M. F. Price & N. Butt, *Forests in sustainable mountain development: A state of knowledge report for 2000. Task Force on Forests in Sustainable Mountain Development.* (pp. 4–19). CABI. https://doi.org/10.1079/9780851994468.0004

Karp, A., & Shield, I. (2008). Bioenergy from plants and the sustainable yield challenge. *New Phytologist*, *179*(1), 15–32. https://doi.org/10.1111/j.1469-8137.2008.02432.x

Kasanke, C. P., Zhao, Q., Bell, S., Thompson, A. M., & Hofmockel, K. S. (2021). Can switchgrass increase carbon accrual in marginal soils? The importance of site selection. *GCB Bioenergy*, *13*(2), 320–335. https://doi.org/10.1111/gcbb.12777

Keenan, T. f., Baker, I., Barr, A., Ciais, P., Davis, K., Dietze, M., Dragoni, D., Gough, C. M., Grant, R., Hollinger, D., Hufkens, K., Poulter, B., McCaughey, H., Raczka, B., Ryu, Y., Schaefer, K., Tian, H., Verbeeck, H., Zhao, M., & Richardson, A. D. (2012). Terrestrial biosphere model performance for inter-annual variability of land-atmosphere CO2 exchange. *Global Change Biology*, *18*(6), 1971–1987. https://doi.org/10.1111/j.1365-2486.2012.02678.x

Keenan, T. F., Prentice, I. C., Canadell, J. G., Williams, C. A., Wang, H., Raupach, M., & Collatz, G. J. (2016). Recent pause in the growth rate of atmospheric CO 2 due to enhanced terrestrial carbon uptake. *Nature Communications*, *7*(1), 1–10. https://doi.org/10.1038/ncomms13428

Keenan, T. F., & Williams, C. A. (2018). The Terrestrial Carbon Sink. *Annual Review of Environment and Resources*, *43*(1), 219–243. https://doi.org/10.1146/annurev-environ-102017-030204

Kicklighter, D. W., Melillo, J. M., Monier, E., Sokolov, A. P., & Zhuang, Q. (2019). Future nitrogen availability and its effect on carbon sequestration in Northern Eurasia. *Nature Communications*, *10*(1), 3024. https://doi.org/10.1038/s41467-019-10944-0

Kitayama, K., & Iwamoto, K. (2001). Patterns of natural 15N abundance in the leaf-to-soil continuum of tropical rain forests differing in N availability on Mount Kinabalu, Borneo. *Plant and Soil*, *229*(2), 203–212.

Krishnaswamy, J., John, R., & Joseph, S. (2014). Consistent response of vegetation dynamics to recent climate change in tropical mountain regions. *Global Change Biology*, *20*(1), 203–215.

Kruse, J., Dietrich, W., Zimmermann, H., Klenke, F., Richter, U., Richter, H., & Thines, M. (2018). Ustilago species causing leaf-stripe smut revisited. *IMA Fungus*, *9*(1), 49–73. https://doi.org/10.5598/imafungus.2018.09.01.05

Kurth, V. J., MacKenzie, M. D., & DeLuca, T. H. (2006). Estimating charcoal content in forest mineral soils. *Geoderma*, *137*(1), 135–139. https://doi.org/10.1016/j.geoderma.2006.08.003

Kuzyakov, Y., Friedel, J. K., & Stahr, K. (2000). Review of mechanisms and quantification of priming effects. *Soil Biology and Biochemistry*, *32*(11), 1485–1498. https://doi.org/10.1016/S0038-0717(00)00084-5

Lai, L., Hong, C. O., Kumar, S., Osborne, S. L., Lehman, R. M., & Owens, V. N. (2018). Soil nitrogen dynamics in switchgrass seeded to a marginal cropland in South Dakota. *GCB Bioenergy*, *10*(1), 28–38. https://doi.org/10.1111/gcbb.12475

Lal, R. (2009). Sequestering carbon in soils of arid ecosystems. *Land Degradation & Development*, *20*(4), 441–454. https://doi.org/10.1002/ldr.934

Lawrence, N. C., Tenesaca, C. G., VanLoocke, A., & Hall, S. J. (2021). Nitrous oxide emissions from agricultural soils challenge climate sustainability in the US Corn Belt. *Proceedings of the National Academy of Sciences*, *118*(46). https://doi.org/10.1073/pnas.2112108118

Le Houérou, H. N. (1984). Rain use efficiency: A unifying concept in arid-land ecology. *Journal of Arid Environments*, *7*(3), 213–247. https://doi.org/10.1016/S0140-1963(18)31362-4

Le Quéré, C., Andrew, R. M., Friedlingstein, P., Sitch, S., Pongratz, J., Manning, A. C., Korsbakken, J. I., Peters, G. P., Canadell, J. G., Jackson, R. B., Boden, T. A., Tans, P. P., Andrews, O. D., Arora, V. K., Bakker, D. C. E., Barbero, L., Becker, M., Betts, R. A., Bopp, L., … Zhu, D. (2018). Global Carbon Budget 2017. *Earth System Science Data*, *10*(1), 405–448. https://doi.org/10.5194/essd-10-405-2018

Lehmann, J., Skjemstad, J., Sohi, S., Carter, J., Barson, M., Falloon, P., Coleman, K., Woodbury, P., & Krull, E. (2008). Australian climate–carbon cycle feedback reduced by soil black carbon. *Nature Geoscience*, *1*(12), 832–835. https://doi.org/10.1038/ngeo358

Leichty, S. I., Kasanke, C. P., Bell, S. L., & Hofmockel, K. S. (2021). Site and Bioenergy Cropping System Similarly Affect Distinct Live and Total Soil Microbial Communities. *Frontiers in Microbiology*, *12*, 3086. https://doi.org/10.3389/fmicb.2021.725756

Lekberg, Y., & Helgason, T. (2018). In situ mycorrhizal function – knowledge gaps and future directions. *New Phytologist*, *220*(4), 957–962. https://doi.org/10.1111/nph.15064

Levine, U. Y., Teal, T. K., Robertson, G. P., & Schmidt, T. M. (2011). Agriculture's impact on microbial diversity and associated fluxes of carbon dioxide and methane. *The ISME Journal*, *5*(10), 1683–1691. https://doi.org/10.1038/ismej.2011.40

Li, Y.-M., Shivas, R. G., & Cai, L. (2017). Cryptic diversity in Tranzscheliella spp. (Ustilaginales) is driven by host switches. *Scientific Reports*, *7*(1), 43549. https://doi.org/10.1038/srep43549

Liao, C., Peng, R., Luo, Y., Zhou, X., Wu, X., Fang, C., Chen, J., & Li, B. (2008). Altered ecosystem carbon and nitrogen cycles by plant invasion: A meta-analysis. *New Phytologist*, *177*(3), 706–714. https://doi.org/10.1111/j.1469-8137.2007.02290.x

Liebig, M. A., Schmer, M. R., Vogel, K. P., & Mitchell, R. B. (2008). Soil Carbon Storage by Switchgrass Grown for Bioenergy. *BioEnergy Research*, *1*(3), 215–222. https://doi.org/10.1007/s12155-008-9019-5

Liu, Y., Wang, C., He, N., Wen, X., Gao, Y., Li, S., Niu, S., Butterbach-Bahl, K., Luo, Y., & Yu, G. (2017). A global synthesis of the rate and temperature sensitivity of soil nitrogen mineralization: Latitudinal patterns and mechanisms. *Global Change Biology*, *23*(1), 455–464. https://doi.org/10.1111/gcb.13372

Lodato, M. B., Boyette, J. S., Smilo, R. A., Jackson, C. R., Halvorson, H. M., & Kuehn, K. A. (2021). Functional importance and diversity of fungi during standing grass litter decomposition. *Oecologia*, *195*(2), 499–512. https://doi.org/10.1007/s00442-020-04838-y

Lugato, E., Leip, A., & Jones, A. (2018). Mitigation potential of soil carbon management overestimated by neglecting N 2 O emissions. *Nature Climate Change*, *8*(3), 219–223. https://doi.org/10.1038/s41558-018-0087-z

Luo, W., Wang, X., Sardans, J., Wang, Z., Dijkstra, F. A., Lü, X.-T., Peñuelas, J., & Han, X. (2018). Higher capability of C3 than C4 plants to use nitrogen inferred from nitrogen stable isotopes along an aridity gradient. *Plant and Soil*, *428*(1), 93–103. https://doi.org/10.1007/s11104-018-3661-2

Lynch, J. A., Clark, J. S., & Stocks, B. J. (2004). Charcoal production, dispersal, and deposition from the Fort Providence experimental fire: Interpreting fire regimes from charcoal records in boreal forests. *Canadian Journal of Forest Research*, *34*(8), 1642–1656. https://doi.org/10.1139/x04-071

MacKenzie, M. D., DeLuca, T. H., & Sala, A. (2004). Forest structure and organic horizon analysis along a fire chronosequence in the low elevation forests of western Montana. *Forest Ecology and Management*, *203*(1), 331–343. https://doi.org/10.1016/j.foreco.2004.08.003

Mackey, B., Prentice, I. C., Steffen, W., House, J. I., Lindenmayer, D., Keith, H., & Berry, S. (2013). Untangling the confusion around land carbon science and climate change mitigation policy. *Nature Climate Change*, *3*(6), 552–557. https://doi.org/10.1038/nclimate1804

Malhi, Y., Girardin, C. A. J., Goldsmith, G. R., Doughty, C. E., Salinas, N., Metcalfe, D. B., Huasco, W. H., Silva-Espejo, J. E., Aguilla-Pasquell, J. del, Amézquita, F. F., Aragão, L. E. O. C., Guerrieri, R., Ishida, F. Y., Bahar, N. H. A., Farfan-Rios, W., Phillips, O. L., Meir, P., & Silman, M. (2017). The variation of productivity and its allocation along a tropical elevation gradient: A whole carbon budget perspective. *New Phytologist*, *214*(3), 1019–1032. https://doi.org/10.1111/nph.14189

Malhi, Y., Silman, M., Salinas, N., Bush, M., Meir, P., & Saatchi, S. (2010). Introduction: Elevation gradients in the tropics: laboratories for ecosystem ecology and global change research. *Global Change Biology*, *16*(12), 3171–3175. https://doi.org/10.1111/j.1365-2486.2010.02323.x

Mariotti, A., Pierre, D., Vedy, J. C., Bruckert, S., & Guillemot, J. (1980). The abundance of natural nitrogen 15 in the organic matter of soils along an altitudinal gradient (Chablais, Haute Savoie, France). *CATENA*, *7*(1), 293–300. https://doi.org/10.1016/S0341-8162(80)80020-8

Marrs, R. H., Proctor, J., Heaney, A., & Mountford, M. D. (1988). Changes in soil nitrogen-mineralization and nitrification along an altitudinal transect in tropical rain forest in Costa Rica. *The Journal of Ecology*, 466–482.

Martinelli, L., Piccolo, M., Townsend, A., Vitousek, P., Cuevas, E., McDowell, W., Robertson, G., Santos, O., & Treseder, K. (1999). Nitrogen stable isotopic composition of leaves and soil: Tropical versus temperate forests. *BIOGEOCHEMISTRY*, *46*(1–3), 45–65.

Martyniak, D., Żurek, G., & Prokopiuk, K. (2017). Biomass yield and quality of wild populations of tall wheatgrass [Elymus elongatus (Host.) Runemark]. *Biomass and Bioenergy*, *101*, 21–29. https://doi.org/10.1016/j.biombioe.2017.03.025

Matthews, H. D., Zickfeld, K., Dickau, M., MacIsaac, A. J., Mathesius, S., Nzotungicimpaye, C.-M., & Luers, A. (2022). Temporary nature-based carbon removal can lower peak warming in a well-below 2 °C scenario. *Communications Earth & Environment*, *3*(1), 1–8. https://doi.org/10.1038/s43247-022-00391-z

McKenzie, E. H. C., & Vánky, K. (2001). Smut fungi of New Zealand: An introduction, and list of recorded species. *New Zealand Journal of Botany*, *39*(3), 501–515. https://doi.org/10.1080/0028825X.2001.9512753

McLauchlan, K. K., Higuera, P. E., Miesel, J., Rogers, B. M., Schweitzer, J., Shuman, J. K., Tepley, A. J., Varner, J. M., Veblen, T. T., Adalsteinsson, S. A., Balch, J. K., Baker, P., Batllori, E., Bigio, E., Brando, P., Cattau, M., Chipman, M. L., Coen, J., Crandall, R., … Watts, A. C. (2020). Fire as a fundamental ecological process: Research advances and frontiers. *Journal of Ecology*, *108*(5), 2047–2069. https://doi.org/10.1111/1365-2745.13403

Meigs, G. W., Donato, D. C., Campbell, J. L., Martin, J. G., & Law, B. E. (2009). Forest Fire Impacts on Carbon Uptake, Storage, and Emission: The Role of Burn Severity in the Eastern Cascades, Oregon. *Ecosystems*, *12*(8), 1246–1267. https://doi.org/10.1007/s10021-009-9285-x

Mendes, R., Kruijt, M., Bruijn, I. de, Dekkers, E., Voort, M. van der, Schneider, J. H. M., Piceno, Y. M., DeSantis, T. Z., Andersen, G. L., Bakker, P. A. H. M., & Raaijmakers, J. M. (2011). Deciphering the Rhizosphere Microbiome for Disease-Suppressive Bacteria. *Science*. https://doi.org/10.1126/science.1203980

Miller, P. R., & Holmes, J. A. (2012). Short Communication: Comparative soil water use by annual crops at a semiarid site in Montana. *Canadian Journal of Plant Science*, *92*(4), 803–807. https://doi.org/10.4141/cjps2011-191

Monson, R. K., Littlejohn, R. O., & Williams, G. J. (1983). Photosynthetic adaptation to temperature in four species from the Colorado shortgrass steppe: A physiological model for coexistence. *Oecologia*, *58*(1), 43–51. https://doi.org/10.1007/BF00384540

Mooshammer, M., Wanek, W., Hämmerle, I., Fuchslueger, L., Hofhansl, F., Knoltsch, A., Schnecker, J., Takriti, M., Watzka, M., Wild, B., Keiblinger, K. M., Zechmeister-Boltenstern, S., & Richter, A. (2014a). Adjustment of microbial

nitrogen use efficiency to carbon:nitrogen imbalances regulates soil nitrogen cycling. *Nature Communications*, *5*(1), 3694. https://doi.org/10.1038/ncomms4694

Mooshammer, M., Wanek, W., Hämmerle, I., Fuchslueger, L., Hofhansl, F., Knoltsch, A., Schnecker, J., Takriti, M., Watzka, M., Wild, B., Keiblinger, K. M., Zechmeister-Boltenstern, S., & Richter, A. (2014b). Adjustment of microbial nitrogen use efficiency to carbon:nitrogen imbalances regulates soil nitrogen cycling. *Nature Communications*, *5*. https://doi.org/10.1038/ncomms4694

Mueller, R. C., Gallegos-Graves, L. V., & Kuske, C. R. (2016). A new fungal large subunit ribosomal RNA primer for high-throughput sequencing surveys. *FEMS Microbiology Ecology*, *92*(fiv153). https://doi.org/10.1093/femsec/fiv153

Nave, L. E., Vance, E. D., Swanston, C. W., & Curtis, P. S. (2011). Fire effects on temperate forest soil C and N storage. *Ecological Applications*, *21*(4), 1189–1201. https://doi.org/10.1890/10-0660.1

Neff, J. C., Townsend, A. R., Gleixner, G., Lehman, S. J., Turnbull, J., & Bowman, W. D. (2002). Variable effects of nitrogen additions on the stability and turnover of soil carbon. *Nature*, *419*(6910), 915–917. https://doi.org/10.1038/nature01136

Nickerson, N. (2016). *Evaluating gas emission measurements using Minimum Detectable Flux (MDF)*. https://doi.org/DOI:10.13140/RG.2.1.4149.2089

Nocentini, C., Certini, G., Knicker, H., Francioso, O., & Rumpel, C. (2010). Nature and reactivity of charcoal produced and added to soil during wildfire are particle-size dependent. *Organic Geochemistry*, *41*(7), 682–689. https://doi.org/10.1016/j.orggeochem.2010.03.010

Nogués-Bravo, D., Araújo, M. B., Errea, M. P., & Martínez-Rica, J. P. (2007). Exposure of global mountain systems to climate warming during the 21st Century. *Global Environmental Change*, *17*(3), 420–428. https://doi.org/10.1016/j.gloenvcha.2006.11.007

Nottingham, A. T., B\aa\aath, E., Reischke, S., Salinas, N., & Meir, P. (2019). Adaptation of soil microbial growth to temperature: Using a tropical elevation gradient to predict future changes. *Global Change Biology*, *25*(3), 827–838.

Nottingham, A. T., Fierer, N., Turner, B. L., Whitaker, J., Ostle, N. J., McNamara, N. P., Bardgett, R. D., Leff, J. W., Salinas, N., Silman, M. R., Kruuk, L. E. B., & Meir, P. (2018). Microbes follow Humboldt: Temperature drives plant and soil

microbial diversity patterns from the Amazon to the Andes. *Ecology*, *99*(11), 2455–2466. https://doi.org/10.1002/ecy.2482

Nottingham, A. T., Turner, B. L., Whitaker, J., Ostle, N. J., McNamara, N. P., Bardgett, R. D., Salinas, N., & Meir, P. (2015). Soil microbial nutrient constraints along a tropical forest elevation gradient: A belowground test of a biogeochemical paradigm. *Biogeosciences*, *12*(20), 6071–6083. https://doi.org/10.5194/bg-12-6071-2015

Nottingham, A. T., Whitaker, J., Ostle, N. J., Bardgett, R. D., McNamara, N. P., Fierer, N., Salinas, N., Ccahuana, A. J. Q., Turner, B. L., & Meir, P. (n.d.). Microbial responses to warming enhance soil carbon loss following translocation across a tropical forest elevation gradient. *Ecology Letters*, *0*(0). https://doi.org/10.1111/ele.13379

Nottingham, A. T., Whitaker, J., Turner, B. L., Salinas, N., Zimmermann, M., Malhi, Y., & Meir, P. (2015). Climate Warming and Soil Carbon in Tropical Forests: Insights from an Elevation Gradient in the Peruvian Andes. *BioScience*, *65*(9), 906–921. https://doi.org/10.1093/biosci/biv109

Odum, E. P. (1964). The New Ecology. *BioScience*, *14*(7), 14–16. https://doi.org/10.2307/1293228

Oertel, C., Matschullat, J., Zurba, K., Zimmermann, F., & Erasmi, S. (2016). Greenhouse gas emissions from soils—A review. *Geochemistry*, *76*(3), 327–352. https://doi.org/10.1016/j.chemer.2016.04.002

Oldfield, E. E., Bradford, M. A., & Wood, S. A. (2019). Global meta-analysis of the relationship between soil organic matter and crop yields. *SOIL*, *5*(1), 15–32. https://doi.org/10.5194/soil-5-15-2019

Page, S. E., Rieley, J. O., & Banks, C. J. (2011). Global and regional importance of the tropical peatland carbon pool. *Global Change Biology*, *17*(2), 798–818.

Paruelo, J. M., & Lauenroth, W. K. (1996). Relative Abundance of Plant Functional Types in Grasslands and Shrublands of North America. *Ecological Applications*, *6*(4), 1212–1224. https://doi.org/10.2307/2269602

Pellegrini, A. F. A., Ahlström, A., Hobbie, S. E., Reich, P. B., Nieradzik, L. P., Staver, A. C., Scharenbroch, B. C., Jumpponen, A., Anderegg, W. R. L., Randerson, J. T., & Jackson, R. B. (2018). Fire frequency drives decadal changes in soil carbon and

nitrogen and ecosystem productivity. *Nature*, *553*(7687), 194–198. https://doi.org/10.1038/nature24668

Pellegrini, A. F. A., Caprio, A. C., Georgiou, K., Finnegan, C., Hobbie, S. E., Hatten, J. A., & Jackson, R. B. (2021). Low-intensity frequent fires in coniferous forests transform soil organic matter in ways that may offset ecosystem carbon losses. *Global Change Biology*, *27*(16), 3810–3823. https://doi.org/10.1111/gcb.15648

Pellegrini, A. F. A., Hobbie, S. E., Reich, P. B., Jumpponen, A., Brookshire, E. N. J., Caprio, A. C., Coetsee, C., & Jackson, R. B. (2020). Repeated fire shifts carbon and nitrogen cycling by changing plant inputs and soil decomposition across ecosystems. *Ecological Monographs*, *90*(4), e01409. https://doi.org/10.1002/ecm.1409

Peterson, G. A., Schlegel, A. J., Tanaka, D. L., & Jones, O. R. (1996). Precipitation Use Efficiency as Affected by Cropping and Tillage Systems. *Journal of Production Agriculture*, *9*(2), 180–186. https://doi.org/10.2134/jpa1996.0180

Pingree, M. R. A., & DeLuca, T. H. (2017). Function of Wildfire-Deposited Pyrogenic Carbon in Terrestrial Ecosystems. *Frontiers in Environmental Science*, *5*. https://doi.org/10.3389/fenvs.2017.00053

Piringer, G., & Steinberg, L. J. (2006). Reevaluation of Energy Use in Wheat Production in the United States. *Journal of Industrial Ecology*, *10*(1–2), 149–167. https://doi.org/10.1162/108819806775545420

Poggio, L., de Sousa, L. M., Batjes, N. H., Heuvelink, G. B. M., Kempen, B., Ribeiro, E., & Rossiter, D. (2021). SoilGrids 2.0: Producing soil information for the globe with quantified spatial uncertainty. *SOIL*, *7*(1), 217–240. https://doi.org/10.5194/soil-7-217-2021

Porder, S., Vitousek, P., Chadwick, O., Chamberlain, C., & Hilley, G. (2007). Uplift, erosion, and phosphorus limitation in terrestrial ecosystems. *ECOSYSTEMS*, *10*(1), 158–170. https://doi.org/10.1007/s10021-006-9011-x

Poulter, B., Frank, D., Ciais, P., Myneni, R. B., Andela, N., Bi, J., Broquet, G., Canadell, J. G., Chevallier, F., Liu, Y. Y., Running, S. W., Sitch, S., & van der Werf, G. R. (2014). Contribution of semi-arid ecosystems to interannual variability of the global carbon cycle. *Nature*, *509*(7502), 600–603. https://doi.org/10.1038/nature13376

Preston, C. M., & Schmidt, M. W. I. (2006). Black (pyrogenic) carbon: A synthesis of current knowledge and uncertainties with special consideration of boreal regions. *Biogeosciences*, *3*(4), 397–420. https://doi.org/10.5194/bg-3-397-2006

Proctor, J., Edwards, I. D., Payton, R. W., & Nagy, L. (2007). Zonation of forest vegetation and soils of Mount Cameroon, West Africa. *Plant Ecology*, *192*(2), 251–269.

Prohic, A., Jovovic Sadikovic, T., Krupalija-Fazlic, M., & Kuskunovic-Vlahovljak, S. (2016). Malassezia species in healthy skin and in dermatological conditions. *International Journal of Dermatology*, *55*(5), 494–504. https://doi.org/10.1111/ijd.13116

Prosser, J. I., Hink, L., Gubry-Rangin, C., & Nicol, G. W. (2020). Nitrous oxide production by ammonia oxidizers: Physiological diversity, niche differentiation and potential mitigation strategies. *Global Change Biology*, *26*(1), 103–118. https://doi.org/10.1111/gcb.14877

Reed, S. C., Vitousek, P. M., & Cleveland, C. C. (2011). Are patterns in nutrient limitation belowground consistent with those aboveground: Results from a 4 million year chronosequence. *Biogeochemistry*, *106*(3), 323–336. https://doi.org/10.1007/s10533-010-9522-6

Reich, P. B., Peterson, D. W., Wedin, D. A., & Wrage, K. (2001). Fire and Vegetation Effects on Productivity and Nitrogen Cycling Across a Forest–Grassland Continuum. *Ecology*, *82*(6), 1703–1719. https://doi.org/10.1890/0012-9658(2001)082[1703:FAVEOP]2.0.CO;2

Revillini, D., Wilson, G. W. T., Miller, R. M., Lancione, R., & Johnson, N. C. (2019). Plant Diversity and Fertilizer Management Shape the Belowground Microbiome of Native Grass Bioenergy Feedstocks. *Frontiers in Plant Science*, *10*, 1018. https://doi.org/10.3389/fpls.2019.01018

Rillig, M. C., Aguilar-Trigueros, C. A., Camenzind, T., Cavagnaro, T. R., Degrune, F., Hohmann, P., Lammel, D. R., Mansour, I., Roy, J., Heijden, M. G. A. van der, & Yang, G. (2019). Why farmers should manage the arbuscular mycorrhizal symbiosis. *New Phytologist*, *222*(3), 1171–1175. https://doi.org/10.1111/nph.15602

Rillig, M. C., Sosa-Hernández, M. A., Roy, J., Aguilar-Trigueros, C. A., Vályi, K., & Lehmann, A. (2016). Towards an Integrated Mycorrhizal Technology: Harnessing

Mycorrhiza for Sustainable Intensification in Agriculture. *Frontiers in Plant Science*, *7*. https://doi.org/10.3389/fpls.2016.01625

Robertson, G. P., Hamilton, S. K., Barham, B. L., Dale, B. E., Izaurralde, R. C., Jackson, R. D., Landis, D. A., Swinton, S. M., Thelen, K. D., & Tiedje, J. M. (2017). Cellulosic biofuel contributions to a sustainable energy future: Choices and outcomes. *Science*, *356*(6345). https://doi.org/10.1126/science.aal2324

Robertson, G. P., Hamilton, S. K., Grosso, S. J. D., & Parton, W. J. (2011). The biogeochemistry of bioenergy landscapes: Carbon, nitrogen, and water considerations. *Ecological Applications*, *21*(4), 1055–1067. https://doi.org/10.1890/09-0456.1

Robertson, G. P., Paul, E. A., & Harwood, R. R. (2000). Greenhouse Gases in Intensive Agriculture: Contributions of Individual Gases to the Radiative Forcing of the Atmosphere. *Science*, *289*(5486), 1922–1925. https://doi.org/10.1126/science.289.5486.1922

Robertson, G. P., & Vitousek, P. M. (2009). Nitrogen in Agriculture: Balancing the Cost of an Essential Resource. *Annual Review of Environment and Resources*, *34*(1), 97–125. https://doi.org/10.1146/annurev.environ.032108.105046

Rütting, T., Cizungu Ntaboba, L., Roobroeck, D., Bauters, M., Huygens, D., & Boeckx, P. (2015). Leaky nitrogen cycle in pristine African montane rainforest soil. *Global Biogeochemical Cycles*, *29*(10), 1754–1762.

Ryan, K. C., Knapp, E. E., & Varner, J. M. (2013). Prescribed fire in North American forests and woodlands: History, current practice, and challenges. *Frontiers in Ecology and the Environment*, *11*(s1), e15–e24. https://doi.org/10.1890/120329

Sainju, U. M., Allen, B. L., Lenssen, A. W., & Mikha, M. (2017). Root and soil total carbon and nitrogen under bioenergy perennial grasses with various nitrogen rates. *Biomass and Bioenergy*, *107*, 326–334. https://doi.org/10.1016/j.biombioe.2017.10.021

Salomé, C., Nunan, N., Pouteau, V., Lerch, T. Z., & Chenu, C. (2010). Carbon dynamics in topsoil and in subsoil may be controlled by different regulatory mechanisms. *Global Change Biology*, *16*(1), 416–426. https://doi.org/10.1111/j.1365-2486.2009.01884.x

Sanderman, J., Hengl, T., & Fiske, G. J. (2017). Soil carbon debt of 12,000 years of human land use. *Proceedings of the National Academy of Sciences*, *114*(36), 9575–9580. https://doi.org/10.1073/pnas.1706103114

Santin, C., Doerr, S. H., Jones, M. W., Merino, A., Warneke, C., & Roberts, J. M. (2020). The Relevance of Pyrogenic Carbon for Carbon Budgets From Fires: Insights From the FIREX Experiment. *Global Biogeochemical Cycles*, *34*(9), e2020GB006647. https://doi.org/10.1029/2020GB006647

Schmer, M. R., Liebig, M. A., Hendrickson, J. R., Tanaka, D. L., & Phillips, R. L. (2012). Growing season greenhouse gas flux from switchgrass in the northern great plains. *Biomass and Bioenergy*, *45*, 315–319. https://doi.org/10.1016/j.biombioe.2012.05.026

Schmer, M. R., Vogel, K. P., Varvel, G. E., Follett, R. F., Mitchell, R. B., & Jin, V. L. (2014). Energy Potential and Greenhouse Gas Emissions from Bioenergy Cropping Systems on Marginally Productive Cropland. *PLOS ONE*, *9*(3), e89501. https://doi.org/10.1371/journal.pone.0089501

Schmidt, R., Mitchell, J., & Scow, K. (2019). Cover cropping and no-till increase diversity and symbiotroph:saprotroph ratios of soil fungal communities. *Soil Biology and Biochemistry*, *129*, 99–109. https://doi.org/10.1016/j.soilbio.2018.11.010

Scholes, R., & Archer, S. (2003). Tree-Grass Interactions in Savannas. *Annual Review of Ecology and Systematics*, *28*, 517–544. https://doi.org/10.1146/annurev.ecolsys.28.1.517

Schrumpf, M., Schulze, E. D., Kaiser, K., & Schumacher, J. (2011). How accurately can soil organic carbon stocks and stock changes be quantified by soil inventories? *Biogeosciences*, *8*(5), 1193–1212. https://doi.org/10.5194/bg-8-1193-2011

Sieg, Carolyn, Joel D. McMillin, James F. Fowler, Kurt K. Allen, José F. Negron, Linda L. Wadleigh, John A. Anhold, Ken E. Gibson, Best Predictors for Postfire Mortality of Ponderosa Pine Trees in the Intermountain West, *Forest Science*, Volume 52, Issue 6, December 2006, Pages 718–728, https://doi.org/10.1093/forestscience/52.6.718

Sena-Souza, J. P., Houlton, B. Z., Martinelli, L. A., & Nardoto, G. B. (2020). Reconstructing continental-scale variation in soil δ15N: A machine learning approach in South America. *Ecosphere*, *11*(8), e03223. https://doi.org/10.1002/ecs2.3223

Sexton, J. O., Song, X.-P., Feng, M., Noojipady, P., Anand, A., Huang, C., Kim, D.-H., Collins, K. M., Channan, S., & DiMiceli, C. (2013). Global, 30-m resolution continuous fields of tree cover: Landsat-based rescaling of MODIS vegetation continuous fields with lidar-based estimates of error. *International Journal of Digital Earth*, *6*(5), 427–448.

Shi, Z., Allison, S. D., He, Y., Levine, P. A., Hoyt, A. M., Beem-Miller, J., Zhu, Q., Wieder, W. R., Trumbore, S., & Randerson, J. T. (2020). The age distribution of global soil carbon inferred from radiocarbon measurements. *Nature Geoscience*, *13*(8), 555–559.

Six, J., Frey, S. D., Thiet, R. K., & Batten, K. M. (2006). Bacterial and Fungal Contributions to Carbon Sequestration in Agroecosystems. *Soil Science Society of America Journal*, *70*(2), 555–569. https://doi.org/10.2136/sssaj2004.0347

Skinner, R. H., & Comas, L. H. (2010). Root Distribution of Temperate Forage Species Subjected to Water and Nitrogen Stress. *Crop Science*, *50*(5), 2178–2185. https://doi.org/10.2135/cropsci2009.08.0461

Smith and Read. (2008). *Mycorrhizal Symbiosis*. Elsevier.

Soong, J. L., Fuchslueger, L., Marañon-Jimenez, S., Torn, M. S., Janssens, I. A., Penuelas, J., & Richter, A. (2020). Microbial carbon limitation: The need for integrating microorganisms into our understanding of ecosystem carbon cycling. *Global Change Biology*, *26*(4), 1953–1961. https://doi.org/10.1111/gcb.14962

Stewart, C. E., Follett, R. F., Pruessner, E. G., Varvel, G. E., Vogel, K. P., & Mitchell, R. B. (2016). N fertilizer and harvest impacts on bioenergy crop contributions to SOC. *GCB Bioenergy*, *8*(6), 1201–1211. https://doi.org/10.1111/gcbb.12326

Stoy, P. C., Ahmed, S., Jarchow, M., Rashford, B., Swanson, D., Albeke, S., Bromley, G., Brookshire, E. N. J., Dixon, M. D., Haggerty, J., Miller, P., Peyton, B., Royem, A., Spangler, L., Straub, C., & Poulter, B. (2018). Opportunities and Trade-offs among BECCS and the Food, Water, Energy, Biodiversity, and Social Systems Nexus at Regional Scales. *BioScience*, *68*(2), 100–111. https://doi.org/10.1093/biosci/bix145

Surawski, N. C., Sullivan, A. L., Roxburgh, S. H., Meyer, C. P. M., & Polglase, P. J. (2016). Incorrect interpretation of carbon mass balance biases global vegetation fire emission estimates. *Nature Communications*, *7*(1), 11536. https://doi.org/10.1038/ncomms11536

Tanner, E., Vitousek, P., & Cuevas, E. (1998). Experimental investigation of nutrient limitation of forest growth on wet tropical mountains. *ECOLOGY*, *79*(1), 10–22.

Taylor, P. G., Cleveland, C. C., Wieder, W. R., Sullivan, B. W., Doughty, C. E., Dobrowski, S. Z., & Townsend, A. R. (2017). Temperature and rainfall interact to control carbon cycling in tropical forests. *Ecology Letters*, *20*(6), 779–788.

Thompson, L. R., Sanders, J. G., McDonald, D., Amir, A., Ladau, J., Locey, K. J., Prill, R. J., Tripathi, A., Gibbons, S. M., Ackermann, G., Navas-Molina, J. A., Janssen, S., Kopylova, E., Vázquez-Baeza, Y., González, A., Morton, J. T., Mirarab, S., Zech Xu, Z., Jiang, L., … Knight, R. (2017). A communal catalogue reveals Earth's multiscale microbial diversity. *Nature*, *551*(7681), 457–463. https://doi.org/10.1038/nature24621

Tilman, D., Reich, P., Phillips, H., Menton, M., Patel, A., Vos, E., Peterson, D., & Knops, J. (2000). Fire Suppression and Ecosystem Carbon Storage. *Ecology*, *81*(10), 2680–2685. https://doi.org/10.1890/0012-9658(2000)081[2680:FSAECS]2.0.CO;2

Tinker, D. B., & Knight, D. H. (2000). Coarse Woody Debris following Fire and Logging in Wyoming Lodgepole Pine Forests. *Ecosystems*, *3*(5), 472–483. https://doi.org/10.1007/s100210000041

Tinker, D., Stakes, G. K., & Arcano, R. M. (2010). Allometric Equation Development, Biomass, and Aboveground Productivity in Ponderosa Pine Forests, Black Hills, Wyoming. *Western Journal of Applied Forestry*, *25*(3), 112–119. https://doi.org/10.1093/wjaf/25.3.112

Tonitto, C., Woodbury, P. B., & McLellan, E. L. (2018). Defining a best practice methodology for modeling the environmental performance of agriculture. *Environmental Science & Policy*, *87*, 64–73. https://doi.org/10.1016/j.envsci.2018.04.009

Tran, B. N., Tanase, M. A., Bennett, L. T., & Aponte, C. (2018). Evaluation of Spectral Indices for Assessing Fire Severity in Australian Temperate Forests. *Remote Sensing*, *10*(11), 1680. https://doi.org/10.3390/rs10111680

Trigg, S., & Flasse, S. (2001). An evaluation of different bi-spectral spaces for discriminating burned shrub-savannah. *International Journal of Remote Sensing*, *22*(13), 2641–2647. https://doi.org/10.1080/01431160110053185

U.S DOE. (2014). *Research for sustainable bioenergy: Linking genomic and ecosystem sciences*. U.S. Department of Energy Office of Science. https://genomicscience.energy.gov/sustainability/SustainableBiofuels-HR.pdf

van der Werf, G. R., Randerson, J. T., Giglio, L., van Leeuwen, T. T., Chen, Y., Rogers, B. M., Mu, M., van Marle, M. J. E., Morton, D. C., Collatz, G. J., Yokelson, R. J., & Kasibhatla, P. S. (2017). Global fire emissions estimates during 1997–2016. *Earth System Science Data*, *9*(2), 697–720. https://doi.org/10.5194/essd-9-697-2017

van der Werf, G. R., Randerson, J. T., Giglio, L., Collatz, G. J., Mu, M., Kasibhatla, P. S., Morton, D. C., DeFries, R. S., Jin, Y., & van Leeuwen, T. T. (2010). Global fire emissions and the contribution of deforestation, savanna, forest, agricultural, and peat fires (1997–2009). *Atmospheric Chemistry and Physics*, *10*(23), 11707–11735. https://doi.org/10.5194/acp-10-11707-2010

van Groenigen, J. W., van Kessel, C., Hungate, B. A., Oenema, O., Powlson, D. S., & van Groenigen, K. J. (2017). Sequestering Soil Organic Carbon: A Nitrogen Dilemma. *Environ. Sci. Technol.*, 2.

Vermeire, L. T., Heitschmidt, R. K., & Rinella, M. J. (2009). Primary Productivity and Precipitation-Use Efficiency in Mixed-Grass Prairie: A Comparison of Northern and Southern US Sites. *Rangeland Ecology & Management*, *62*(3), 230–239. https://doi.org/10.2111/07-140R2.1

Vicca, S., Luyssaert, S., Peñuelas, J., Campioli, M., Chapin III, F. S., Ciais, P., Heinemeyer, A., Högberg, P., Kutsch, W. L., Law, B. E., Malhi, Y., Papale, D., Piao, S. L., Reichstein, M., Schulze, E. D., & Janssens, I. A. (2012). Fertile forests produce biomass more efficiently. *Ecology Letters*, *15*(6), 520–526. https://doi.org/10.1111/j.1461-0248.2012.01775.x

Vitousek, P. M., & Howarth, R. W. (1991). Nitrogen limitation on land and in the sea: How can it occur? *Biogeochemistry*, *13*(2), 87–115. https://doi.org/10.1007/BF00002772

Vitousek, P. M., Matson, P. A., & Turner, D. R. (1988a). Elevational and age gradients in Hawaiian montane rainforest: Foliar and soil nutrients. *Oecologia*, *77*(4), 565–570.

Vitousek, P. M., Matson, P. A., & Turner, D. R. (1988b). Elevational and Age Gradients in Hawaiian Montane Rainforest: Foliar and Soil Nutrients. *Oecologia*, *77*(4), 565–570.

Vitousek, P. M., Mooney, H. A., Lubchenco, J., & Melillo, J. M. (1997). Human Domination of Earth's Ecosystems. *Science*, *277*(5325), 494–499. https://doi.org/10.1126/science.277.5325.494

Vitousek, P. M., & Sanford, R. L. (1986). Nutrient Cycling in Moist Tropical Forest. *Annual Review of Ecology and Systematics*, *17*, 137–167.

Vitousek, P. M., Van Cleve, K., Balakrishnan, N., & Mueller-Dombois, D. (1983). Soil development and nitrogen turnover in montane rainforest soils on Hawai'i. *Biotropica*, 268–274.

Wang, G.-J., Nyren, P., Xue, Q.-W., Aberle, E., Eriksmoen, E., Tjelde, T., Liebig, M., Nichols, K., & Nyren, A. (2014). Establishment and Yield of Perennial Grass Monocultures and Binary Mixtures for Bioenergy in North Dakota. *Agronomy Journal*, *106*(5), 1605–1613.

Wang, L., Qian, Y., Brummer, J. E., Zheng, J., Wilhelm, S., & Parton, W. J. (2015). Simulated biomass, environmental impacts and best management practices for long-term switchgrass systems in a semi-arid region. *Biomass and Bioenergy*, *75*, 254–266. https://doi.org/10.1016/j.biombioe.2015.02.029

Wang, L., Qian, Y. L., Brummer, J., Wilhelm, S. J., & Leach, J. E. (2019). Biomass Production and Soil Carbon Analysis of Switchgrass under Rainfed or Minimal Irrigation in a Semiarid Environment. *Agronomy Journal*, *111*(4), 1704–1711. https://doi.org/10.2134/agronj2018.09.0568

Wanga, W., Ohse, K., Liu, J., Mo, W., & Oikawab, T. (2005). Contribution of root respiration to soil respiration in a C3/C4 mixed grassland. *Journal of Biosciences*, *30*(4), 507–514. https://doi.org/10.1007/BF02703725

Weintraub, S. R., Cole, R. J., Schmitt, C. G., & All, J. D. (2016). Climatic controls on the isotopic composition and availability of soil nitrogen across mountainous tropical forest. *Ecosphere*, *7*(8), e01412. https://doi.org/10.1002/ecs2.1412

Whitman, T., Enders, A., & Lehmann, J. (2014). Pyrogenic carbon additions to soil counteract positive priming of soil carbon mineralization by plants. *Soil Biology and Biochemistry*, *73*, 33–41. https://doi.org/10.1016/j.soilbio.2014.02.009

Wieczorek, A. S., Schmidt, O., Chatzinotas, A., von Bergen, M., Gorissen, A., & Kolb, S. (2019). Ecological Functions of Agricultural Soil Bacteria and Microeukaryotes in Chitin Degradation: A Case Study. *Frontiers in Microbiology*, *10*. https://www.frontiersin.org/article/10.3389/fmicb.2019.01293

Wilson, G. W. T., Rice, C. W., Rillig, M. C., Springer, A., & Hartnett, D. C. (2009). Soil aggregation and carbon sequestration are tightly correlated with the abundance of arbuscular mycorrhizal fungi: Results from long-term field experiments. *Ecology Letters*, *12*(5), 452–461. https://doi.org/10.1111/j.1461-0248.2009.01303.x

Wolf, K., Veldkamp, E., Homeier, J., & Martinson, G. O. (2011). Nitrogen availability links forest productivity, soil nitrous oxide and nitric oxide fluxes of a tropical montane forest in southern Ecuador. *Global Biogeochemical Cycles*, *25*(4). https://doi.org/10.1029/2010GB003876

Wright, L., & Turhollow, A. (2010). Switchgrass selection as a "model" bioenergy crop: A history of the process. *Biomass and Bioenergy*, *34*(6), 851–868. https://doi.org/10.1016/j.biombioe.2010.01.030

Wright, S. J. (2019). Plant responses to nutrient addition experiments conducted in tropical forests. *Ecological Monographs*, *89*(4), e01382.

Xue, Q., Nyren, P. E., Wang, G., Eriksmoen, E., Bradbury, G., Halverson, M., Aberle, E., Nichols, K., & Liebig, M. (2011). Biomass composition of perennial grasses for biofuel production in North Dakota, USA. *Biofuels*, *2*(5), 515–528. https://doi.org/10.4155/bfs.11.123

Zeng, Z., Wang, D., Yang, L., Wu, J., Ziegler, A. D., Liu, M., Ciais, P., Searchinger, T. D., Yang, Z.-L., Chen, D., Chen, A., Li, L. Z. X., Piao, S., Taylor, D., Cai, X., Pan, M., Peng, L., Lin, P., Gower, D., … Wood, E. F. (2020). Deforestation-induced warming over tropical mountain regions regulated by elevation. *Nature Geoscience*, 1–7. https://doi.org/10.1038/s41561-020-00666-0

Zhalnina, K., Hawkes, C., Shade, A., Firestone, M. K., & Pett-Ridge, J. (2021). Managing Plant Microbiomes for Sustainable Biofuel Production. *Phytobiomes Journal*, *5*(1), 3–13. https://doi.org/10.1094/PBIOMES-12-20-0090-E

Zhou, Y., Singh, J., Butnor, J. R., Coetsee, C., Boucher, P. B., Case, M. F., Hockridge, E. G., Davies, A. B., & Staver, A. C. (2022). Limited increases in savanna carbon stocks over decades of fire suppression. *Nature*, *603*(7901), 445–449. https://doi.org/10.1038/s41586-022-04438-1

Zimmermann, M., & Bird, M. I. (2012). Temperature sensitivity of tropical forest soil respiration increase along an altitudinal gradient with ongoing decomposition. *Geoderma*, *187–188*, 8–15. https://doi.org/10.1016/j.geoderma.2012.04.015